Climatic and geomorphological controls of rock glaciers in the Andes of Central Chile:

Combining statistical modelling and field mapping

D I S S E R T A T I O N

zur Erlangung des akademischen Grades
doctor rerum naturalium
(dr. rer. nat.)
im Fach Geographie

eingereicht an der
Mathematisch-Naturwissenschaftlichen Fakultät II
Humboldt-Universität zu Berlin

von
Herrn Dipl.-Math. Alexander Brenning
geboren am 15.09.1975 in Bamberg

Präsident der Humboldt-Universität zu Berlin:
Prof. Dr. rer. nat. Jürgen Mlynek

Dekan der Mathematisch-Naturwissenschaftlichen Fakultät II:
Prof. Dr. rer. nat. Uwe Küchler

Gutachter:
1. Prof. Dr. Wilfried Endlicher
2. Prof. Dr. Lothar Schrott
3. Prof. Donald Friend, PhD
4. Prof. Dr. Otti Margraf

Eingereicht am:	19. April 2005
Tag der mündlichen Prüfung:	31. August 2005

Abstract

Rock glaciers are ubiquitous landforms in the dry Andes, and significant, but unheralded stores of frozen water. In this study, statistical modelling techniques and geomorphological mapping are applied to quantify and analyze the distribution of rock glaciers in the Andes of Central Chile (27–35° S) as related to climate and topography. Special emphasis is put on the the Andes of Santiago (33–34.5° S).

A statistical sample survey and a logistic regression model were designed to quantitatively estimate distribution patterns and characterize the geomorphological niche of rock glaciers based upon digital elevation models. These methods proved to be efficient instruments that are complementary to field mapping and remote-sensing techniques.

The amount of water stored within rock glaciers of the Andes of Santiago per unit area is by one order of magnitude higher than in the Swiss Alps, reaching an average 0.7–1.1 km^3 of water equivalent per 1000 km^2 in the Andes. At least one fifth of the high-mountain area of the Andes of Santiago drains through intact rock glaciers. This statistical estimate underlines the importance of rock glaciers within the Andean hydrological and debris-transport system.

On a local scale, the optimal rock glacier niche in the Andes of Santiago is characterized by a convergent contributing area of 0.5–1 km^2 and modern mean annual air temperatures of $+1$ to -1°C, corresponding to 3500–3800 m a. s. l. Sporadic intact rock glaciers reach down to 3000 m a. s. l. at places with favorable morphography and topoclimate including low incoming solar radiation. Huge rock glaciers of more than 1.5 km^2 are in contrast favored by north-facing glacier-free cirques at higher elevations. They are among the largest known rock glaciers on Earth.

The overall distribution pattern of rock glaciers in Central Chile is influenced by precipitation, past and modern glaciation, topography and volcanism. These act as combined controls at the northern (27° S) and southern (35° S) limit of rock glacier occurrence in the Chilean area of winter precipitation.

Rock glacier sediment budgets revealing Holocene denudation rates, and the use of rock glaciers as permafrost indicators give further insight into the periglacial environment of the Andes of Central Chile.

Keywords:
Rock glacier, statistical modelling, geomorphometry, Andes

Zusammenfassung

Die Blockgletscher der trockenen Anden sind weitverbreitete Oberflächenformen sowie bedeutende, aber unauffällige Bodeneisvorkommen. In der vorliegenden Arbeit werden statistische Methoden angewandt und geomorphologische Kartierungen durchgeführt, um die Verbreitung dieser Formen in den Anden von Zentralchile (27–36° s. Br.) in ihrem Bezug zu Klima und Topographie zu quantifizieren und analysieren. Besondere Aufmerksamkeit gilt den Anden von Santiago (33–34,5° s. Br.).

Eine stichprobenbasierte statistische Erhebung und eine logistische Regressionsmodellierung wurden durchgeführt, um Verbreitungsmuster quantitativ zu schätzen und die geomorphologische Nische von Blockgletschern unter Verwendung von digitalen Geländemodellen zu charakterisieren. Diese Methoden haben sich als effiziente Instrumente erwiesen, die als komplementär zu Geländekartierung und Fernerkundungsmethoden anzusehen sind.

Das in Blockgletschern der Anden von Santiago gespeicherte Wasseräquivalent von durchschnittlich 0,7–1,1 km^3 je 1000 km^2 Gebirgsfläche ist um eine Größenordnung größer als in den Schweizer Alpen. Mindestens ein Fünftel der Hochgebirgsfläche der Anden von Santiago wird durch Blockgletscher hindurch entwässert. Diese statistische Schätzung unterstreicht die Bedeutung von Blockgletschern im andinen hydrologischen System und Schutttransportsystem.

Auf lokaler Ebene ist die optimale Blockgletschernische der Anden von Santiago gekennzeichnet durch ein konvergierendes Einzugsgebiet von etwa 0,5–1 km^2 Fläche sowie rezente mittlere Jahrestemperaturen von etwa $+1$ bis -1°C in 3500–3800 m Höhe. Sporadisch reichen intakte Blockgletscher bis 3000 m Höhe hinab, sofern besonders günstige morphographische und topoklimatische Verhältnisse wie etwa eine niedrige Sonneneinstrahlung vorliegen. Außerordentlich große Blockgletscher von mehr als 1,5 km^2 Fläche treten dagegen in höhergelegenen, nordexponierten unvergletscherten Karen auf. Sie gehören zu den größten bekannten Blockgletschern der Erde.

Das überregionale Verbreitungsmuster von Blockgletschern in Zentralchile wird gesteuert durch Niederschlag, vergangene und gegenwärtige Vergletscherung, Topographie und Vulkanismus. Diese Faktoren wirken in Kombination auch an der nördlichen und südlichen Verbreitungsgrenze der Blockgletscher des Winterregengebiets bei 27° bzw. 35° s. Br.

Die Verwendung der Blockgletscher-Sedimentbilanzen zur Abschätzung von holozänen Denudationsraten sowie von Blockgletschern als Permafrostindikatoren vermittelt weitere Einblicke in die Umweltverhältnisse der zentralchilenischen Anden.

Schlagwörter:
Blockgletscher, statistische Modellierung, Geomorphometrie, Anden

Resumen

Los glaciares de escombros o glaciares rocosos de los Andes semiáridos son geoformas omnipresentes y reservorios de agua importantes, aunque poco llamativos. En el presente trabajo se aplican el modelamiento estadístico y la cartografía geomorfológica para cuantificar y analizar la distribución de los glaciares de escombros en los Andes de Chile Central (27–35° S) en relación con el clima y la topografía. Especial atención reciben los Andes de Santiago (33–34.5° S).

Una encuesta estadística por muestreo aleatorio y un modelo de regresión logística fueron diseñados para estimar cuantitativamente el patrón de distribución, y caracterizar el nicho geomorfológico de los glaciares de escombros usando modelos digitales de terreno. Estos métodos han demostrado ser instrumentos eficientes, complementarios a la cartografía en terreno y las técnicas de percepción remota.

El equivalente en agua almacenado dentro de los glaciares de escombros de los Andes de Santiago alcanza en promedio los 0,7–1,1 km^3 por 1000 km^2 de montaña, siendo esta cantidad un orden de magnitud superior al valor para los Alpes suizos. Por lo menos la quinta parte de los altos Andes de Santiago desagua a través de los glaciares de escombros. Esta estimación estadística subraya la importancia de los glaciares de escombros en los sistemas hidrológico y de denudación andinos.

A escala local, el nicho óptimo para los glaciares de escombros de los Andes de Santiago se caracteriza por un área de captación de 0,5–1 km^2 y temperaturas medias anuales actuales de $+1$ a -1°C, correspondiente a una altitud de 3500–3800 m s. n. m. El límite inferior de los glaciares de escombros intactos esporádicos se ubica a los 3000 m s. n. m. en lugares con condiciones morfográficas y topoclimáticas favorables, incluyendo una reducida insolación. Enormes glaciares de escombros de más de 1,5 km^2, en cambio, se encuentran preferentemente en circos expuestos hacia el Norte, situados a mayores altitudes. Estos figuran entre los glaciares de escombros más grandes conocidos en la Tierra.

El patrón de distribución suprarregional de los glaciares de escombros en Chile Central es controlado por las precipitaciones, las glaciaciones pasadas y actual, la topografía, y el volcanismo. Estos factores actúan en combinación en los límites Norte (27° S) y Sur (35° S) de la occurrencia de glaciares de escombros en la zona de precipitaciones invernales.

Los balances de sedimentos de los glaciares de escombros, los cuales revelan las tasas de denudación holocenas, y el uso de los glaciares de escombros como indicadores del permafrost, entregan conocimientos adicionales acerca del ambiente altoandino de Chile Central.

Palabras claves:
Glaciar de escombros, modelamiento estadístico, geomorfometría, Andes

Acknowledgements

First, I would like to thank my Chilean friends and companions, who cordially received me when I first arrived at Pontificia Universidad Católica de Chile in March 1998, and who were very helpful: Muchísimas gracias a María Constanza Cabrera y su familia, y a Alvaro Zúñiga! I am also very grateful to him and to the students Sebastián Grau, Esteban Sagredo, Magdalena García and Cristián Vásques from Santiago and Tobias Wittkopf and Andreas Lamm from Berlin for their collaboration in venturesome field work.

The invaluable logistic support by Prof. Dr. Belisario Andrade and the Instituto de Geografía at Pontificia Universidad Católica de Chile, Santiago, is gratefully acknowledged. Thanks to Prof. Dr. Hilmar Schröder for giving me the opportunity of carrying out this work while I was employed as scientific assistant. I am furthermore grateful to Dr. Dario Trombotto and Pepe Hernández (Instituto Argentino de Nivología, Glaciología y Ciencias Ambientales, Mendoza) for their constructive collaboration and the opportunity of expanding the statistical analyses to the Andes of Mendoza.

Since the present dissertation would be completely different without access to the complete coverage of air photos of the 1950s, I am very grateful to the Centro de Investigación de Recursos Hídricos at the Dirección General de Aguas in Santiago the unbureaucratic support that they gave me. Valuable data is also due to Rachel Bernardin (Ondeo, Aguas Andinas), Alejandro Contreras (Compañía Minera Disputada de Las Condes), and the Servicio Geológico Minero Argentino at Mendoza. The access permits issued by GASCO S. A. and Aguas Andinas for working on their ground are gratefully acknowledged.

Regarding my work in Germany, I am very indebted to Ronny Poppschötz for his comments on the manuscript and for countless discussions. Thanks to Prof. Donald Friend (Minnesota State University) for kindly revising the English and for encouraging discussions. I am very grateful to Prof. Wilfried Endlicher for his support in a decisive phase of the work.

The present work has greatly benefited from free access to ASTER and especially SRTM data provided by NASA and USGS, and from the capabilities of the open-source data analysis environment R. Thanks to Olaf Conrad (University of Göttingen) for providing the terrain analysis software SAGA.

Financial support for field work is due to the German Academic Exchange Service (DAAD).

Last but not least, many thanks to Bettina, Yannick and Saskia for their understanding and support!

Contents

List of Figures

List of Tables

Chapter 1

Introduction

1.1 Motivation and goals

Rock glaciers (figure 1.1) are both complex landforms and unheralded stores of frozen water. Although they constitute important mesoscale landforms in the Central Chilean High Andes (figure 1.2) and contain a significant amount of ground ice, very little is known about their actual distribution and significance in the region until now. Furthermore, the semi-arid Andes are among the mountain areas with greatest rock glacier density and best rock glacier development worldwide (Brenning, 2004a).

Therefore, both geomorphological curiosity and the practical need of a better knowledge of this store of water provided the impetus to study the vast periglacial environment of Central Chile and in particular of the Andes of Santiago, and for focusing on rock glaciers.

The motivation and goals of this work are summarized as follows:

- Why are rock glaciers so abundant in Central Chile? Where are they best developed? Which morphographic controls favor or inhibit rock glacier formation?
- How abundant are rock glaciers in quantitative terms? What amount of water is stored within these bodies of ice-rich permafrost?
- Which are the least favorable places where rock glaciers can be found? How do they compete with glaciers? How is rock glacier distribution affected by extreme aridity?
- What do rock glaciers tell us about their environment? Of which order are rock glacier ages and denudation rates in their talus shed? What is the relation between rock glacier distribution and (palaeo-) climate in the study area?

In summary, the goals of this work are to analyze the distribution of rock glaciers in the Andes of Central Chile as related to climate and topography, and to draw conclusions on their geomorphological and hydrological importance. The study area is limited to the Chilean Andes with winter precipitation regime, i. e. it lies south of the South American Arid Diagonal, which crosses the Andes at $\sim$24–25° S (figure 1.2).

Figure 1.1: Rock glaciers in the upper Yeso valley, Andes of Santiago, between ∼3250 and 3500 m a. s. l. Photograph: 28 Mar 2004.

1.2 Methodological overview

Geomorphological and glaciological research in high mountain areas follows a variety of approaches: On one hand, at local scales, technically demanding quantitative studies have gained importance compared to traditional approaches such as geomorphological mapping and genetic interpretation, though numeric results are mostly of local significance. (Cf. Ahumada 1992; Corripio and Purves 2003; Kull et al. 2002; Paskoff 1970; Rivera and Casassa 1999; Scholl 2002; Schröder and Makki 1998; Schrott 1994). On the other hand, regional scale investigations are often rather descriptive and mainly contain qualitative interpretations (cf. Fox and Strecker, 1991; Garleff, 1977; Jenny and Kammer, 1996; Schröder, 1999). Quantitative studies on a regional scale, in contrast, are often inventory-like (Bishop et al., 2004; Corte and Espizua, 1981; Marangunic, 1979) and aim at obtaining a "complete" data base of certain phenomena. This "complete" numeric coverage paradoxically often seems to obstruct the extraction of further knowledge, since it is difficult to recognize regularities within huge amounts of data embedded within a complex environment.

Based on these observations, and taking into account the lack of detailed local rock glacier research in the Chilean Andes, the methodological approach chosen for this work is twofold: Locally, geomorphological mapping and interpretation aim at enhancing the rock glacier knowledge base of the Chilean Andes and exploring the periglacial environment of selected catchments. Complementarily, on a regional scale, a statistical sampling and modelling approach is used to derive quantitative information on high-Andean geomorphology.

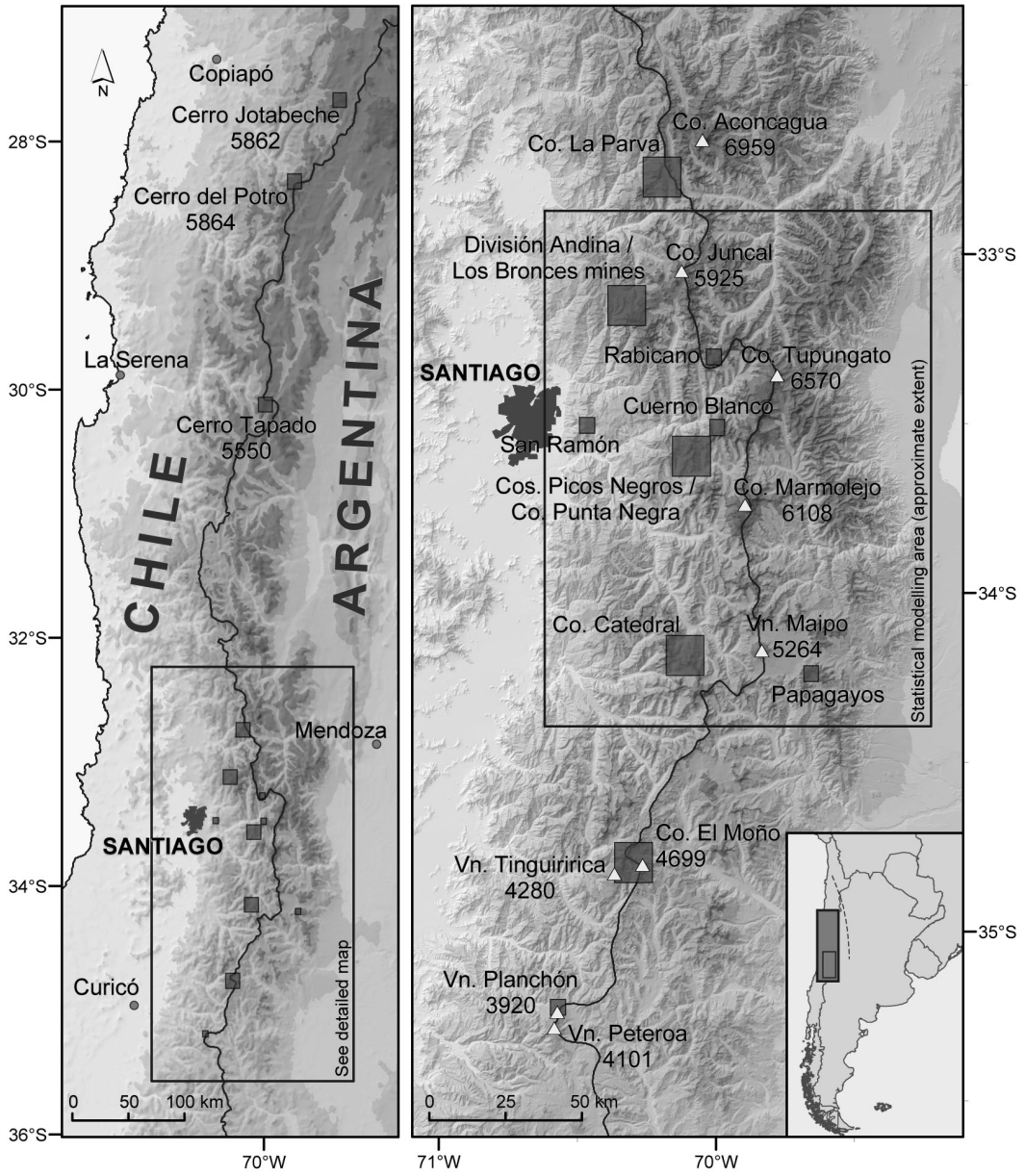

Figure 1.2: Overview of the Central Andes, the Andes of Santiago and Mendoza and the areas studied in detail. The small map of southern South America shows the position of the South American Arid Diagonal as a dashed line. The map is based on SRTM topography and ESRI World Basemap Data.

The different goals and methods of this work are reflected in three different scales used, which are visualized in figure 1.3. The methods are briefly introduced in the following sections; further details and references are given in each chapter's methodological section.

1.2.1 Geomorphological mapping and quantification

Twelve areas in the Andes of Central Chile were studied by means of geomorphological field mapping, field reconnaissance, and the interpretation of aerial photographs (figure 1.2, table 1.1). The study areas were selected in order to represent different climatic regions, but similar topographic conditions. Several areas of particular theoretical or applied interest (huge rock glaciers; impact of mining on rock glaciers) were also included. The scale of the resulting geomorphological maps, all of which are in Appendix C, ranges between 1:25 000 and 1:50,000, depending on the available field data.

Rock glaciers and relevant glacigenic mesoscale features are the main objects of interest within the present work. Information on small periglacial forms such as patterned ground was included when available, but the size of the mapped catchments, the limited time in the field, and logistic constraints in high mountain terrain made it impossible to present a complete survey and analysis of their distribution.

Topographic sequences of geomorphological forms and processes, and altitudinal belts in the sense of idealized representations of these sequences, were derived from the distribution of rock glaciers and other geomorphological phenomena.

The altitudinal distribution of rock glaciers, glaciers and thermokarst areas was quantified in order to assess the relative geomorphological and hydrological importance of these features. (Compare section 1.4.2 for remarks on the use of the term "thermokarst area" in this work.)

1.2.2 Statistical sample survey and statistical estimation

According to Raj (1968), "it is a curious fact that the results from a carefully planned and well-executed sample survey are expected to be more accurate (nearer to the aim of the study) than those from a complete census that can be taken." This is due to the fact that quality control is much easier to implement on a small amount of data, and statistical methods may be applied in order to get error estimates.

In the context of the present work, this statistical experience implies that complete, inventory-like data is not needed to determine the distributional characteristics and patterns of a particular landform type. In fact, instead of maps or inventories, a finite, well-formed (random) sample should be sufficient for this purpose on a regional scale.

Turning to the peculiarities of mountain areas and relief-dependent data, it is important to control the effects of unbalanced distributions, especially of elevation, aspect and slope. This can best be achieved by means of stratified random sampling of observational sites for statistical modelling.

Following that approach, a stratified random sample of high-elevation locations was generated based on a digital elevation model (DEM) and evaluated using aerial photographs (Appendix A). Stratification was implemented with respect to elevation and aspect classes.

This random sample of land surface

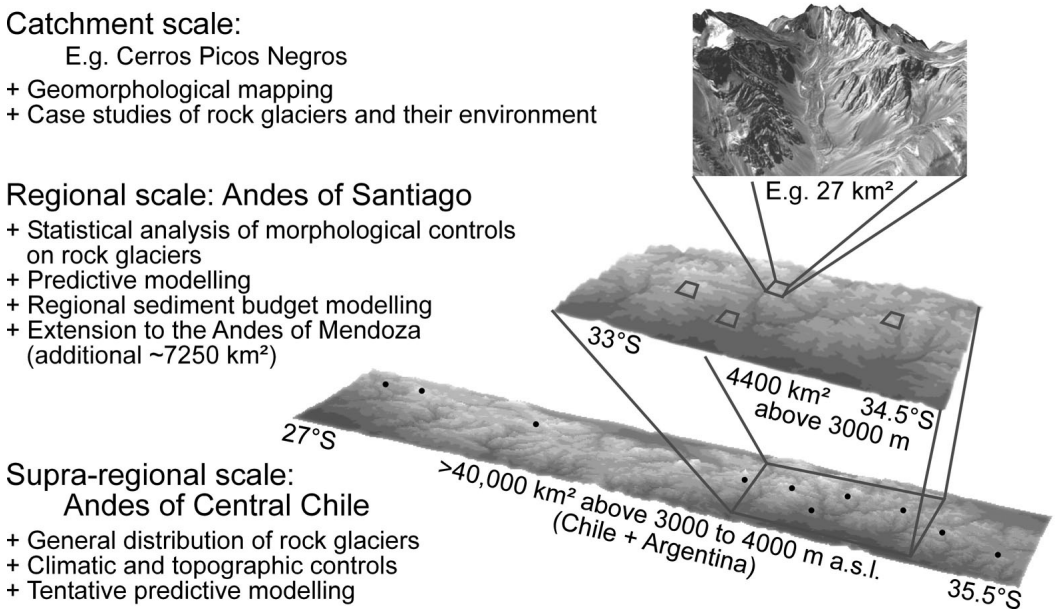

Figure 1.3: Overview of the scales and main methodological approaches used in this work.

Area	Latitude	Max. alt. [m a. s. l.]	Field mapping	Field reconnaissance	Air photo interpretation	Quantification
Cerro Jotabeche	27° 42′ S	5862		X	X	
Cerro del Potro	28° 23′ S	5864			X	X
Cerro Tapado	30° 08′ S	5550		X	X	X
Cerro La Parva	32° 45′ S	4831	X		X	X
Los Bronces	33° 09′ S	4910			X	
Cerro San Ramón	33° 29′ S	3253		X	X	
Co. Cuerno Blanco[a]	33° 31′ S	5038			X	
Cerros Picos Negros	33° 33′ S	4542	X		X	X
Cerro Punta Negra	33° 34′ S	4655		X	X	
Cerro Catedral	34° 12′ S	4765	X		X	X
Cerro El Moño	34° 45′ S	4699	X		X	X
Volcán Planchón	35° 13′ S	3920		X	X	

Table 1.1: Overview of the areas studied in chapter 2, and of methods used in each area. Compare the overview maps shown in figure 1.2. Remark: [a] Together with the Cuerno Blanco rock glacier, two Argentinian features (at Morro Rabicano and in the Papagayos valley) are discussed.

observations was used for the statistical estimation of the altitudinal and directional distribution of rock glaciers and other relevant features (section 3.1). Furthermore, simple assumptions of average ice contents served to estimate rock glacier water equivalence (section 3.1.2).

The sampling and estimation procedure was first designed for and applied to the Andes of Santiago in 2003 (Brenning, 2004a, 2005a). In fact, neither a reasonable estimate of the number of rock glaciers nor of their total area and volume were available before this work. In 2004, the study was extended to the Argentinian side of the Andes at the same latitude in order to cover the wide range of climatic conditions on both sides (Brenning et al., 2005).

To the author's knowledge, random sampling of surface points and statistical estimation techniques have seldom been applied in the field of mountain geomorphology before the author's work (Brenning, 2004a, 2005a).

1.2.3 Logistic regression modelling

Logistic regression models are well-established generalized linear models for the analysis and prediction of binary data. More specifically, logistic regression is capable of relating the presence versus the absence of a feature (e. g. success versus failure of medical treatment) to some explanatory variables, and it predicts probabilities of the presence of this feature based upon known explanatory variables.

Logistic regression models were applied in order to discriminate between rock glacier, glacier and other areas based upon relief parameters as derived from DEMs (section 3.2). The goal of this approach is to recognize morphometric parameters that control rock glacier distribution, and to determine "optimum" conditions of rock glacier formation within the given environment.

To the author's knowledge, logistic regression models have not been applied within rock glacier or glacier studies before the work of Brenning (2004a).

1.2.4 Rock glacier and site characteristics

It is important to note that both statistical estimation and logistic regression modelling refer to rock glaciers as pointwise (or pixelwise) presence–absence information, not to the population of rock glaciers as objects. The sample of rock glaciers obtained in the mentioned stratified random sampling procedure can be used for further analyses of the rock glacier population (section 3.3).

First, morphographic attributes describing the sample of rock glaciers are obtained manually and computationally, and their distribution is statistically evaluated and visualized. The results include the estimated rock glacier size distribution, an estimated total number of rock glaciers, and a more detailed characterization of the geomorphological niche of rock glaciers.

1.2.5 Modelling rock glacier sediment budgets and advance

A simple approach towards the estimation of average talus production in mountain environments is based upon sediment budget models that assume a closed debris-transport system. Three alternative model formulations are applied to a sample of rock glaciers in order to assess rock glacier ages, talus production, and rates of rock glacier advance (Chapter 4).

1.2.6 A note on the software used

Though "spatial modelling" is in geography often associated with "GIS modelling", Geographical Information Systems (GIS) do not offer the same flexibility for data analysis as statistical programming environments. Most of this work's quantitative analyses were therefore performed within the open-source data analysis environment R, versions 1.6.1–2.0.1 (R Development Core Team, 2005), which is increasingly being applied in connection with GIS (Bivand, 2000; Brenning and van den Boogaart, 2001; Grunsky, 2002). ArcGIS 8.1 was used for data base management and visualization purposes, and the terrain analysis software SAGA (written by O. Conrad, Göttingen; Olaya, 2004) for computing geomorphometric parameters from DEMs.

1.3 An overview of the study area

The study area covers a wide range of climatic, topographic and geological characteristics both in longitudinal and in meridional direction (figure 1.2). They culminate both topographically and demographically in the area of Santiago (33.5° S) and Mendoza (33° S, Argentina). These cities depend heavily on meltwater runoff from the Andes, with up to 60 % of Santiago's water supply being provided by the El Yeso reservoir at 2475 m a. s. l. (Aguas Andinas, 2003[1]).

1.3.1 Geology and topography

The Andes in the study area are situated at an active continental margin at which the denser Pacific Nazca Plate is subducted beneath the South American Plate. The Andes were mainly formed by tectonic uplift, with parallel faulting predominating over folding (Zeil, 1986). They are therefore generally divided into several chains running parallel in meridional direction. The Southern Andes (south of 33° S) are delimited in westward direction against the Chilean Longitudinal Depression by a fault (in the Andes of Santiago, the Ramón or Pocuro fault), and are dominated by one main range. In contrast to this, north of 33° S the Precordillera constitutes a significant eastern mountain chain on the Argentinian side. Starting at the northern edge of the study area, from 27.5° S northward a basin–range topography with largely internal drainage hosts salt lakes (*salares*) within tectonic depressions and announces the graben structure of the Altiplano, which characterizes the Atacama desert.

While Quaternary volcanism is almost absent in the Andes between 27° and 33° S, a zone of more than 5000 m high stratovolcanoes starts at the latitude of Santiago and Mendoza and is related to the strong tectonic uplift (González-Ferrán, 1994; Zeil, 1964, 1986). Volcanism becomes a dominant landforming process, even during the Holocene, south of 35° S (González-Ferrán, 1994; Naranjo and Haller, 2002; Naranjo et al., 1999).

The Andes of Santiago are composed of a basement of Jurassic to Early Tertiary age, intrusive units and Quaternary stratovolcanoes (figure 1.4). The basement consists of marine and continental sediments and andesitic to rhyolitic volcanic rocks with intercalated pyroclastic series (Klohn, 1960; Zeil, 1986). Its vertical extent exceeds 8000 m.

[1] URL: `http://www.aguasandinas.cl`

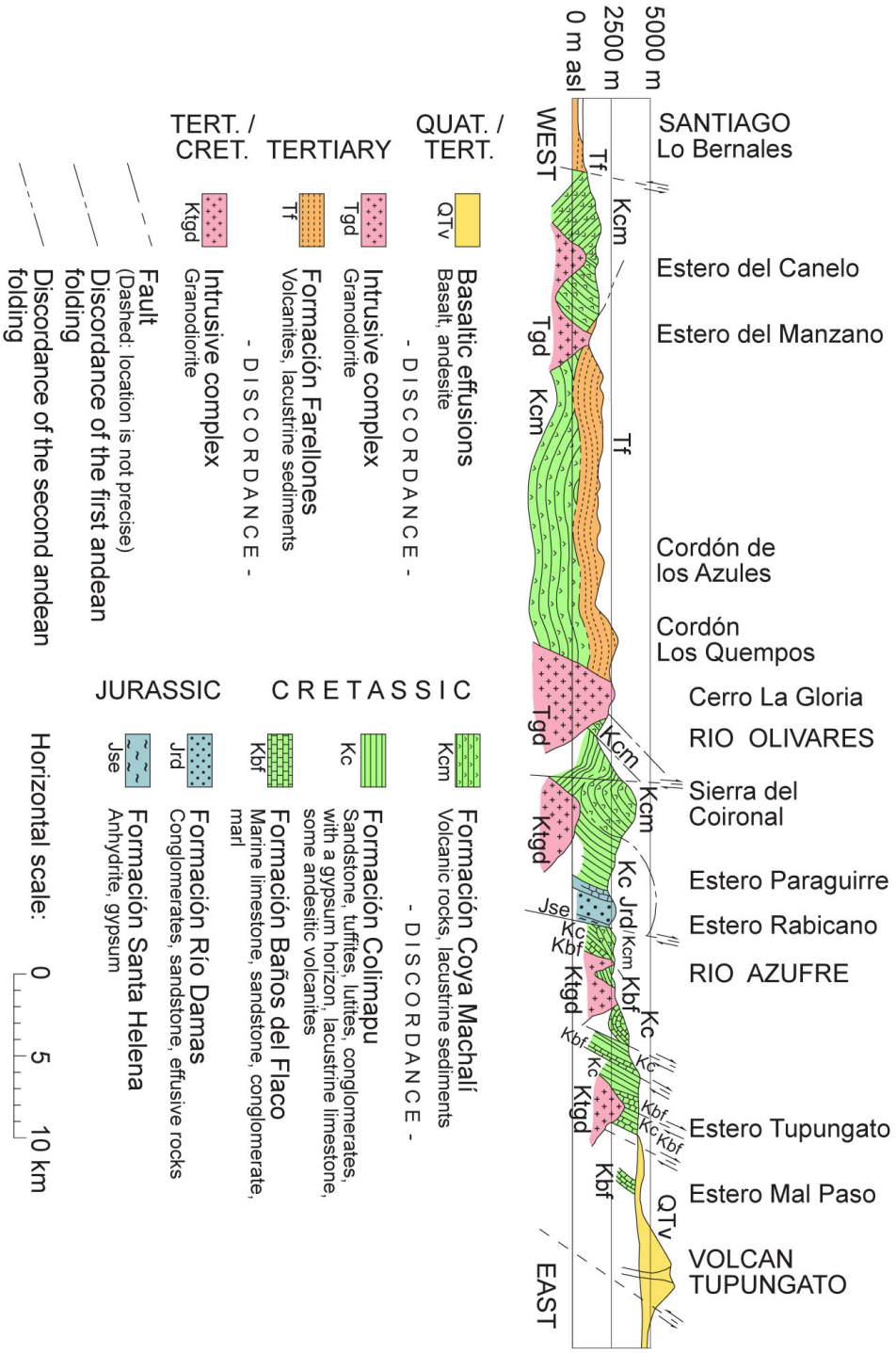

Figure 1.4: Geological cross-section of the Andes of Santiago (Lo Bernales – Tupungato). After Klohn (1960).

Figure 1.5: The High Andes of Santiago (and Mendoza), seen from 32° S looking southwards, with Cerro Aconcagua (left, 6959 m), Volcán Tupungato (center, 6570 m) and in the background further summits of the main range. Photograph: 4 Mar 2004.

These strata are weakly folded and divided into lifted and subsided blocks. The Oligocene and Miocene were characterized by the planation of the basement (Klohn, 1960). The time from the Jurassic to the middle Tertiary includes three intrusive periods.

Strong uplifting since the Pliocene is responsible for the formation of the Andes of Santiago. Its vertical magnitude can be observed at the Ramón fault just east of Santiago with an impressive vertical displacement of more than 2000 m. The volcanic edifices of Tupungatito, San José, Maipo and other stratovolcanoes in the area go back to the same period and are composed of basaltic and andesitic volcanics.

The topography of the Andes of Santiago reflects their geological history as described above (figures 1.4 and 1.5): The western parts are mainly characterized by relatively low relief between ∼2000 and 3250 m a. s. l., corresponding to a Tertiary planation surface that has been incised during the Quaternary. Towards the east, summit elevations rise rather suddenly to about 4500 m and reach more than 5500 m a. s. l. at the continental divide, which marks the border between Chile and Argentina. The highest summits of the main range are Cerro Tupungato (6570 m), Nevado de los Piuquenes (6019 m) and Cerro Marmolejo (6108 m). However, several important mountains are situated away from the main divide, for instance Cerro Altar (5180 m), which is linked with the main range at the Node of Juncal, and Cerro Aconcagua (6959 m, Argentina), the highest mountain of the Americas (figure 1.5).

The geologic structure and petrographic composition of the Andes of Santiago have several consequences for weathering intensity and slope development that are relevant for rock glacier formation. In the Western Andes, valleys are cut into almost horizontal strata, which are often reflected by a terrace-like subdivision of the valley slopes due to differential weathering and de-

nudation. The main range, in contrast, presents a more varied mosaic of folded and lifted blocks of different lithology. This geological mosaic, which in addition has been more intensively eroded by Pleistocene glaciers, therefore also shows a greater variety of morphographic conditions, though many valleys run in a north–south direction. Furthermore, the weathering resistivity of young volcanics of the highest massifs is greater than that of the Mesozoic stratified partly sedimentary rocks (including gypsum).

Although most of the highest summits are concentrated within the Andes of Santiago, altitudes above 5000 m a. s. l. are also common in the northern part of the study area between 30° and 27° S (e. g. Nevado Jotabeche, 27° 42′ S, 5862 m; Cerro del Potro, 28° 23′ S, 5864 m; Cerro de las Tórtolas, 29° 48′ S, 6160 m). In contrast to this, most summit elevations in the Chilean Andes between 30° and 32° S are below 4500 m a. s. l. South of 34.5° S, maximum elevations also decrease; Volcán Peteroa (35° 17′ S, 4101 m) is one of the southernmost summits of South America that surpasses 4000 m a. s. l.

1.3.2 Climate and vegetation

The study area between 27° and 35.5° S is characterized by a southward transition from arid to semi-humid climates with a strong winter precipitation maximum (Romero, 1985). This pattern is produced by the interplay of the persistent subtropical east Pacific anticyclone and maritime polar air masses in the south Pacific (Rumney, 1968; Weischet, 1996). The Pacific anticyclone, centered about 1500 km west of northern Chile, weakens and moves towards the Equator in winter, allowing polar air masses to move northward. Migrating cyclones from the south Pacific can therefore reach lower latitudes and provide winter precipitation. This seasonal pattern is superimposed by El Niño Southern Oscillation (ENSO) events, which increase precipitation in El Niño periods and often reduce it in subsequent La Niña (or Anti-Niño) years in Central and Northern Chile (Caviedes and Waylen, 1991; Enfield, 1989; Escobar et al., 2000). Furthermore, precipitation patterns show a great inter-annual variability (Caviedes and Waylen, 1991; Waylen and Caviedes, 1990).

North of the study area and also on the eastern side of the Andes, summer precipitation mainly of tropical convective origin plays an increasing role (Vuille, 1996). The transition between the summer and winter precipitation regime coincides with the South American Arid Diagonal, which crosses the Andes in the area of Volcán Llullaillaco (24° 43′ S, 6739 m) (Messerli et al., 1992; Richter and Schröder, 1996; Schröder and Schmidt, 1997).

Lowland vegetation around Santiago is a Mediterranean scrub woodland, although sclerophyllic forests were more widespread prior to human settlement in the region. While irrigation embraces vast areas in the Longitudinal Depression around Santiago, north of Río Aconcagua (32° S) it is restricted to river terraces. These river oases are surrounded by steppe vegetation of the semi-arid to arid Chilean *Norte Chico*. The transition to the Atacama desert of the *Norte Grande* is finally found at the latitude of Vallenar between 28° and 29° S (Weischet, 1970).

The climate parameters are depicted on a regional scale in figure 1.7 and in more detail for the Andes of Santiago in figure 1.6.

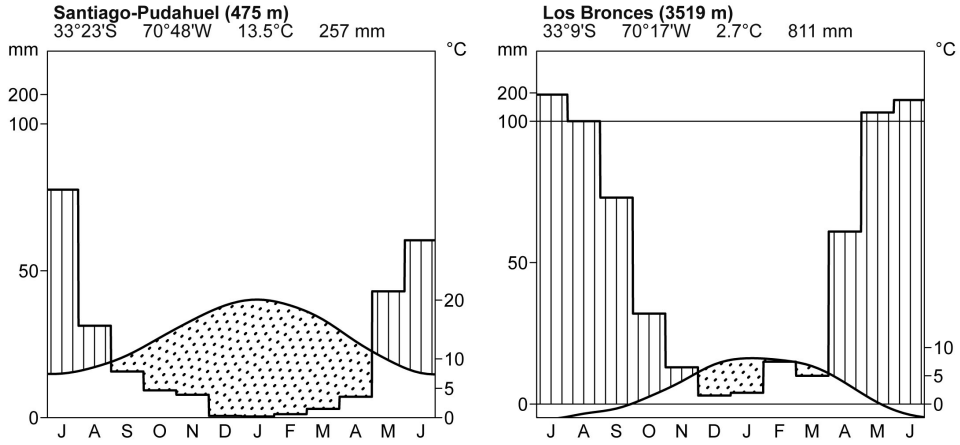

Figure 1.6: Mean monthly air temperature and precipitation in the Andes of Santiago and their forelands.
Data from Los Bronces are from A. Contreras (Disputada de Las Condes; temperature: 1980–2001; precipitation: 1980–1998).

The Andes of Santiago

The modern 0°C isotherm of mean annual air temperature (MAAT) in the Andes of Santiago is situated at ∼3600 m a. s. l. This estimate is based upon data from Embalse El Yeso (figure 1.6, MAAT +8.4°C at 2475 m a. s. l.; 1962–2000; source: DGA), Cristo Redentor (MAAT −1.5°C at 3830 m a. s. l., 1941–1983; Leiva et al., 1989) and El Infiernillo (−5.3°C at 4343 m a. s. l. in 1969; Puig and Valdivia, 1977), which yields a lapse rate of ∼0.7°C per 100 m. Data from Los Bronces mine (figure 1.6, MAAT +2.7°C at 3519 m a. s. l., 1980–2001; Disputada de Las Condes) and an estimation made by Lliboutry (1986) (MAAT 0°C at 3700 m a. s. l.) suggest significantly warmer conditions in the same area.

At Los Bronces (3519 m a. s. l.), more than 95 % of the precipitation is solid; more than two-thirds are concentrated in winter between May and August. Above 2000 m a. s. l., annual precipitation sums vary around 1000 mm of water equivalent (Ereño and Hoffmann, 1978) subject to high spatial and inter-annual variability. However, technical limitations to precipitation measurements under high-mountain conditions must be kept in mind (cf. Dessens and Bücher 1997).

Between 32.5° and 35.5° S, approximately, a strong southward increase in mean annual precipitation can be observed (Ereño and Hoffmann, 1978; Romero, 1985). Although climatic data are scarce, it can be deduced that this southward change in precipitation is in the order of a factor of 3 to 4 in this area. Regarding the availability of these amounts of precipitation for geomorphological processes and vegetation, high sublimation and evaporation rates have to be taken into account in comparison with Southern Europe, where Mediterranean climates are found at higher latitudes than in Chile.

The altitudinal zonation of vegetation in the Andes of Santiago has been described in detail by Muñoz et al. (2000). The vegetation above 2000 m a. s. l. may be divided into an Andean matorral or shrubland (2000–2700 m a. s. l.), a high-Andean steppe

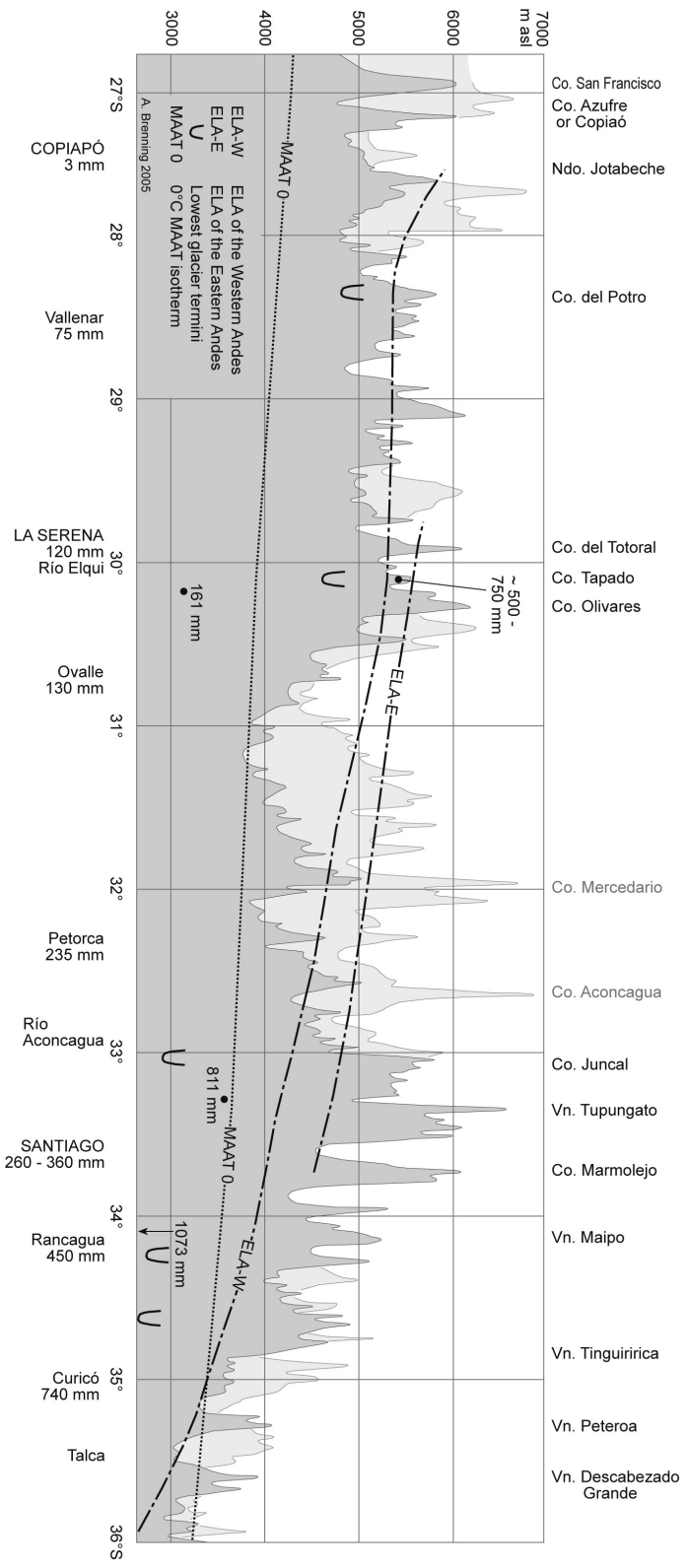

Figure 1.7: A north–south profile of modern climate and glacierization in Central Chile. The black and gray relief outlines represent maximum elevations in the Chilean and Argentinian Andes, respectively. Sources: Partly based on Lliboutry (1956) and Lliboutry (1999), with additional data from Escobar et al. (1995); Toledo and Zapater (1991); Veit (1991) and Kull et al. (2002).

Figure 1.8: The terminus of the debris-covered Pirámide glacier at ∼3200 m a. s. l. in the upper Yeso valley, Andes of Santiago. The ∼7 km long completely covered glacier originates from a huge south-exposed cirque at Cerro Hoff (33° 32′ S, 5170 m) and Cerro Pirámide (33° 32′ S, 5484 m). Note the stratification of the (essentially sedimentary) glacier ice especially in the upper parts of the front. Photograph: March 1999.

belt of gramineae, subshrubs and cushion plants (2700–3300 m; mean density 25 %), and above 3300 m a. s. l. a high-Andean desert belt of gramineae and cushion plants (Muñoz et al., 2000). The latter is characterized by densities below 10 %; the actual upper limit of vegetation is often lowered to about 3000 and 3300 m a. s. l., depending on the substratum and on the governing geomorphological processes.

1.3.3 Late Quaternary glaciations

The extreme aridity around the South American Arid Diagonal (∼24°–25° S) is responsible for a potential snow-line altitude that surpasses most summit elevations in the area. Therefore Volcán Llullaillaco (24° 43′ S, 6739 m), which hosts only a penitentes firn field above 6000 m a. s. l., is at present the highest non-glacierized mountain on Earth (Schröder and Makki, 1998).

In contrast, the topographic culmination of the Andes of Mendoza and Santiago under semi-arid climatic conditions produces a considerable modern glacierization, but glacier sizes do not reach magnitudes known from the Alps (compare figure 1.5). Many glaciers in the semi-arid and semi-humid Andes are debris-covered in their ablation areas (figure 1.8, Lliboutry, 1956, 1999).

The modern equilibrium line altitude (ELA) of glaciers in the study area behaves concordantly with the meridional changes in precipitation and temperature (figure 1.7). It easily surpasses 5000 m a. s. l. north of 30° S, and drops to 4300–4400 m around 32.5°–33° S and to about 3200 m a. s. l. at 35° S (Hastenrath, 1971; Kull et al., 2002; Lliboutry, 1956, 1986, 1999). The northern glacier of Cerro Juncal (5925 m; 33° 03′ S) constitutes the northernmost valley glacier of the Chilean Andes south of the Arid Diagonal of South America.

In the western Andes of Santiago, the 25-year mean ELA at the (small) Echaurren Norte glacier (33° 35′ S, 70° 08′ W) is situated at 3800 m a. s. l., but it fluctuates between 3600 and 4000 m depending on the amounts of precipitation and espe-

cially on ENSO events (Escobar et al., 2000, 1995). Figure 1.9 shows the orographic effects on the extent of modern glaciers in a cross-section through the Andes of Santiago and Mendoza.

South of the Andes of Santiago, the divide between the Maipo (Andes of Santiago in the strict sense) and Cachapoal catchments around 34° 15′ S constitutes a rather marked step within the regional pattern of glacier extent, since significant tongue glaciers such as the Cachapoal glacier (length 14 km) are found south of this divide.

At the Cachapoal glacier, Röthlisberger (1986) identified glacier advances at the beginning of the 14th century and around 1860. More generally, two cool–moist pulses of the so-called Little Ice Age (LIA) have been reported for Central Chile and Patagonia around AD 1400–1600 (possibly 1300–1700) and during the 19th century (Cioccale, 1999; Jenny et al., 2002; Villagrán and Varela, 1990; Villalba, 1994a,b). During the 20th century, temperatures rose in Central and Northern Chile by about 1–2°C (Rosenblüth et al., 1997).

The Pleistocene glaciations of the Andes of Santiago have been studied by Borde (1966); Brüggen (1946); Caviedes (1972) and Caviedes and Paskoff (1975). According to these works, the maximum extent of Pleistocene glaciations would either have reached the Andean foreland (in the Maipo catchment, at about 700 m a. s. l.), or San Alfonso (1100 m a. s. l.) in the lower Cajón del Maipo. However, since G. Abele convincingly identified several of the former "moraines" as being huge mega-landslides or debris-flows (Abele, 1981, 1984), the chronology and extent of Pleistocene glaciations in the Maipo and Aconcagua valleys are not sufficiently known.

1.4 Periglacial high-mountain environments

Cold non-glacierized environments of the polar regions and mountain areas present distinct geomorphological phenomena that are related to frozen ground and its freezing and thawing (French, 1976; Washburn, 1973; Weise, 1983). The geomorphological characteristics of these glacier-free cold regions are referred to as being "periglacial"; rock glaciers are a characteristic landform of the periglacial environments especially of dry and continental mountain areas (Barsch, 1996a; Gorbunov, 1983; Wahrhaftig and Cox, 1959).

1.4.1 The periglacial environment and periglacial belt

Periglacial processes are due to seasonal or diurnal freezing and thawing of the ground, such as cryoturbation and gelifluction (Washburn, 1973). Periglacial environments are consequently defined as areas where frost action and/or frozen ground are geomorphologically effective phenomena (Karte and Liedtke, 1981; Troll, 1947). The periglacial environment is not restricted to permafrost areas, nor is it necessarily adjacent to glacial environments, in contrast to the literal meaning of the term (Greek *peri* = around; Latin *glacial* = related to the ice).

As a consequence of the hypsometric decrease of temperature, modern periglacial environments exist in many high-mountain regions of all latitudes. These periglacial zones however present a manifold of conditions and processes that are also characteristic of non-periglacial mountain envi-

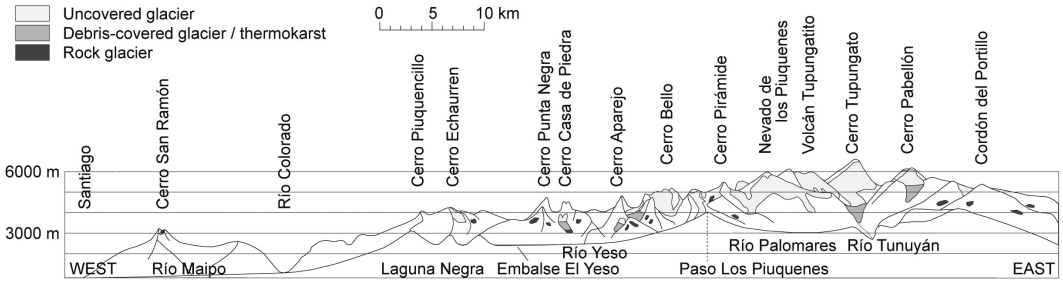

Figure 1.9: South-exposed glaciological cross-section through the Andes of Santiago. The westernmost glacier is Glaciar Echaurren (size 0.4 km^2, length 1.2 km; Vergara and Escobar, 2003), which is monitored by Dirección General de Aguas (Santiago). The borderline between Chile and Argentina passes through Paso Los Piuquenes, Nevado de los Piuquenes and Cerro Tupungato. The figure has been modified by Brenning et al. 2005 based on Lliboutry (1956, 1999), who presented a rock glacier-free version.

ronments. The importance of gravitational denudation processes associated with steep slopes and tectonic uplift, as well as the imprint of past glaciations on the landscape and its sediments have to be emphasized (Barsch and Caine, 1984). This contributes, on one side, to the great variety of geomorphological form association within and beyond the periglacial altitudinal zone; on the other side, it makes it difficult to delimit a periglacial altitudinal zone or periglacial belt. This becomes an important issue in semi-arid and arid environments, where a timberline does not exist and the snow-line is variable (Barsch, 1983, 1986).

1.4.2 Rock glaciers

Active rock glaciers are the geomorphological expression of creeping mountain permafrost (Barsch, 1996a; figure 1.1). They consist of a debris–ice mixture that physically deforms and slowly moves downslope or downvalley, developing a tongue-shaped or lobate landform with a front scarp and characteristic surface structures like furrows and ridges as rheological expressions.

Rock glaciers that stopped moving but still contain ice are called inactive, and the sediment body that remains after a rock glacier has melted out is called a relict (or fossil) rock glacier. Active and inactive ones are also referred to as "intact" rock glaciers (Barsch, 1996a) .

Inactivity may be caused by climatic or dynamic factors. In the former case, the seasonally unfrozen block mantle has grown as a consequence of permafrost degradation. A rock glacier may in contrast also become inactive in permafrost areas after entering into flat terrain (dynamic inactivity). While the front scarp of active rock glaciers generally reaches inclinations between 35° and up to 45°, inactive ones show front slopes at or below the angle of repose with a smooth convex transition upward to the rock glacier's surface. Relict rock glaciers can be recognized from their collapsed appearance and irregular surface structure (Barsch, 1996a,b; Ikeda and Matsuoka, 2002). These criteria are however sometimes ambiguous (cf. Ikeda and Matsuoka 2002).

In this work, rock glacier terminology and further classification criteria follow Barsch (1996a)

Rock glaciers contain on the aver-

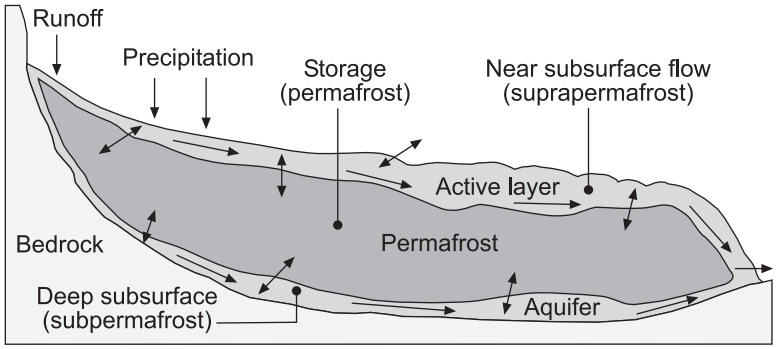

Figure 1.10: Rock glacier hydrology after Burger et al. (1999), redrawn.

age about 40 to 60 % of ice by volume and constitute therefore sizeable stores of water (Arenson et al., 2002; Barsch, 1977a, 1988; Corte, 1976a; Croce and Milana, 2002; Haeberli, 1985; Hoelzle et al., 1998; Schrott, 1994, 1996). Furthermore, the active layer and sub-permafrost material constitute temporal aquifers (figure 1.10; Burger et al., 1999, 1997; Haeberli, 1985). This aspect is demonstrated by streams flowing from frontal slopes of many alpine rock glaciers (Giardino et al., 1992).

After an early description of rock glaciers by Steenstrup (1883), the comprehensive work of Wahrhaftig and Cox (1959) marked a milestone in rock glacier research. In spite of this long tradition, even today there persists some (partly terminological) confusion concerning the differentiation of rock glaciers and glaciers (compare the discussion by Barsch 1996a).

The development of rock glaciers is a consequence of the enrichment of debris with percolating snow meltwater, which freezes under permafrost conditions and forms interstitial and segregation ice (Arenson et al., 2002; Barsch, 1988; Haeberli, 1985; Wayne, 1981). Massive ice —sometimes buried surface ice (Guglielmin et al., 2004)— may add to the predominant component of congelation ice (Haeberli, 2000). Rock glaciers are therefore of periglacial origin. They may form out of talus accumulations (talus rock glaciers) or morainic debris (debris rock glaciers). Due to the association of debris rock glaciers with moraines and similarities with debris-covered glaciers, theories of a glacigenic origin of rock glaciers have also been developed (e. g. Whalley, 1974; Whalley et al., 1994); cf. Barsch 1996a for a discussion of the topic.

In the semi-arid Andes, it is important to distinguish rock glaciers from other ground ice bodies (figure 1.11). There exists a continuum of forms between "vital" debris-covered glaciers and stagnant buried "dead" ice bodies. Stagnant massive ice bodies in general are in many cases subject to a steady decay unless they are protected under permafrost conditions by a thick, isolating debris cover. Such stagnancy and decay can be recognized from widespread melt-out ponds ("thermokarst") and an irregular surface topography (Clayton, 1964; Haeberli, 2000; Wayne, 1981). In the semi-arid Andes, thermokarst affects mainly huge massive-ice bodies of glacigenic origin (compare section 2.3.2 and Brenning 2003). In contrast to these, rock glaciers present a well-defined frontal slope and a characteristic surface topography of furrows and ridges. In the present work, "thermokarst areas" are operationally distinguished from

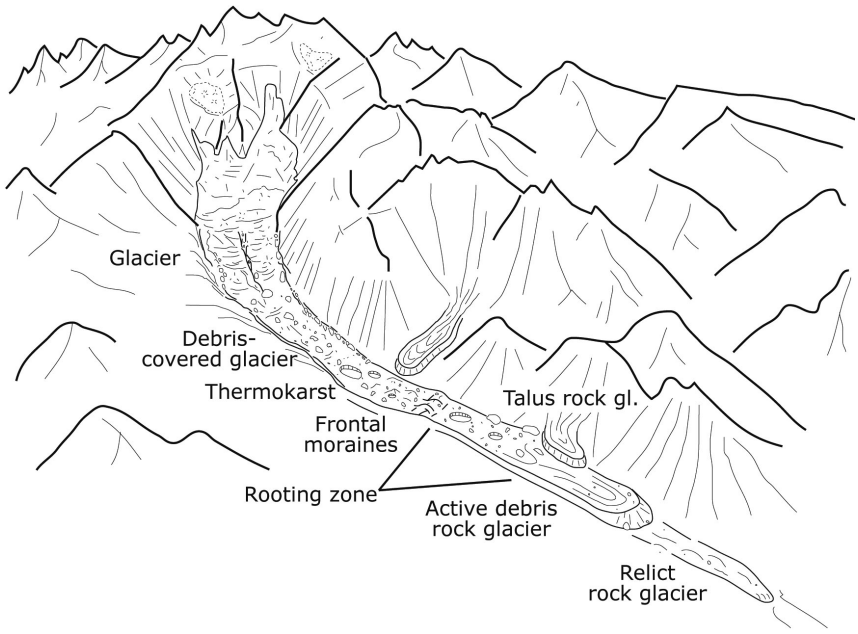

Figure 1.11: Sketch of a debris rock glacier connected to a thermokarst area and a cirque glacier, together with valley-side talus rock glaciers. Figure by D. Trombotto (in Brenning et al. 2005).

rock glaciers and debris-covered glaciers independently of the actual development of these ice masses, and though thermokarst may in principle exist on both features.

1.4.3 Mountain permafrost

Permafrost is usually thermally defined as a zone of the lithosphere whose temperatures remain below 0°C for at least two consecutive years (Barsch, 1977a; Furrer and Fitze, 1970; Haeberli, 1975; Muller, 1947; van Everdingen, 2002; Washburn, 1973). While permafrost is generally attributed to polar and subpolar climates, it exists in most high-mountain areas of the world (Furrer and Fitze, 1970; Gorbunov, 1978; Haeberli, 1975; Ishikawa et al., 2003; Jin et al., 2002; Trombotto, 2000).

The scientific investigation of permafrost has often been driven by (civilian and military) engineering problems especially in the Arctic (Washburn, 1973). Frozen ground is however also of general geographic interest because of its effects on and complex interactions with economic activities, vegetation, snow cover and geomorphological processes, especially in the context of natural hazards and a changing climate (Dramis et al., 1995; Gruber et al., 2004; Hoelzle, 1994; Keller, 1994; Smith, 1975).

Currently there exist different permafrost taxonomies: The North American usage, which has mainly been adapted to Arctic environments, considers a continuous permafrost region, of which more than 90 % is underlain by permafrost, and a discontinuous permafrost region (van Everdingen, 2002). Barsch (1978), in contrast, follows Ives (1974) as he argues in favor of a division of mountain permafrost into three zones, namely sporadic, discontinuous and continuous permafrost. He considers active rock glaciers as part of and indicators for the modern discontinuous permafrost zone of the Alps, and

uses the attribute "sporadic" for extra-zonal permafrost that exists below the lower limit of active rock glaciers and in some cases even below the timberline (Barsch, 1978; Kneisel et al., 2000) or in low-altitude ice-caves and scree slopes (Delaloye et al., 2003; Gude et al., 2003; Luetscher et al., 2003; Wakonigg, 1996).

Within this work, the general differentiation of (quasi-) continuous, discontinuous and sporadic permafrost of Barsch shall be maintained, while recognizing that only preliminary conclusions on permafrost distribution can be drawn without geophysical investigations.

In addition to rock glaciers, which have been used as indicators for discontinuous to sporadic permafrost in the semi-arid Andes (Garleff and Stingl, 1986; Schrott, 1994), in the Rocky Mountains of Colorado (Janke, 2005), and originally in the Alps (Barsch, 1978), there exists a series of other signs of mountain permafrost (cf. Haeberli 1975 for an overview in an alpine context). In particular, perennial snow patches have often been associated with permafrost in different high-mountain areas of the world (Barsch, 1977a; Furrer and Fitze, 1970; Garleff and Stingl, 1986; Haeberli, 1975, 2000; Harris and Corte, 1992; Ishikawa et al., 2003; Trombotto, 1991). They have either been treated as permafrost indicators or even as features that force the development of mountain permafrost. These relations must be reanalyzed taking into account the current knowledge of soil–atmosphere heat transfer and the climatic peculiarities of each mountain area. Long-lasting and perennial snow patches are important controls for the ground thermal regime in mountain areas. They act as effective barriers for conductive heat transfer into the ground in summer, provided that snow depths exceed 80–100 cm (Haeberli, 1973). In addition, they are excellent reflectors of incoming solar radiation, which plays a major role in the Andes of Central Chile (Schrott, 1994).

A long-lasting snow cover that disappears in autumn or late summer and that is built up again in early winter, when air temperatures already have fallen considerably, may however be more favorable for permafrost than a perennial snow cover, which inhibits ground cooling at the beginning of the cold season (Iijima and Fukui, 2003; Keller, 1994; Smith, 1975). Based on these observations, distribution patterns of long-lasting and perennial snow patches will be of further interest within the present work.

Coarse debris on the surface of rock glaciers and on talus slopes allows the penetration of cold air at night and in the colder seasons. Extra-zonal and marginal permafrost occurrences at positive MAAT have frequently been observed within talus accumulations and attributed to cold air circulation (Delaloye et al., 2003; Gude et al., 2003; Harris and Pedersen, 1998; Ishikawa et al., 2003; Keller and Tamás, 2003; Luetscher et al., 2003; Wakonigg, 1996). This effect might be of particular importance in the semi-arid Andes, where a snow-cover forms late in autumn and is less stable than in the Alps, facilitating air flow in winter.

1.4.4 Other periglacial processes and forms

At a micro-scale, periglacial processes in arid and semi-arid mountains include frost weathering, sorting, cryoturbation and solifluction, which produce angular weathering products, patterned ground, frost mounds and stone- or turf-banked terraces, among other forms (Bolch and Schröder, 2001; Lewkowicz, 1988; Lliboutry, 1961; Schröder and Makki, 1998;

Trombotto, 2000; Washburn, 1973; Weise, 1983). Depending on the size and nature of periglacial forms, they are to a varying degree related to modern and past climate and have therefore different diagnostic values for determining modern periglacial zones or inferring climatic conditions (Karte, 1979).

Relevant mesoscale forms include cryoplanation terraces and rock glaciers (Trombotto, 1991). Rectilinear slopes (see the next section 1.4.5) are also generally associated with and attributed to periglacial processes and environments (Garleff and Stingl, 1983; Stingl and Garleff, 1983), but they are not restricted to them (Höllermann, 1983).

1.4.5 Slope development

Slopes of semi-arid and arid high mountains are in general characterized by gravitational and periglacial processes of weathering and transport, while the importance of fluvial processes is limited.

Talus accumulations, including talus cones and scree slopes, are the typical gravitational deposits that are developed below steep rock faces (figure 1.12). Their development is weathering-controlled, and slope inclination is equal to the angle of repose of the deposited material. Talus cones are often associated with rockfall or avalanche couloirs in the free rock faces above them (Cooke et al., 1993).

The upper part of talus slopes, especially when situated below rock cliffs, presents favorable conditions for local snow accumulations; their meltwater may produce erosion rills and debris flows on these slopes (figure 1.12). At places with larger, convergent local contributing areas, fluvial processes gain importance. However in the semi-arid High Andes, gravitational processes still play an important role in most cases, according to grain shape and slope inclination. Mixed fluvio-gravitational cones are the resulting accumulation type at the transition between talus cones and alluvial cones (figure 1.12).

Rectilinear slopes, or, more precisely, rectilinear accumulation slopes and Richter denudation slopes, present a characteristic profile and inclinations of 27–30° (Höllermann, 1983; Stingl and Garleff, 1983; Weischet, 1969). They are the geomorphological expression of an equilibrium between talus production and transport, which is ideally independent of lithology. Dry creep and solifluction are important transport processes on rectilinear slopes (Garleff and Stingl, 1983; Veit, 1991). Rectilinear slopes may in their uppermost part present a convexity or be limited, if their development is still in progress, by a rock cliff. The footslope may be transport-limited and therefore concave.

In recently deglacierized terrain and glacier forefields, slopes are often oversteepened and consequently subject to intensified denudation including fast mass movements. These non-glacial processes that are directly conditioned by (past or present) glaciation are called paraglacial processes (Ballantyne, 2002; Ballantyne and Benn, 1994; Church and Ryder, 1972). Especially late glacial and early Holocene geomorphological activity in now glacier-free mountain areas was strongly controlled by these processes. Late- and post-glacial megalandslides such as those identified by Abele (1981, 1984) may be considered as part of the paraglacial cycle, and the catastrophic 1987 rock slide also originated from a steep headwall of a Pleistocene glacial cirque (Casassa and Marangunic, 1993; González-Ferrán, 1994).

a)

b)

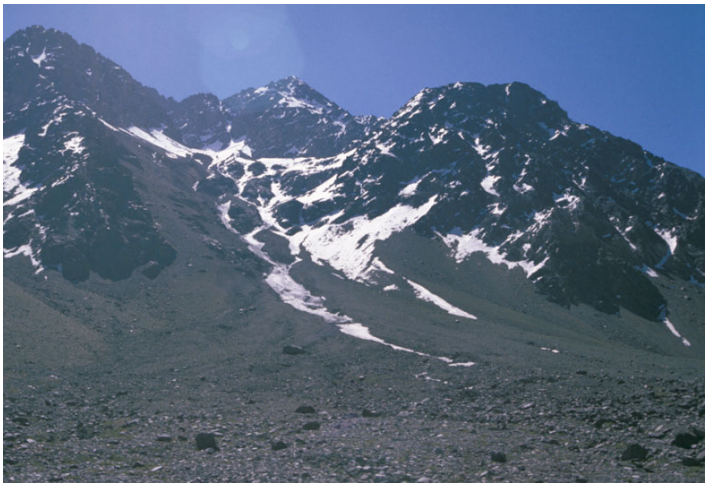

c)

Figure 1.12: Selected slopes in the Andes of Central Chile.
a) Talus cone with a debris flow; Río de las Damas valley, Volcán Tinguiririca and Cerro El Moño area. Photograph: 19 Mar 2002.
b) Fluvio-gravitational cone; Cajón de la Casa de Piedra, Andes of Santiago, 22 Dec 1998.
c) Rectilinear slope; Cajón de la Casa de Piedra, 22 Dec 1998.

1.5 Periglacial environments of Central Chile: the knowledge base

Before entering into the main part of this study, a look back into the history of periglacial research in the Andes of Central Chile is necessary.

Although Charles Darwin must have seen several rock glaciers in March 1835 on his way from Santiago to Mendoza through the Yeso valley and across the Paso Los Piuquenes (figure 1.9), the French glaciologist Louis Lliboutry is, to the author's knowledge, the first scientist to describe these landforms in Chile in the 1950s (Lliboutry, 1953, 1955, 1956). In this early period of rock glacier research, Lliboutry already recognized the periglacial character of rock glaciers, and indicated that they are characteristic of the semi-arid Andes. He later published more detailed studies of the periglacial environment in the area of the Los Bronces mine, Andes of Santiago (33° S), including a valuable map of rock glaciers in that area (Lliboutry 1961, 1986; compare section 2.3.6).

Jean Borde later referred to rock glaciers in his work on the geomorphology of the Andes of Santiago (Borde, 1966). He presented a cartography of rock glaciers in the area of Lo Valdés and Baños Colina in the Andes of Santiago at 34° S. At the same time, the French geomorphologist Roland Paskoff described and mapped rock glaciers in the area of Cerro Tapado (30° S) within his work on the geomorphology of the semi-arid Andes (Paskoff, 1967, 1970; see section 2.2.3).

The Chilean geologist Cedomiro Marangunic is apparently the first scientist to measure the displacement rate of a South American rock glacier. For one month of March, he determined a surface velocity of $1.28\,\mathrm{cm\,d^{-1}}$ for the Pedregoso rock glacier at 32° S (Marangunic, 1976).

Ice masses in general were systematically registered since the 1970s within the glacier inventories of the Chilean Water Directorate (Dirección General de Aguas, DGA; Garín, 1987; Marangunic, 1979; Valdivia, 1979, 1984a). However, only a very small fraction of rock glaciers (especially debris rock glaciers) is included, and the inventories do not distinguish between rock glaciers, debris-covered glaciers and thermokarst. They are therefore not directly comparable with Argentinian glacier inventories at the same latitude (Corte and Espizua, 1981; cf. Corte 1980).

With the boom of mining activities in the periglacial belt of the Andes of Santiago since the 1980s, a series of comprehensive geotechnical studies on rock glaciers have been executed (Arcadis Geotécnica, 2001; Contreras and Illanes, 1992; C. Marangunic, 2003, personal communication). Apparently the work by Contreras and Illanes (1992) is the only scientific publication of such results from the mining industry. These results and the effects of mining on rock glaciers (Brenning, 2004b) are evaluated in section 2.3.6.

More recently, Hintermayr (1997), Kammer (1998) and Schröder (1999, 2001) investigated rock glacier distribution and periglacial environments in the arid Andes of Northern Chile. According to these authors, the extreme aridity in the area of the Arid Diagonal of South America appears to inhibit rock glacier development or activity, but information on the actual gap within rock glacier distribution remained contradictory.

Palaeoclimatic conclusions on the late glacial temperature depression in Northern Chile were drawn by Veit (1991) and Payne (1998) based on the

distribution of active and relict rock glaciers. According to these works, the offset of rock glacier distribution reaches 400–500 m, which would correspond to a temperature depression of about 3°C.

In contrast to the sporadic rock glacier research in the Chilean Andes, there is a long tradition in Argentina, especially at the Instituto Argentino de Nivología, Glaciología y Ciencias Ambientales (IANIGLA) in Mendoza (Ahumada, 1992; Buk, 1983; Corte, 1976a,b, 1978, 1980; Corte and Espizua, 1981; Croce and Milana, 2002; Trombotto, 1991; Trombotto et al., 1997, 1999; Trombotto and Villalba, 2002). German geomorphologists have also contributed to the current knowledge base in the dry Andes of Northwest Argentina (Barsch and Happoldt, 1985; Barsch and King, 1989; Garleff and Stingl, 1986; Happoldt and Schrott, 1992; Schrott, 1991, 1994, 1996, 1998).

Recently published articles of this author include case studies of rock-glacierized areas (Brenning, 2003, 2004b) as well as first results on the statistical quantification and analysis on a regional scale (Brenning, 2004a, 2005a,b; Brenning et al., 2005); most of these results are also included in this dissertation.

Chapter 2

Geomorphological mapping and quantification in Central Chile

A fundamental part of the present work consists of geomorphological mapping of selected areas in the field and from aerial photographs. Though field work is very time-consuming, this kind of "ground truthing" is crucial for a qualified interpretation of aerial photographs or statistical modelling results. It is furthermore needed for obtaining a more comprehensive knowledge of the complex geoecological conditions within the periglacial and nival environments of the Andes.

2.1 Methods

During the summers of 2002–2004, the author visited nine high-elevation catchments in the Andes of Central Chile, and three further mapping areas were studied by means of aerial photographs (figure 1.2, table 1.1). In addition, the vertical distribution of periglacial landforms and glaciers was quantified in six of these areas.

The selection of comparable mapping areas aims at covering the whole central Chilean rock glacier distribution and was subject to logistical constraints of time and accessibility.

Field work focused on geomorphological mapping and morphometric measurements on rock glaciers. Front slope inclinations of selected rock glaciers were measured with a hand-held clinometer as an average of at least three readings, and front slope length with a tape, when possible.

Morphographic criteria for determining the activity of rock glaciers and for distinguishing between rock glaciers, thermokarst areas and debris-covered glaciers are discussed in section 1.4.2.

Geomorphological maps at scales between 1:25,000 and 1:50,000 were prepared based on sketches made in the field, the interpretation of aerial photographs (approximate scale 1:50,000 to 1:60,000), and topographic data (maps 1:50,000 and/or SRTM DEMs; see Appendix A). The symbology is based on Kneisel et al. (1998).

The altitudinal distribution of rock glaciers, glaciers and thermokarst areas was quantified at discrete elevation intervals for comparison with the regional altitudinal distribution derived

Average rock glacier ice content[a]	40–60 % by volume
Thickness of ice-rich r. gl. permafrost[b] [m]	$50 \cdot (\text{area}\,[\text{km}^2])^{0.2}$
Glacier thickness[c] [m]	$28.5 \cdot (\text{area}\,[\text{km}^2])^{0.357}$
Density of glacier and r. gl. ice[d]	$0.9\,\text{g/cm}^3$

Table 2.1: Assumptions for estimating rock glacier and glacier water equivalence, based upon: [a] Arenson et al. (2002); Barsch (1977a, 1996a); Haeberli et al. (1998); Hoelzle et al. (1998); [b] present work; [c] Chen and Ohmura (1990); [d] Paterson (1994).

later and in order to visualize the hypsometric change in the distribution of landforms and compare different catchments (Bolch and Schröder, 2001; Brenning, 2003). Furthermore, total areas were determined, and water equivalence of rock glaciers and glaciers was estimated for each study area making the assumptions shown in table 2.1. The estimation of rock glacier thickness is based upon morphometric field measurements in the Andes of Santiago and is conservative if compared to the area–thickness relation used by Barsch (1977c) in the Swiss Alps. The empirical relationship that was applied to glacier thickness estimates (Chen and Ohmura, 1990) is more conservative than the one used in the Chilean glacier inventories (cf. Garín 1987; Marangunic 1979).

Though cryogenic microforms, slope form and glacigenic landforms were not mapped to their full extent, they are used to give a more comprehensive impression of the high-mountain environment and to delimit, in conjunction with rock glaciers, the periglacial altitudinal zone.

The large amount of morphometric data produced for the rock glaciers of the study areas is summarized in the respective sections. The full database will be submitted to the Frozen Ground Data Center at the National Snow and Ice Data Center[1] (NSIDC) after publication of the present dissertation. Numeric rock glacier identifiers indicated in the text refer to the geomorphological maps, which are included in Appendix C, and to the mentioned database.

[1] URL: `http://nsidc.org/fgdc/`

2.2 The arid North

The Atacama desert, the driest mountain area of the world (Richter and Schmidt, 2002), is characterized by non-glacierized peaks of more than 6000 m height in its central part, where the South American Arid Diagonal crosses the Andes (24°–25° S; figure 1.2).

Rock glacier distribution is interrupted within the Arid Diagonal, for example at Volcán Lullaillaco (24° 43′ S, 6739 m; Schröder and Makki, 1998). The actual gap within the distribution of active rock glaciers has been determined by Kammer (1998); it extends at most between Cerro Lejía (23° 33′ S, 5793 m) and Cerro San Francisco (26° 55′ S, 6018 m), where Hintermayr (1997) already described active rock glaciers. The gap comprises therefore about 400 km of distance in north–south direction. In contrast to the findings of Hintermayr (1997) (who described active features on Cerro Sairécabur; 22° 43′ S, 5971 m) and Kammer (1998), Schröder (1999, 2001) later maintains that active rock glaciers are absent between about 21.5° and 29° S.

The following sections present three mapping areas that cover the semi-arid to arid Andes south of the Altiplano. In these areas, precipitation, predominantly provided during the cold season, already becomes more notorious ($\geq$ 200 mm a^{-1}; Ammann, 1996; Richter and Schmidt, 2002), and glaciers exist, but are limited to the highest peaks.

2.2.1 Nevado Jotabeche: scarce rock glaciers in extreme aridity

Nevado Jotabeche (27° 42′ S, 69° 13′ W, 5862 m; figure 2.1) is a Tertiary volcano complex at the southern end of the Chilean Altiplano (Mpodozis et al., 1995). The mountain's summit plateau above 5500 m a. s. l. is defined by an escarpment, which is superimposed by cirques and valley heads (figure C.1 on page 126). South and west of the mountain, the Nevado and Yeguas Heladas valleys impose a strong fluvial imprint and an exorheic drainage, while its northern slope faces the basin of Salar del Negro Francisco (about 4100 m a. s. l.), the southernmost significant salt lake of the Chilean Andes.

The Jotabeche Massif formed at the end of an Oligocene–Miocene period of volcanic activity in the Maricunga Belt of the southern Altiplano; its geological development has been described by Mpodozis et al. (1995). Nevado Jotabeche itself and the Pastillitos valley are characterized by ignimbrites, lavas and rhyolitic tuffites of late Miocene age, while the upper Gallinas valley presents andesitic rocks of the same age. The neighboring Cordón Yeguas Heladas to the west and Volcán Jotabeche Norte to the north are mainly composed of middle Miocene andesitic lava sequences, domes and pyroclastic flows. The mentioned Miocene volcanics are deeply eroded due to the great tectonic uplift of the Altiplano. Specifically, the Nevado and Yeguas Muertas valleys, which are of particular interest here, have been cut down through the subhorizontal Miocene layers into a late Cretassic–Palaeocene basement of intrusive, volcanic and sedimentary rocks.

Pleistocene glaciations at Nevado Jotabeche are reported to extend down to the Llano del Negro Francisco, but last glacial frontal moraines on all sides of the mountain reach only 4300–4550 m; the corresponding LGM (Last Glacial Maximum) ELA was located at 4700–4750 m a. s. l. (Jenny and Kammer, 1996).

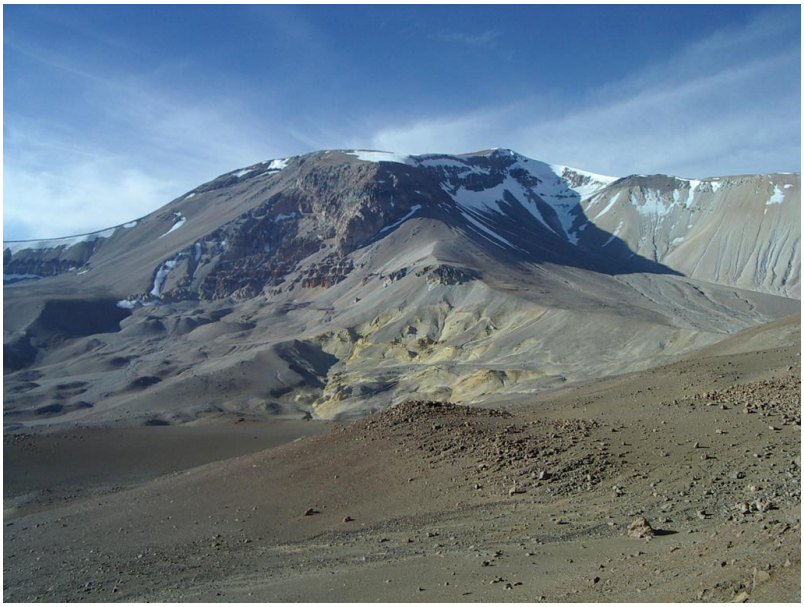

Figure 2.1: Nevado Jotabeche, seen from south. Photograph: 14 Mar 2003.

There is no modern glaciation at Nevado Jotabeche, but perennial snow fields partly cover the summit plateau.

Probably active rock glaciers exist at Nevado Jotabeche above 4650 m, probably inactive features above 4550 m a. s. l. (figure C.1). Most of them are concentrated within three areas: (1) A south-exposed cirque below the mountain's peak; (2) a small cirque in the Gallinas catchment; and (3) the valley slopes (especially footslopes) of the Yeguas Heladas valley.

Slopes are gentle, valleys are open, and concave–convergent niches such as Pleistocene cirques are less frequent and prominent than in more humid areas. Overall, the development of rectilinear slopes is a dominant landforming process in the area. On the other hand, the presence of small rock glaciers at the foot of talus slopes in the Yeguas Heladas valley shows that rates of talus production and supply are sufficiently high for the development of talus-derived rock glaciers in spite of the aridity.

In conclusion, rock glacier formation in the area is strongly limited due to morphographic reasons, which are partly the consequence of limited Quaternary glaciation and therefore of aridity.

2.2.2 Cerro del Potro: well-developed rock glaciers in the arid North

Cerro del Potro is a glacierized mountain that is surrounded by huge valleys both on its Chilean and Argentinian side. Its southern side is limited by a steep rock wall towards the trough-shaped Río Blanco valley (Argentina), which presents a wide valley floor; the other sides of the mountain are characterized by well-developed Pleistocene cirques (figure C.2).

The summit plateau of Cerro del Potro hosts a 7 km^2 large, mainly east-exposed glacier. The lowest of its three termini reaches ∼4800 m a. s. l. (figure C.2 on page 127). The glacier's margins are disintegrated into *penitentes*. According to Jenny and Kammer (1996),

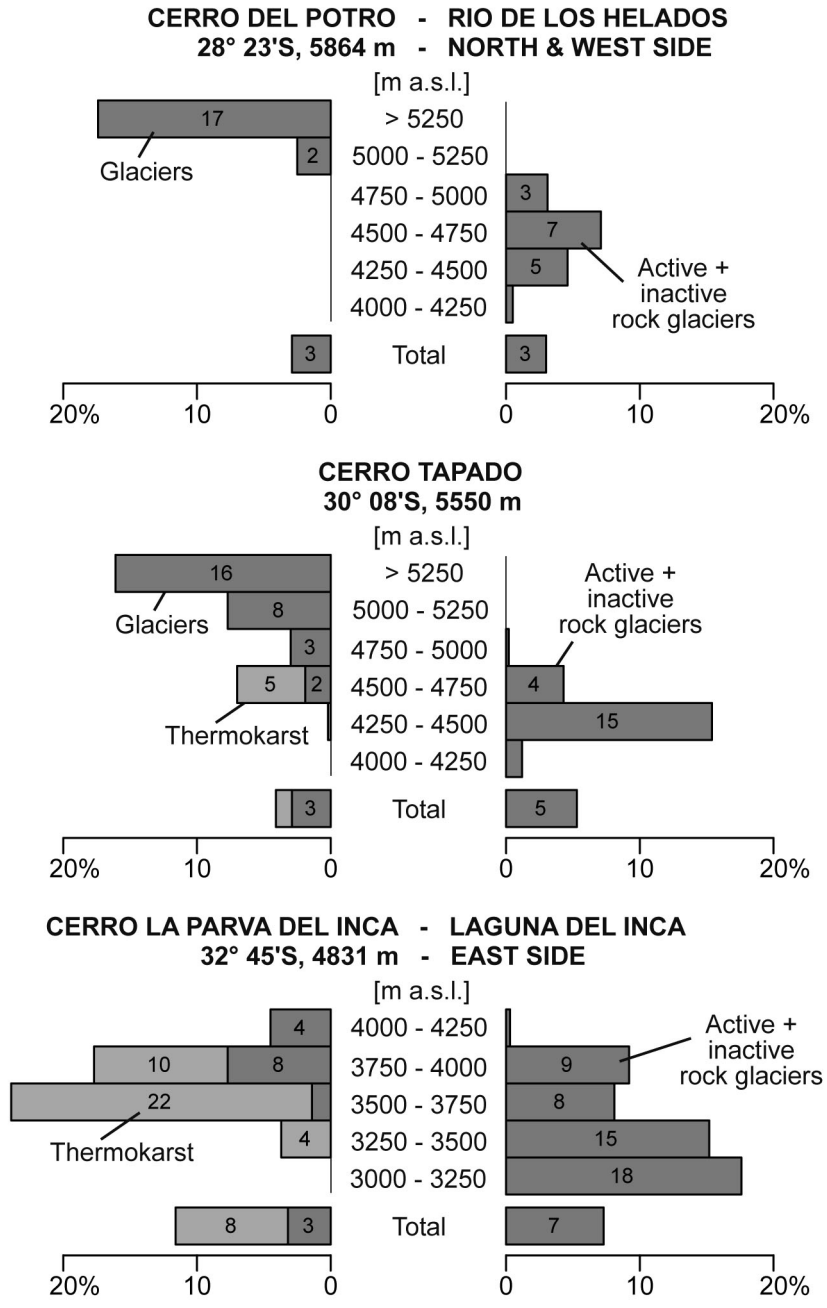

Figure 2.2: Quantification of rock glacier and glacier surfaces in the Potro, Tapado and La Parva areas. Compare figure 2.10 on page 40.

the modern 4:1 to 2:1 ELA lies between 5250 and 5400 m a. s. l.

The last glaciation of Cerro del Potro was characterized by four large valley glaciers; LGM ELA was estimated to be situated around 4350 m a. s. l. in the case of cirque glaciers (Jenny and Kammer, 1996).

Active rock glaciers exist as low as at 4150 m a. s. l., but they are associated with inactive features up to 4500–4600 m (figure C.2). However, the differentiation between inactive and active features in this area is only based on the interpretation of aerial photographs and must therefore be considered as preliminary. Rock glaciers are most abundant in cirques, but they are also frequent at the foot of valley slopes. The location with respect to late Pleistocene moraines as determined by Jenny and Kammer (1996) clearly indicates that all intact rock glaciers are of post-glacial age.

A huge relict debris rock glacier (no. 135) is situated in the Río de los Helados valley in an area of late glacial recessional moraines; its toe lies at ∼3960 m a. s. l. The rock glacier's lower part consists of two lobes that moved from the moraine down onto a river terrace. This suggests ongoing activity during late-glacial climatic change even after further glacier retreat.

The quantitative analysis of rock glacier and glacier distribution in the Chilean part of the Potro area is shown in figure 2.2 and table 2.2. Both features are restricted to distinct altitudinal zones because of the high elevation of modern ELA with respect to the MAAT 0°C isotherm.

Late Quaternary slope development is governed by several processes, which vary according to slope length and water supply: North and west of Cerro del Potro, steep rock faces provide direct talus supply to rock glacier rooting zones. Talus and alluvial cones as related to gravitational and fluvial processes are scarce and develop only below extremely high, steep rock faces, for example in the Blanco valley. Shorter and less steep slopes close to the angle of repose are often rectilinear and represent different stages of development. At lower altitudes, where the last glaciation had minor or no geomorphological impact, the rock cliff has often been dissolved, and where linear valley drainage is absent, a concave footslope indicates that equilibrium transport conditions have been abandoned.

In summary, rectilinear slopes and rock glaciers are the dominant mesoscale landforms above 4000 m a. s. l.. The latter are particularly favored in the immediate surroundings of Cerro del Potro due to Pleistocene glacial landforming and sedimentation. The hypsometric distribution of rock glaciers and glaciers is clearly separated as a consequence of aridity.

2.2.3 Cerro Tapado

Rock glaciers in the surroundings of Paso de Agua Negra at 30° S have early been mapped from aerial photographs of Cerro Tapado in Chile (Paskoff, 1967, 1970) and later on the Argentinian side (Barsch et al., 1994; Croce and Milana, 2002; Happoldt and Schrott, 1992; Scholl, 1992, 2002; Schrott, 1991, 1994, 1996, 1998). Past and present periglacial environments of the Cordillera de Elqui have furthermore been studied by Veit (1991, 1992).

While the highest summits of the Cordillera de Elqui, Cerro de las Tórtolas (6160 m) and Cerro Olivares (6252 m), host firn and snow fields without apparent signs of movement (Paskoff, 1970), Cerro Tapado (5550 m) presents a southeast-exposed hanging glacier (fig-

	Number of features	Area [km^2]	[%]	Water equiv. [10^6 m^3]
Intact rock glaciers	42	3.9	3	53–80
Glaciers	0.5	3.7	3	186

Table 2.2: Areas and water equivalence of intact rock glaciers and glaciers in the upper Río de los Helados catchment (127 km^2), Cerro del Potro area. Note that only part of the Potro glacier lies within this Chilean catchment. Assumptions: See table 2.1

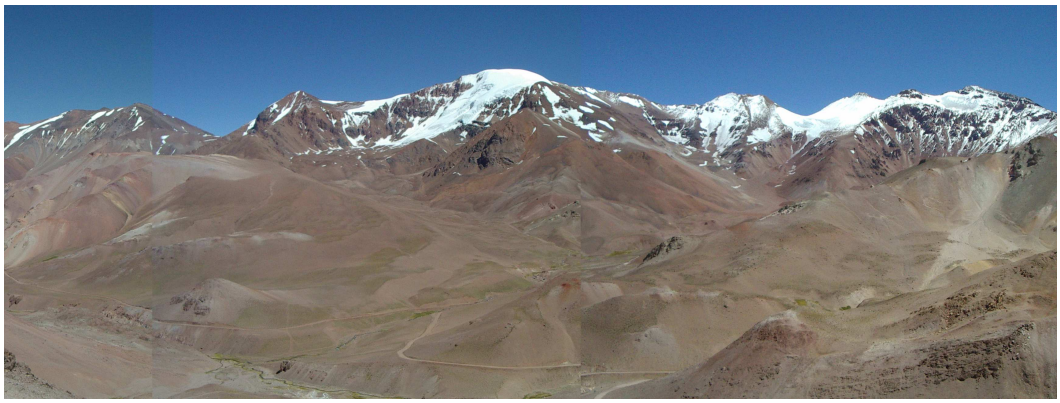

Figure 2.3: Panoramic view of the eastern side of Cerro Tapado (5550 m a. s. l.) and its surroundings. Composite of three photographs taken on 10 Mar 2003 at 4150 m a. s. l. from the road to Paso de Agua Negra.

	Number of features	Area [km^2]	[%]	Water equiv. [10^6 m^3]
Intact rock glaciers	22	3.3	5	47–70
Glaciers	4[a]	1.8	3	41
Thermokarst areas	3	0.7	1	11

Table 2.3: Areas and water equivalence of intact rock glaciers, glaciers and thermokarst at Cerro Tapado (62 km^2). Assumptions: See table 2.1.
Remark: [a] Includes possible firn fields.

	Mean thickness	Area	Ice content	Ice volume
Active rock glaciers	50 m	2.07 km^2	60 %	$62 \cdot 10^6$ m^3
Glaciers	50 m	1.78 km^2	100 %	$89 \cdot 10^6$ m^3
Continuous permafrost	20–30 m	9 km^2	20 %	$36–54 \cdot 10^6$ m^3
Discontinuous permafrost[a]	20–30 m	44 km^2	20 %	$44–66 \cdot 10^6$ m^3

Table 2.4: Inventory of rock glaciers, glaciers and permafrost in the upper Agua Negra catchment (Argentina, 30° S). Data from Schrott (1996).
Remark: [a] Assumed to be underlain by 25 % of permafrost.

Figure 2.4: Snow penitentes between Cerro Tapado and Paso de Agua Negra. Photograph: 10 Mar 2003.

ure 2.3). It extends down to 4650 m a. s. l. covering ∼1.2–1.5 km^2, and modern ELA is situated around 5300 m a. s. l. (Hastenrath, 1971; Kull et al., 2002). Kull et al. (2002) indicate that local climatic conditions are responsible for the existence of the Tapado glacier. Their model results suggest that precipitation at the Tapado glacier at 5500 m a. s. l. is of 750 mm a^{-1} instead of the regional mean of 580 mm a^{-1} estimated by Vuille (1996).

Active rock glaciers exist at Cerro Tapado above 4200 m a. s. l., while inactive features reach down to 4000 m (figure C.3 on page 128). The absence of intact rock glaciers at lower altitudes may however here be a consequence of topographic rather than thermal conditions. Specifically, mapped areas below 4200 m consist mainly of gentle valley floors and are affected by fluvial processes. Schrott (1991) mentions active rock glaciers above 4000 m a. s. l. in the nearby Agua Negra catchment. Veit (1991) indicates that relict features reach down to 3800–3900 m in the Cordillera de Elqui; he assigns a late glacial age to them.

In contrast to the Jotabeche and Potro areas, where thermokarst was absent, thermokarst-affected massive-ice bodies do exist at Cerro Tapado and in the Agua Negra catchment, where they are connected to debris rock glaciers. In fact, these two features dominate the cirques on the south side of Cerro Tapado. The largest debris rock glacier (no. 97) reaches a size of 0.8 km^2 and a length of 1800 m. The hypsometric distribution of landforms reflects a depression of the glacial environment and a compression of the periglacial belt in south exposition.

An estimation of rock glacier and glacier volumes in the Tapado and Agua Negra areas indicates that the amount of water contained within both types of stores is of a similar order of magnitude (tables 2.3 and 2.4).

Penitentes above 4000 m a. s. l. in the Cordillera de Elqui are formed under the influence of high direct solar radiation, which results in an effective firnification (figure 2.4; Lliboutry, 1954; Paskoff, 1970; Reichert, 1910). Many of these firn

Chile	Argentina	Phenomenon
5300 m		Modern ELA of the Tapado glacier
4900	5050	Upper limit of active rock glaciers
4650	4750	Lower limit of Agua Negra and Tapado glaciers, resp.
4200		Lower limit of patterned ground
4000–4100		Modern 0°C isotherm
4100–4200	4000	Lower limit of active rock glaciers
3800–3900	3900	Lower limit of the periglacial belt (stone-banked terraces, formation of rectilinear slopes)
3800–3900		Lower limit of relict rock glaciers
3500		Lower limit of the Andean belt (pipkrake, shallow patterned ground, increasing vegetation density)
$\leq$ 3500		Subandean belt (patchy vegetation, conservation of rectilinear slopes; pipkrake, dry creep)
2900		Lower limit of the conservation of rectilinear slopes

Table 2.5: Modern altitudinal zonation in the Andes at 30° S, according to Croce and Milana (2002); Kull et al. (2002); Schröder (2001); Schrott (1996); Veit (1991).

fields are discontinuous in time. According to Paskoff (1970), *penitentes* of more than 2 m of height had formed after strong snowfall events in July/August 1965 and practically disappeared after two consecutive dry years (1967/68).

Intensive physical weathering and the lack of fluvial incision provide excellent conditions for the development of rectilinear slopes in the area (Schröder, 2001; Schrott, 1994; Stingl and Garleff, 1983; Weischet, 1969). They exist mainly in areas that are not affected by Holocene glacier advances as indicated by debris-covered massive ice and fresh moraines (cf. Veit 1991 and section 2.2.2).

Table 2.5 summarizes the altitudinal distribution of periglacial phenomena in the Andes at 30° S.

To conclude, Holocene and lateglacial glaciation has left its geomorphological imprint in the periglacial zone, as most rock glaciers in the area are debris rock glaciers. In contrast to areas further to the north, at Cerro Tapado the periglacial and glacial environments show a more complex pattern depending on topographic conditions. Rectilinear slopes are still in general the dominant mesoscale landforms of the periglacial belt.

2.3 The Andes of Santiago

The area between the Andes of La Serena and Santiago has not been studied in this work because of the rather low topography on the Chilean side. The significant changes in topography, precipitation sums and glacierization over the distance of ∼300 km have to be recalled therefore (compare figure 1.7).

The following mapping areas are intended to cover the wide range of rock glaciers and their environments in the Andes of Santiago (e. g. sections 2.3.1, 2.3.2, 2.3.4, 2.3.5). Certain emphasis is however put on medium-elevation catchments with limited modern glaciation (sections 2.3.3, 2.3.2, 2.3.7), which are "typical" away from the central range. Applied aspects especially as related to mining are also addressed (section 2.3.6).

2.3.1 Cerro San Ramón: permafrost 10 km from Santiago

The San Ramón Massif constitutes the westernmost mountain range of the Andes of Santiago. Its highest summit, Cerro San Ramón (3253 m a. s. l.; 33° 29′ S, 70° 26′ W), rises within only 10 km of horizontal distance ∼2500 m above the nearby basin of Santiago forming an imposing wall just east of the Chilean capital (figure 2.5). In spite of its proximity to Santiago, the San Ramón Massif has attracted little touristic or scientific interest, except from hydrological studies related to sudden floods that originate in the *quebradas* (V-shaped valleys) on its steep western flank (Corvalán et al., 1997). As a consequence, periglacial geomorphology and in particular the existence of a rock glacier at the San Ramón Massif, which will be described in this section, have not been mentioned in the literature before.

The summit of Cerro San Ramón can be divided into three geomorphological units: To the west, the steep and incised rocky slopes drop off towards Santiago; to the north, relatively smooth surfaces and ridges connect the massif with Cerro de la Provincia (2751 m); and east of the summit, a small, elongated cirque of glacial origin can be found, which opens towards south. The cirque floor is situated at ∼3000 m a. s. l., being surrounded by ridges of about 3200 m a. s. l. Depending on the season, there are two or three small lakes on the cirque floor.

The San Ramón rock glacier

On the northeastern side of the mentioned cirque, a tongue-shaped talus rock glacier emerges from the short, vegetation-free talus slopes that reach up to about 3150 m a. s. l. (figure 2.6). The rock glacier's toe is situated at 3020 m a. s. l. just north of one of the lakes.

Field observations suggest that the rock glacier is inactive:

- Lateral talus aprons are inclined at an angle of ∼31°, which is at or below the angle of repose.
- Though frontal slope angles are greater (35–37°), the smoothed upper part of the front slope suggests inactivity.
- On the rock glacier's surface, vegetation is extremely scarce, but present. According to field observations throughout the Andes of Santiago, rock glacier activity as deduced from front slope appearance is closely related to the complete absence even of vegetation.

Rock glacier inactivity at Cerro San Ramón is attributed to the thermal con-

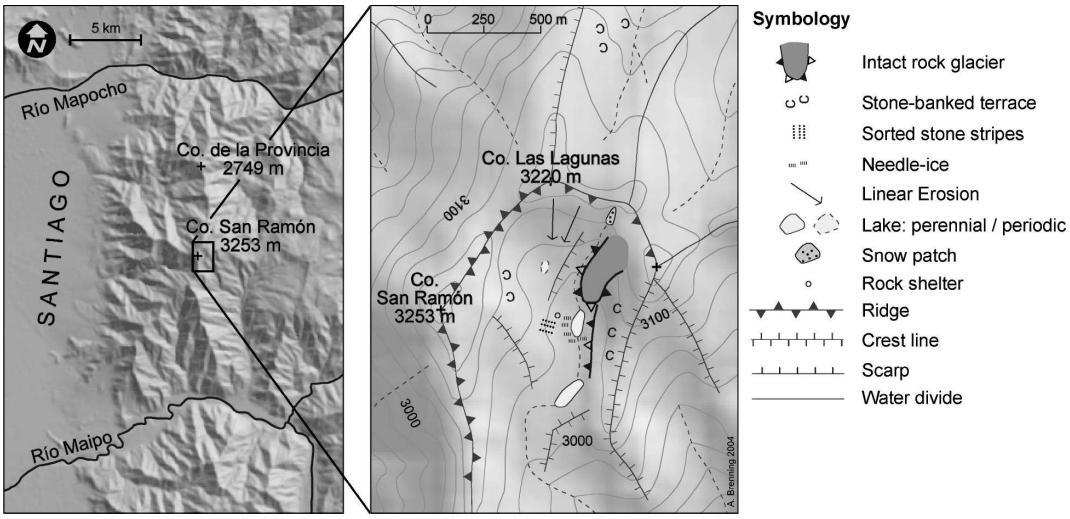

Figure 2.5: Location of the study area and geomorphological map sketch of the San Ramón Massif.

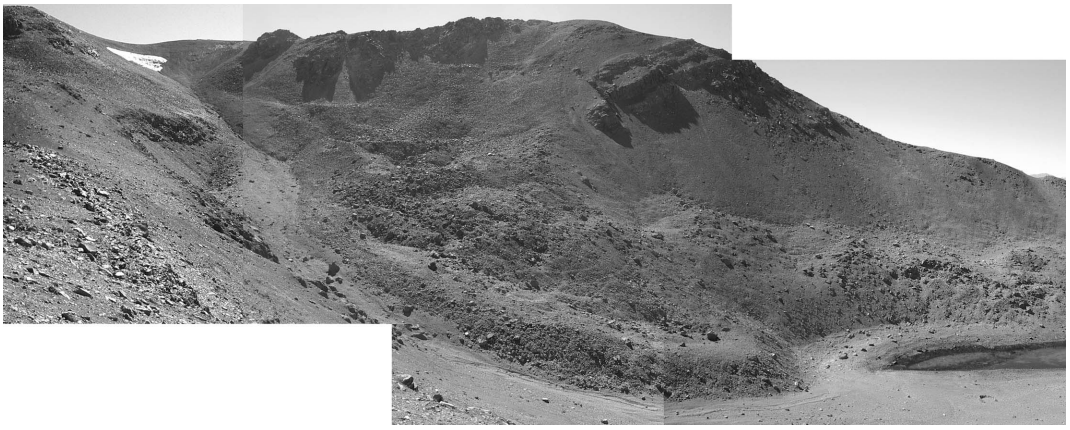

Figure 2.6: The inactive rock glacier east of the summit of Cerro San Ramón. Note that perspective makes the snow patch on the left hand side appear smaller than it is. Composite of four photographs, 7 Mar 2004, looking northeastwards.

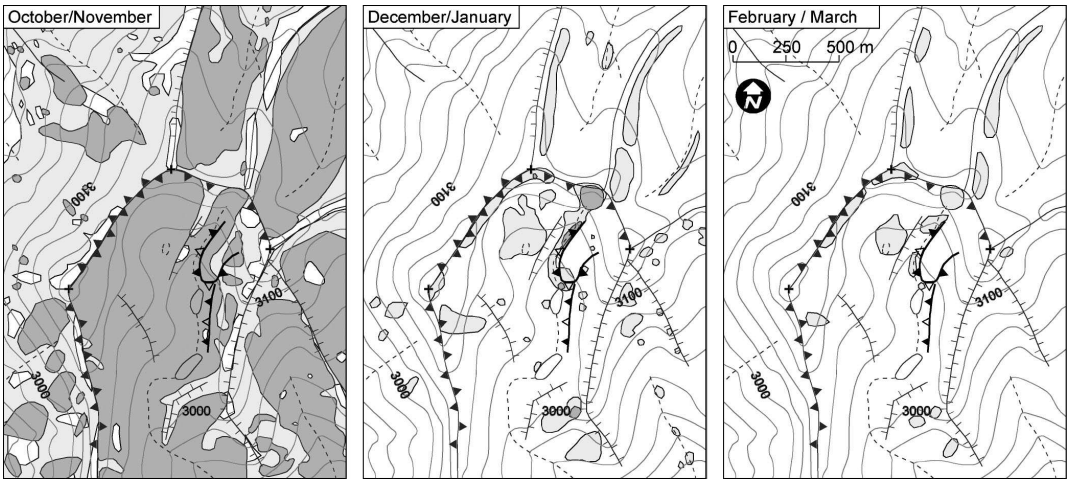

Figure 2.7: Spatio-temporal distribution of snow cover on Cerro San Ramón. "Typical" conditions are shown in dark grey, maximum snow extent in light grey. Compare the symbology of figure 2.5.

ditions imposed by a modern regional-scale MAAT of about +4°Cat 3000 m a. s. l. (section 1.3.2).

Long-lasting snow patches

In the south-exposed cirque of Cerro San Ramón, several protected places host long-lasting snow patches on a regular basis, according a visual evaluation of remotely-sensed imagery (figure 2.7; summers of 1989, 1997, 2001, 2003, 2004 and 2005; see Appendix A.2).

A characteristic pattern of long-lasting snow patches persists at topographically favored places during great part of the summer. These are situated in south and east exposition below ridges, south and west of the rock glacier, and around the location of the periodic lake. One snow patch north of the San Ramón rock glacier appears to survive some summers entirely (such as 2003), while it was absent in 2004 only during less than one month, and it may in some years (e. g. 1989, 1997) disappear before March (compare figures 2.5 and 2.6).

In winter, in contrast, west-exposed areas below ridges are generally snow-free. The rock glacier's surface remains partly snow-free during winter, allowing cold air penetration into the blocky material.

Periglacial microforms are frequent in the cirque (compare section 2.3.8). Especially the nocturnal formation of needle-ice along the lake side even during the field visit in late summer 2004 shall be mentioned here, since it gives evidence of cooler topoclimate inside the cirque.

Conclusions

The presence of an inactive rock glacier, long-lasting snow patches and periglacial microforms at 3000–3200 m a. s. l. are the consequence of favorable topoclimatic conditions within the south-facing cirque of Cerro San Ramón. Permafrost may be present within the rock glacier itself, but possibly also locally in its surroundings due to the interaction of snow cover and the air circulation within coarse debris.

2.3.2 Cerro Punta Negra and Cerros Picos Negros: Rock glaciers and remnant glaciers

The Cerro Punta Negra[2] and Cerros Picos Negros areas are situated within the Yeso catchment close to Laguna Negra and the Embalse El Yeso reservoir, which contribute up to two thirds of Santiago's drinkwater in dry summers, according to the water supplier Aguas Andinas[3].

The highest peaks of the area are Cerro Punta Negra (4655 m a. s. l.) and Cerros Picos Negros (4542 m), both of which present small valley glaciers. Downvalley, these glaciers turn into debris-covered glaciers and finally into decaying dead-ice bodies with melt-out depressions and an extremely irregular relief (figures 2.8, 2.9, and C.4).

Cajón de la Casa de Piedra / Cerros Picos Negros

In the Cajón de la Casa de Piedra, southeast of Cerros Picos Negros, the lowest partly active rock glacier (no. 208) is connected to the Casa de Piedra massive-ice body and reaches down to 3000 m a. s. l. (figure 2.8). It consists of three superimposed units, the lowest of which is relict. The uppermost unit is classified as active due to front slope morphometry (36° inclination) and appearance, and the middle unit as inactive (33°). The three units present well-developed furrows and ridges on their surface, which is distinct from the chaotic and instable surface structure of the neighboring massive-ice body. Both areas can therefore be distinguished in the field and by air photo stereoscopy.

A lateral moraine divides the Casa de Piedra glacier tongue into an older lower part that is strongly affected by ice-decay, and a less affected upper part. The latter ends in a second active debris rock glacier no. 209, which is a single-unit feature. The difference in complexity of these debris rock glaciers no. 208 and 209 (single-unit versus multi-unit composition) is attributed to different rock glacier ages that correlate with two Holocene advances of the Casa de Piedra glacier.

A series of relict, inactive and active rock glaciers (no. 48) exists within a southwest-exposed cirque between 3000 and 3700 m a. s. l. (figure C.4). The spatial association of this sequence of rock glaciers suggests that it is the hypsometric expression of a temporal series of rock glacier development periods under increasingly warm climatic conditions within the Holocene. The uppermost part of the cirque's talus slopes furthermore hosts several initial rock glaciers that form around 3600 m a. s. l. just below the rocky head walls.

The rooting zones of the highest rock glacier in the Casa de Piedra catchment reach about 3820 m a. s. l. The lack of topographically suitable niches and talus sheds at higher altitudes imposes this altitudinal limit, which coincides with the 25-year mean ELA of nearby Echaurren glacier.

The rock glacier-free parts of the mentioned cirque and further to the south the eastern slope of the lower Casa de Piedra valley between ∼2800 and 3600 m a. s. l. are characterized by rectilinear slopes (figure 1.12). Their lower parts below 3000 m a. s. l. present vegetation and are therefore being conserved in modern times, while the development of the upper parts is still in progress. The valley slopes of the much greater

[2] Lliboutry (1956) refers to Cerro Punta Negra as Cerro Aguja Helada. Here the place names of the topographic map 1:50,000 Embalse El Yeso are used.

[3] URL: `http://www.aguasandinas.cl`

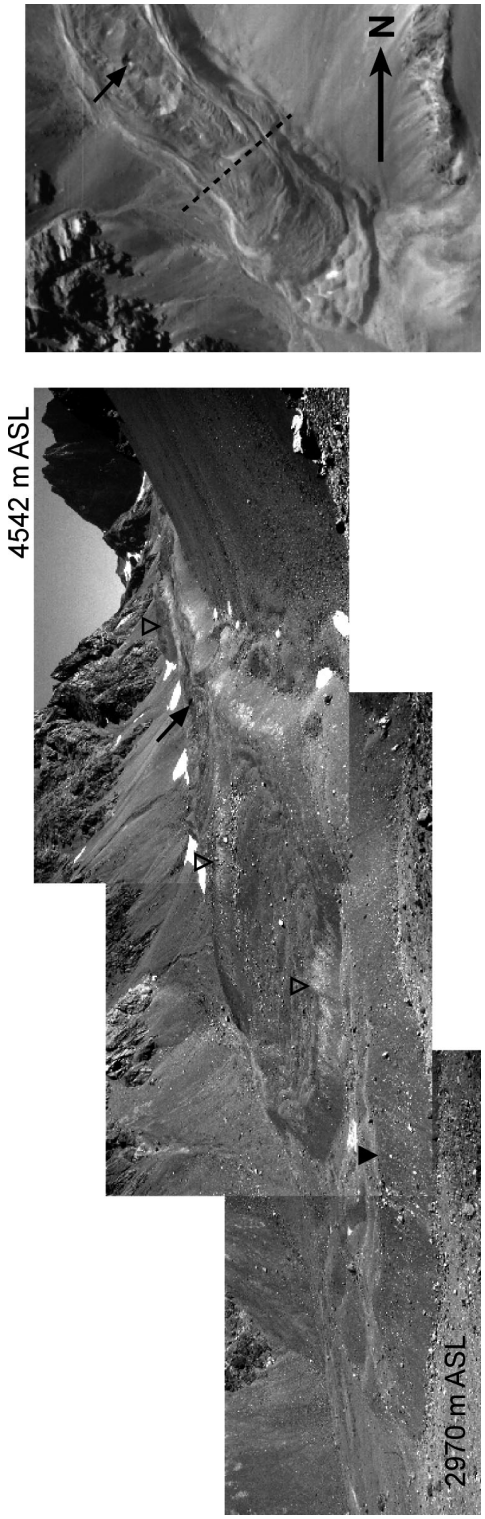

Figure 2.8: The relict, inactive and active units of the debris rock glacier no. 208 in the Casa de Piedra catchment, Cerros Picos Negros (33° 33′ S, 4542 m), at around 3000 m a. s. l. The arrow indicates a thermokarst melt-out pond, and the dashed line represents the approximate limit between rock glacier and debris-covered massive-ice. In the background, the active debris rock glacier no. 209 is also indicated by a triangle. Adapted from Brenning (2003); aerial photograph of the SAF, 1996.

	Number of features	Area [km^2]	[%]	Water equiv. [10^6 m^3]
Intact rock glaciers	14	0.7	5	8–11
Glaciers	1	0.2	1	3
Thermokarst areas	1	0.6	5	13

Table 2.6: Areas and water equivalence of intact rock glaciers, glaciers and thermokarst areas in the upper Cajón de la Casa de Piedra (13 km^2), Cerros Picos Negros area. Several initial rock glaciers are included. Assumptions: See table 2.1.

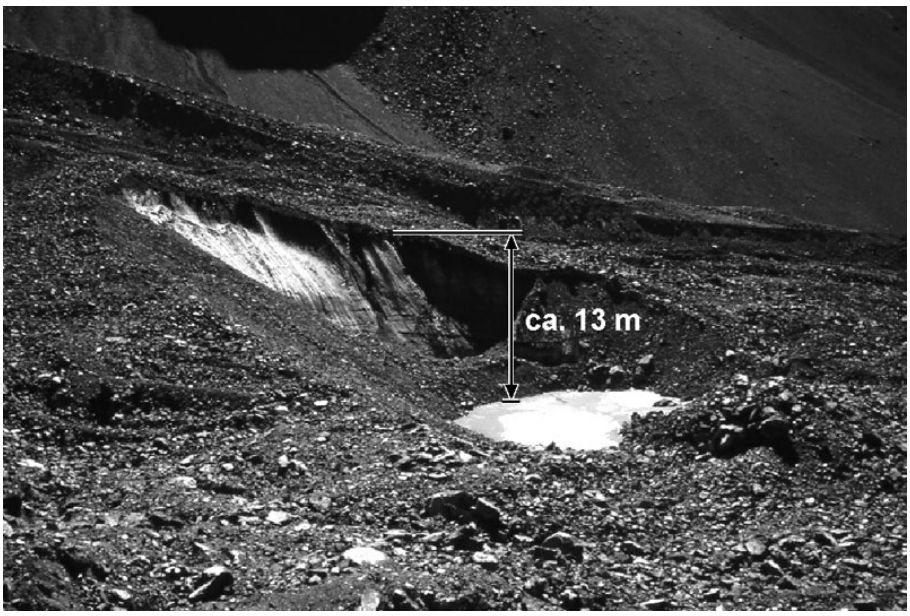

Figure 2.9: A thermokarst melt-out depression and lake situated at 3120 m a. s. l. on the dead-ice body of Cajón de la Casa de Piedra. The morainic debris cover is approximately 1 m thick. Photograph: 12 Mar 2002.

western part of the catchment are in contrast controlled by Holocene fluvial and gravitational processes. These result in fluvial incision of hanging valleys and fluvio-gravitational cones below ∼3000 m, and active talus cones and scree slopes above this altitude. However, it has to be noted that the upper Casa de Piedra hydrological catchment is endorheic and practically lacks even periodic superficial drainage. The endorheism is due to a closed depression at 2900 m a. s. l., which episodically hosts a meltwater lake in spring and summer.

Turning to the glacierization, the snow-line of the Casa de Piedra glacier is depressed to less than 3800 m a. s. l. because of the contribution of avalanches, but it is hard to give a precise figure due to the great inter-annual variability (Escobar et al., 2000; Lliboutry, 1953).

Furthermore there exist several firn fields above 3700–3800 m a. s. l. at topographically favored locations. Long-lasting snow patches are found in vicinity to most active rock glaciers in the catchment. In particular, low-elevation snow patches persist in many years until late February or March especially in the surroundings of the lower Casa de Piedra rock glacier (sources: aerial photographs, field observation, Landsat and ASTER imagery of 1955, 1975, 1989, 1996, 2001–04; compare Appendix A). On the other hand, snow conditions during a visit of the area in late October 1998, after a dry La Niña winter, rather resembled typical February snow conditions, with only patchy snow distribution even at 4000 m a. s. l.

Cerro Punta Negra / Laguna Negra

The ground thermal regime and rock glacier displacement rates in the adjacent catchment of Laguna Negra, just west of the Casa de Piedra valley, are currently being studied by Andreas Lamm and Tobias Wittkopf (both Humboldt-Universität zu Berlin). Only selected observations shall here be anticipated.

The Laguna Negra catchment hosts only two small glaciers, namely the Echaurren glacier on Cerro Echaurren (4028 m), which is being monitored by the DGA (Escobar et al., 2000, 1995), and one glacier below the south face of Cerro Punta Negra (4655 m). The latter is connected to a huge debris-covered massive-ice body with thermokarst features, from which a debris rock glacier emerges. According to an evaluation of aerial photographs (1955/1996), the massive-ice body has lost significant amounts of ice during the last decades and is therefore considered as dead ice. Its chaotic, instable surface with its melt-out depressions and remnant debris-covered ice towers and irregular ridges contrasts clearly with the rock glacier's more regular furrows and smoother ridges.

Active and inactive rock glaciers in this study area extend down to 3250 and 3050 m a. s. l., respectively.

Perennial snow fields exist above *c.* 3600 m a. s. l. along the southeastern side of the Punta Negra debris rock glacier, but long-lasting snow has also been observed in late March 2003 at the toe of an active rock glacier at ∼3250 m. Stronger evidence of modern permafrost conditions can be seen in an ice-fall that was present both in late summer 2003 and 2004 at a protected rock wall around 3450 m a. s. l. Furthermore, near-surface ice was encountered locally at ∼3400 m in a void between boulders aside an active rock glacier.

Conclusions

The Picos Negros and Punta Negra study areas are characterized by abundant Holocene rock glacier development, while decaying massive ice of former glacier tongues indicates periods of more extensive Holocene glaciation. Based upon field observations, it is proposed that permafrost is discontinuous above 3500 m and sporadic down to 3000 m a. s. l. at south-exposed places with additional favorable topoclimatic conditions.

2.3.3 Cerro La Parva: rock glaciers and remnant glaciers

Cerro La Parva (4831 m, 32° 45′ S) is situated in the upper Aconcagua river basin near the limit to Argentina, just a few kilometers away from the Portillo ski resort. Though the study area drains into the Aconcagua river, there is no hydrological connection to Cerro Aconcagua (6959 m), which is situated some 15 km further to the northeast in the Río Mendoza catchment of Argentina.

The Andean catchment studied here is that of Laguna del Inca (or del Portillo), a tongue-shaped lake that was dammed by the deposits of a prehistoric (probably late glacial) mega-landslide (Abele, 1981, 1984). A glacigenic origin had previously been suggested by Caviedes (1969, 1972) and Caviedes and Paskoff (1975).

East of Cerro La Parva, great surfaces within the the Laguna del Inca catchment surpass the 0°C-isotherm of ∼3600 m a. s. l. A debris-covered massive ice body with thermokarst features dominates this area (figure C.5, table 2.7). It is connected to remnant glaciers and firn fields on the east-facing valley side below the Las Coloradas range. On the opposite valley side, active rock glaciers accompany the massive-ice body.

Further downvalley, multiple units of an intact debris rock glacier (no. 164) emerge from the thermokarst area and reach down to 3130 m a. s. l. Front slope inclinations of 40–43° and a lateral slope of 46° are clear signs of activity (compare figure 2.17).

At the toe of this rock glacier, a spring emerges as the only superficial watercourse in the upper catchment. Its water is presumably provided by the mentioned massive-ice body. In the decaying thermokarst area, percolating meltwater was omnipresent in the melt-out structures. This meltwater flows above, below and within the massive ice and permafrost (compare figure 1.10). The downward narrowing valley concentrates this water toward the rock glacier spring.

The regional MAAT at the snout elevation of rock glacier no. 164 is of about +3°C, but its south-southeast orientation and the emplacement within a narrow valley may produce a significant departure of local thermal conditions from the regional mean.

Firn fields exist above 3200 m a. s. l. especially in avalanche accumulation areas such as footslopes and furrows beside rock glaciers, always in south exposition. On north-facing slopes (north of the mapping area), there are no significant snow patches even at elevations above 4000 m a. s. l., according to the available remotely-sensed data and field evidence.

In summary, the Cerro La Parva area presents similar conditions as the Punta Negra and Picos Negros areas. The thermal regime of a clearly active debris rock glacier, which reaches down to 3200 m a. s. l., benefits from specific topoclimatic conditions.

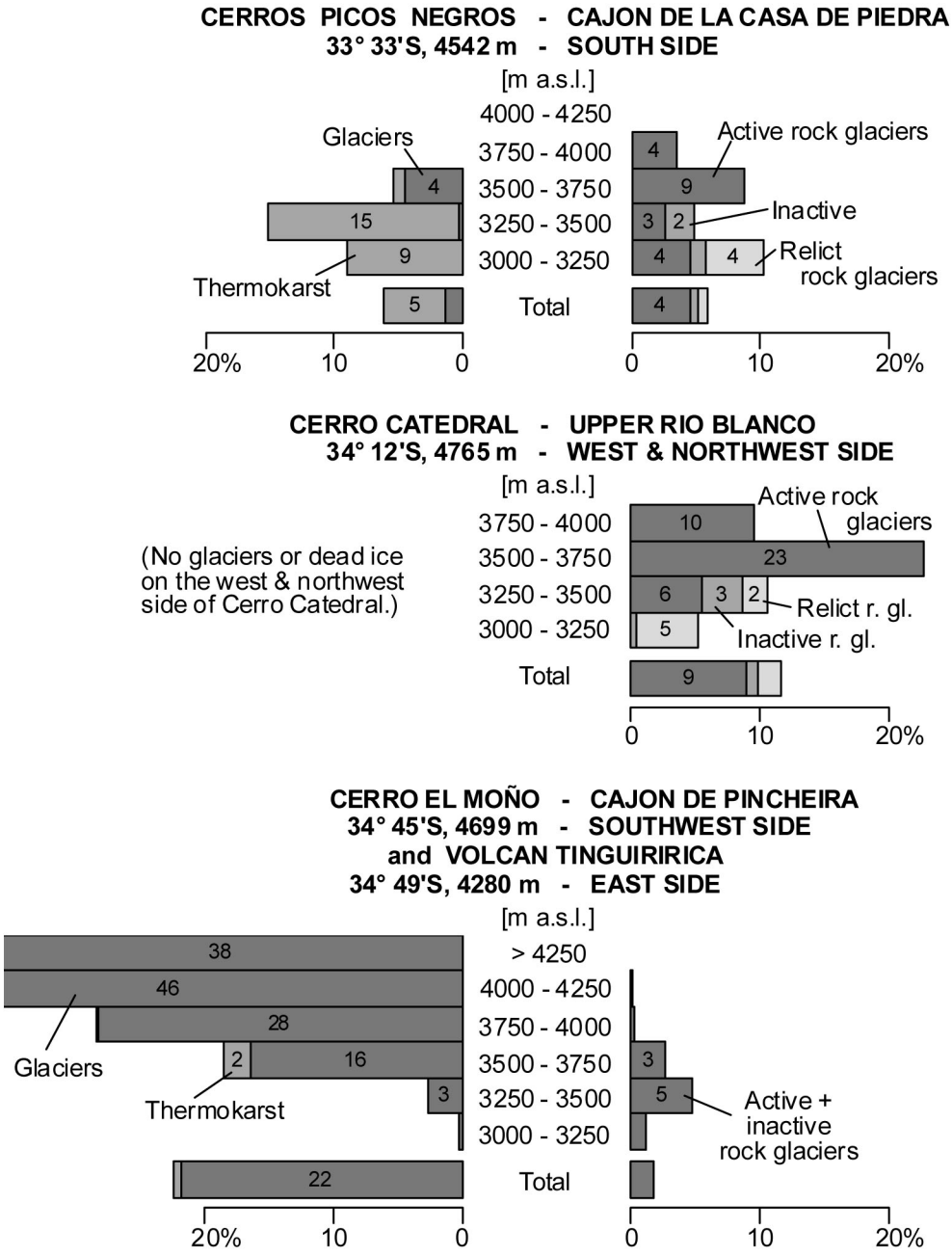

Figure 2.10: Quantification of rock glacier and glacier surfaces in the Picos Negros, Catedral and El Moño areas. Compare figure 2.2 on page 27.

2.3.4 Exceptionally huge rock glaciers

The three largest known rock glaciers in the Andes of Mendoza and Santiago are presented in this section. There may exist larger ones further to the north, especially in the Argentinian Andes. Table 2.8 shows a comparison with other extremes reported in the literature. Clearly, the semi-arid Andes have produced rock glaciers that are among the largest of our planet (cf. Bachrach et al. 2004; Barsch 1996a; Gardner and Bajewsky 1987; Gorbunov 1983).

The Cuerno Blanco rock glacier

The Chilean Cuerno Blanco rock glacier (figure 2.11) is an active coalescent rock glacier that incorporates both morainic debris and talus from the Chacayal valley head. It is bipartite, forming out of a predominantly debris-fed tongue-shaped western part and an elongated eastern part that extends more than 1000 m below the steep north face of Cerro Cuerno Blanco (33° 31′ S, 69° 57′ W, 5038 m). Some smaller debris and talus rock glaciers exist within the contributing area of the Cuerno Blanco rock glacier.

Cerro Cuerno Blanco's south side is covered by the 4.8 km^2 large Bello glacier (Marangunic, 1979), while its steeper north face is almost completely snow-free. The steepness of this north-exposed mountain face is, on one side, responsible for the absence of an ice glacier, and on the other, for the talus supply needed for the growth of such a huge rock glacier. The valley head's floor below the mountain's north face is situated slightly above the modern regional 0°C isotherm. At least the western part of the rock glacier has benefited from Holocene glaciations of the adjacent Cerro Aguja Delgada (4652 m) and Cerro Yeguas Muertas (4912 m).

The Cuerno Blanco rock glacier certainly carries the latent conflict between ice glaciers and rock glaciers in the semi-arid Andes to the extremes: It fills out the geomorphological niche of a huge cirque, while the mountain's strongly glacierized south face recalls that the presence of such a glacier-free niche at this altitude is by no means a matter of course.

The Rabicano rock glacier

About 22 km noth of the Cuerno Blanco rock glacier, another striking feature is found just north of the Argentinian border, which here runs westward across Morro Rabicano (33° 18′ S, 5277 m). The Rabicano rock glacier is an active spatulate debris rock glacier whose rooting zone is situated around 4400 m a. s. l. within a glacier-free cirque (figure 2.12a). The rock glacier is connected to a debris-covered massive-ice body that is considered to be remnant

	Number of features	Area [km^2]	Area [%]	Water equiv. [10^6 m^3]
Intact rock glaciers	8	1.1	7	15–23
Glaciers	2	0.5	3	9
Thermokarst areas	1	1.3	8	37

Table 2.7: Areas and water equivalence of intact rock glaciers, glaciers and thermokarst areas in the Laguna del Inca catchment (15 km^2), Cerro La Parva area. Assumptions: See table 2.1.

a)

b)

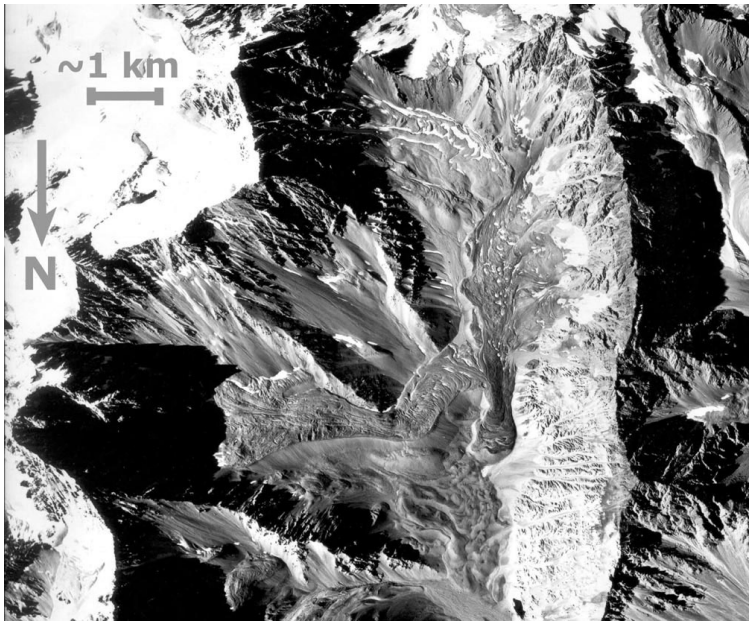

Figure 2.11: Perspective view and aerial photograph of Cuerno Blanco rock glacier. a) Conaf-Conama image (2001) draped over the SRTM DEM. b) Aerial photograph, flight Hycon (1956), Instituto Geográfico Militar.

Rock glacier	Location	Altitude at toe	Length	Mean width	Area	Talus shed	Ridge height[a]
Andes of Santiago							
Cuerno Blanco	33° 30′ S, 69° 58′ W	3600 m	—[b]	—[b]	2.0 km^2	4.7 km^2	800 m
Andes of Mendoza							
Papagayos	34° 14′ S, 69° 38′ W	3730 m	3100 m	700 m	2.5 km^2	3.2 km^2	300 m
Rabicano	33° 17′ S, 69° 59′ W	3950 m	2200 m	700 m	1.3 km^2	1.9 km^2	650 m
Zailijskiy Alatau							
Pjamoy shcheli	∼43° N, 77° E	—	4400 m	400 m	1.6 km^2	7 km^2 [c]	—
Canadian Rocky Mountains							
Hilda	52° 02′ N, 117° 00′ W	2185	2185 m	—	1.5 km^2	—	—

Table 2.8: Selected huge rock glaciers in the mountains of the world. Data from Bachrach et al. (2004); Gardner and Bajewsky (1987); Gorbunov (1983), and own data for Chilean and Argentinian rock glaciers.
Remarks: [a] Mean ridge crest height above the rooting zone. [b] Not measured because of complex shape. [c] After maximum glacier retreat: 11–12 km^2.

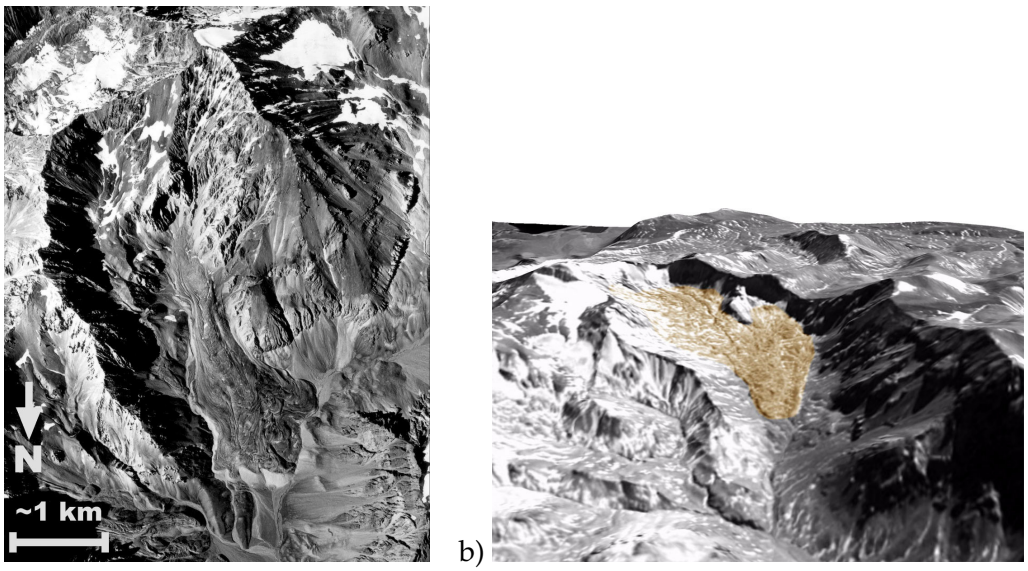

Figure 2.12: a) Aerial photograph of Rabicano rock glacier, Andes of Mendoza. Aerial photograph, flight Hycon (1956), Instituto Geográfico Militar.
b) Perspective view of Papagayos rock glacier, Andes of Mendoza. ASTER near-infrared channel draped over the SRTM DEM (rock glacier highlighted by the author).

dead-ice because of the absence of firn fields in the potential contributing area. The rock glacier moves into the Morado valley, where it spreads out in divergent flow forming several lobes. Estero del Morado is diverted by the rock glacier's front and forced into a narrow remnant valley. Though the advance might dam the creek in the future, a "rock glacier outburst flood" is unlikely to happen because of the low advance rates and the permeability of the involved material.

The Papagayos rock glacier

The largest observed rock glacier reaches a size of 2.5 km^2 and is here called the Papagayos rock glacier as it is situated in the upper Papagayos valley, about 15 km east-southeast of Volcán Maipo (figure 2.12b). This debris rock glacier is rimmed by relatively low cirque walls (compare table 2.8). Its contributing area is rather small compared to its size (ratio 1.3:1) in spite of the low relief. The incorporation of morainic debris and possibly of volcanic ashes of windward Volcán Maipo may explain this ratio.

Conclusions

If general conclusions can be drawn from individual occurrences of huge rock glaciers, then the most important issue is that these occupy cirques that have been neglected by modern glaciation due to a specific topographic situation including north exposition, steep rock faces, or (in the case of Papagayos) low summit elevation. In other words, the contributing areas of these features are in modern times "almost glaciated", since a slight modification of topographic situation (or climate) would be expected to produce a new glaciation within these cirques. Furthermore, only complex debris rock glaciers appear to be able to become that huge since they take advantage of morainic debris and dead ice left behind by melting glaciers. It is therefore questionable whether rock glaciers of comparable size can be found north of Cerro Aconcagua or Cerro Mercedario (32° S), where the extent of late Quaternary glaciations rapidly diminishes.

2.3.5 The highest peaks: Glaciers versus rock glaciers

The highest mountains of the area, which are mainly situated on the continental divide and in the Node of Juncal, present large valley glaciers especially in south and southeast exposition. These glaciers, together with local late Quaternary volcanic activity and the morphodynamic effects of more extensive Holocene glacier advances, reduce both the number and size of the remaining potential rock glacier niches. Similar effects will be discussed in more detail in section 2.4.1 in the context of the Cerro El Moño area, which is situated close to the southern limit of rock glacier distribution.

2.3.6 D. Andina and Los Bronces: large-scale mining in periglacial environments

In the area of Los Bronces and División Andina mines (figure 2.13, rock glaciers were studied for the first time in Chile in the 1950s by the French glaciologist L. Lliboutry (Lliboutry, 1953, 1956, 1961, 1986). The area was later also visited by D. Barsch in 1982 (compare the photographs of Barsch 1988 and Barsch 1996a, p. 26), at a time when morphology still had not been much altered by mining. Since then, the tremendous growth of both copper mines situated in the area mapped by Lliboutry has pro-

duced a strong geomorphological impact, which shall be studied in this section. Along with the mining activities, geophysical studies have been executed, which have only partly been published. Some of the few published results will be recalled in the present section.

Excursus: Historical background

The historical development of the Los Bronces mine started in the 1830s at several small copper and silver extraction sites situated around 3500 m a. s. l. Exxon Minerals, the former owner of the mining company Disputada de Las Condes and of the Los Bronces mine, in the 1980s initiated a process of modernization that increased copper production (Editec, 2000; Minería Chilena, 1993). Disputada belongs since 2001 to the South African company Angloamerican.

Just north of Los Bronces, the state-owned Corporación Nacional del Cobre de Chile (Codelco) exploits at División Andina in the upper Blanco catchment (Aconcagua drainage basin) the same copper reserve as Disputada de Las Condes. In 1980, open-pit mining of high-grade minerals began at the Sur-Sur pit (Arcadis Geotécnica, 2001). Since then, several expansion projects have boosted copper production with the goal of reaching an output of 400,000 t a^{-1} of refined copper from 2006 on (Arcadis Geotécnica, 2001; Editec, 2000; Holmgren and Vela, 1991).

Figure C.6 (page 131) gives a cartographic impression of the development of the mining activities at Los Bronces and División Andina since 1955 and shows the original distribution of rock glaciers in the area.

Removal and alteration of rock glaciers

The vast rock glacier areas in the upper Blanco catchment have been affected by mining activities at least since the Sur-Sur pit of División Andina began to operate in 1980. Since then, two rock glaciers have disappeared almost completely compared to the situation found by Lliboutry (1961) (figure C.6, table 2.9).

Codelco is currently implementing an expansion project at División Andina, which provides for an enlargement of the Sur-Sur mine to a total area of 375 ha and the construction of two new waste rock disposal areas with a total surface of 497 ha, according to the corresponding environmental impact study (Arcadis Geotécnica, 2001; table 2.9). The operations imply the destruction or degradation of about 1.4 km^2 of rock glaciers present in the area, according to the same study, which was approved by the environmental agency Comisión Nacional del Medio Ambiente (Conama).

In the area of the Los Bronces mine of Disputada de Las Condes, a comparison of aerial photographs of 1955 and 1997 shows that rock glaciers have also been removed and altered there (table 2.9). Most information available from Los Bronces concerns however the deposition of waste rock on top of the Infiernillo rock glacier since 1990.

Infiernillo rock glacier creep

The Infiernillo rock glacier is an active tongue-shaped multi-part rock glacier of 2.5 km of length. It extends from $\sim$3600 to 4300 m a. s. l. covering 1.0 km^2. The rock glacier's rooting zone is situated within a cirque between Cerro Fortuna (4611 m) and Cerro La Paloma (4860 m), and its tongue leans against a west-exposed valley side producing a very high and long lateral slope to-

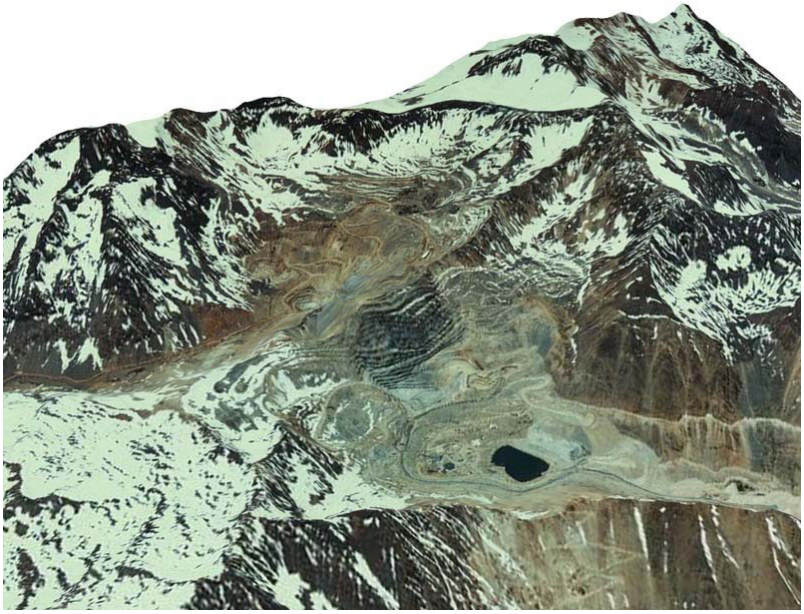

Figure 2.13: Perspective view of Los Bronces (foreground) and División Andina (left, middleground) mines, generated from a Conaf-Conama aerial photograph (2001) and SRTM elevation data.

		Andina	Los Bronces
Original rock glacier area[a]	[km^2]	2.6	1.9
Alteration until 1997[a]			
— Removed by open-pit mining	[km^2]	0.5	0.2
— Covered by waste rock deposits	[km^2]	—	0.2
— Affected by mining infrastructure	[km^2]	0.2	0.4
Water equivalent affected until 1997[b]	[10^6 m^3]	6 – 12	7 – 14
Alteration 1997–2005[c]			
— Removed by open-pit mining	[km^2]	0.82	n/a
— Degraded (waste rock, infrastructure)	[km^2]	0.58	n/a
Water equivalent affected 1997–2005[b]	[10^6 m^3]	12 – 24	n/a

Table 2.9: Rock glacier area and water equivalent affected by División Andina and Los Bronces mines.

Remarks: [a] Own calculations based on aerial photographs (Hycon 1955, Geotec 1997) and the environmental impact studies of Geotécnica Consultores (1996) and Arcadis Geotécnica (2001). [b] Own calculations assuming an average thickness of the ice-rich permafrost of 20–40 m, an ice content of 50 % and an ice density of 0.9 g cm^{-3}. [c] Expansion project of División Andina, data from Arcadis Geotécnica (2001).

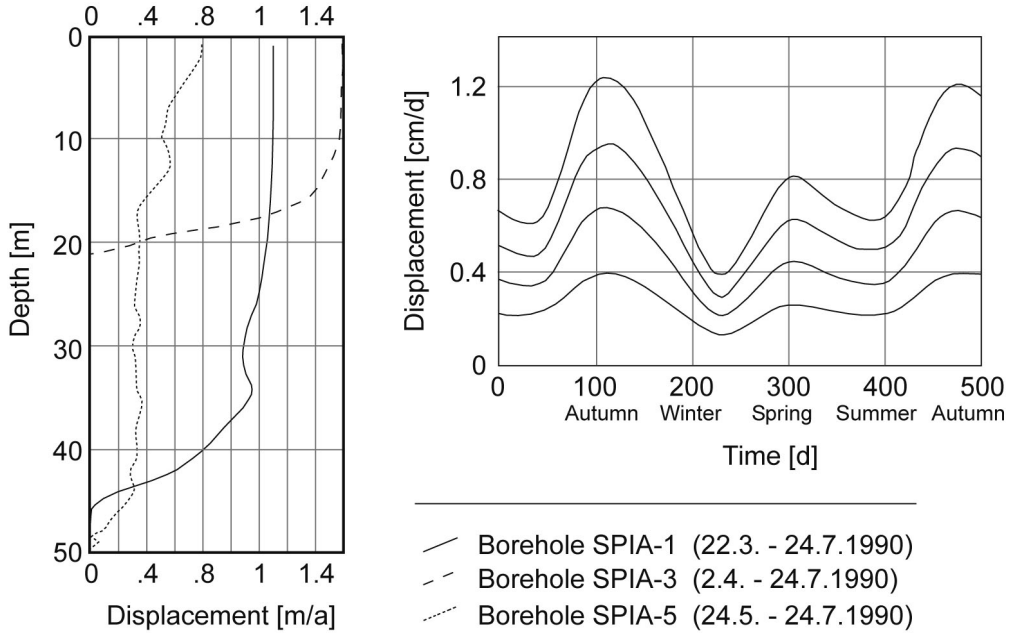

Figure 2.14: Horizontal displacement rates of Infiernillo rock glacier, Los Bronces mine, after Contreras and Illanes (1992). Left: Displacement rates within three boreholes during autumn 1990 before the beginning of the disposal of waste rock on the rock glacier. Right: The natural regime of superficial displacement at four control points; the original temporal resolution of measurements is unknown.

wards the valley floor. This flow pattern might be explained in the following way: The debris mantle of the lateral slope is thicker than at the front slope, thus increasing downslope friction and favoring cross-slope displacement and rock glacier elongation.

The upper central part ($\sim$0.2 km^2) of the Infiernillo rock glacier at $\sim$4000 m a. s. l. has been covered with waste rock from Los Bronces since August 1990. Its displacement has been monitored at several topographic points and boreholes since before the beginning of the deposition; the results have partly been published by Contreras and Illanes (1992) (figure 2.14).

According to Contreras and Illanes (1992), the rock glacier mainly consists of granular material cemented by ice. Furthermore, there exist lenses of clear ice of up to 12 m of thickness. The rock glacier's superficial debris mantle is 1–3 m thick, and its mean thickness is 35 m.

Superficial displacement ranged between 0.3 and 1.2 cm d^{-1} under natural (pre-depositional) conditions, and reflect strong seasonal variation with highest velocities in spring and especially autumn, confirming observations made in other places (Barsch, 1996a; Barsch and Hell, 1975; Haeberli, 1985; no seasonal differences were in contrast encountered by Roer 2003).

Pre-depositional creep rates measured in boreholes on the Infiernillo rock glacier show a general decrease of velocity with depth, with greatest vertical changes within 5–10 m above the base and almost constant velocities at smaller depths. Borehole SPIA-5 constitutes an exception, since the velocity decrease concentrates at two depths, 12–16 m below the surface and at the base (45–

49 m), suggesting the presence of a shear plane within the rock glacier (cf. Arenson et al. 2002).

The initial deposition of 14 million tons of waste rock led to a strong increase in rock glacier surface velocity up to 20 cm d^{-1} immediately after deposition. Velocities stabilized afterwards, but on a higher level than before the deposition (Contreras and Illanes, 1992). The further development of waste rock deposition and creep rates has not been published, but it was originally planned to add another 30 million tons of waste between 1992 and 1997.

The artificial deposition of debris on a rock glacier may have several long-term effects, some of which are rather speculative until now. First, geochemical weathering of the waste rock is likely to produce acid rock drainage (ARD) that may affect water discharge from the rock glacier even after mine closure (Andía et al., 1999; EPA, 2001; Ripley et al., 1995). Second, natural geothermal heating may raise the lower permafrost boundary within decades after deposition and affect rock glacier stability, which is partially temperature-driven (Burger et al., 1999). Third, new permafrost may develop within years to decades within the waste rock. This permafrost is however not likely to be ice-rich due to its distance from the rock glacier's rooting zone and the artificial compactation of the deposited material, and it will probably be patchy and present varying ice contents depending on local material properties. (Compare however Grebenets et al. 1998 for an example of the development of a fast-moving rock glacier out of mine waste rock.)

Conclusions

The periglacial environment of División Andina and Los Bronces has strongly been intervened by large-scale mining. The potential hydrological and geomorphological hazards would inevitably affect the adjacent lowlands. The effects of mining on rock glaciers has seldom been discussed in the scientific literature or in the Chilean public so far.

2.3.7 Cerro Catedral: a huge relict rock glacier

Cerro Catedral is a 4765 m high peak situated on the southern limit of the Maipo catchment towards the Cachapoal catchment. It is characterized by steep rock faces and pointed rock towers (figure 2.15).

Glaciers

Just below the summit of Cerro Catedral, a south-exposed glacier of 0.2 km^2 extends down to 4080 m a. s. l. (Marangunic, 1979), where it ends in a glacier fall. This glacier fall nourishes one of three debris-covered glaciers south of Cerro Catedral (figure C.7). The lowest termini reach ∼2950 m a. s. l. Further glaciers exist north of Cerro Catedral on the eastern side of a ridge (0.1 km^2), and east of the summit in a north-exposed cirque (1.6 km^2), extending down to 3710 m a. s. l. (Marangunic, 1979). In contrast to this, glaciers are absent in the upper Blanco catchment on the north and northwest side of Cerro Catedral.

In the western Blanco catchment, a partly debris-covered glacier of 0.5 km^2 in size can be recognized in an air photo of the year 1955 (cf. Marangunic 1979). This glacier has disappeared since then, leaving a fresh frontal moraine at 3050 m

a)

b)

Figure 2.15: a) Active rock glaciers no. 185–187 on the west side of Cerro Catedral (34° 12′ S, 70° 05′ W; 4765 m) above 3500 m a. s. l.
b) The front of rock glacier no. 57, with a height of more than 100 m.
Photographs: 5 Mar 2002.

	Number of features	Area [km^2]	[%]	Water equiv. [10^6 m^3]
Intact rock glaciers	13	2.3	9	36–53

Table 2.10: Areas and water equivalence of intact rock glaciers in the upper Río Blanco catchment (24 km^2), Cerro Catedral area. Assumptions: See table 2.1.

a)

b)

Figure 2.16: a) Initial rock glacier no. 102 at ∼3600 m a. s. l. in SW-exposition; note the outflow of permafrost meltwater from the scree slope above and to the right of the rock glacier.
b) Rock glacier no. 177, west side of Cerro Catedral. Part of the rock glacier is covered with rock fall debris of up to 2 m in diameter.
Photographs: 3/4 Mar 2002.

a. s. l. (figure C.7).

On the south side of Cerro Catedral, lateral and frontal moraines indicate presumably Holocene glacier extents. Two well-developed debris rock glaciers grow out of such lateral moraines. If their development had started during the first cool–moist pulse of the LIA in the 14th century (compare section 1.3.3; Jenny et al., 2002; Röthlisberger, 1986), average rock glacier advance rates of 60–70 cm a^{-1} were required. These values are high, but possible (Barsch, 1996a), and impose a minimum age on the corresponding glacier advance.

Rock glaciers

While on the south side of Cerro Catedral medium-sized debris rock glaciers occupy only the gaps between currently glacierized areas down to 3120 m a. s. l., the upper Blanco catchment is characterized by an abundant rock glacier distribution (figures C.7 and 2.10, table 2.10). Active rock glaciers reach down to 3250–3300 m a. s. l. and fill several now glacier-free cirques. The largest features appear

to have originated as debris rock glaciers, although talus is now supplied directly from the cirque walls (figure 2.15). Sequences of relict, inactive and active rock glaciers are frequent.

An active initial talus rock glacier (no. 192) is situated at 3600 m a. s. l. in west exposition (figure 2.16). The recent activity of this small feature indicates that permafrost at this altitude is not restricted to huge (and therefore old, persistent) rock glaciers representing a smoothed and delayed climate signal.

Palaeoclimatic implications of the Catedral rock glacier

Turning to the most prominent rock glaciers in the mapped area, the valley on the northwest side of Cerro Catedral presents a unique series of relict, inactive and active rock glaciers in an altitudinal range between 2630 and almost 4000 m a. s. l. The lower, relict rock glacier complex consists of three superimposed tongue-shaped features with a total length of 2.2 km and approximate front heights of 150 m (lowest) and 80 m (middle and upper fronts), respectively. The complex ends upvalley at 3350 m a. s. l., where it is superimposed by an inactive feature. Active units (no. 57) follow above ∼3430 m a. s. l. The largest active front is more than 100 m high, and boulders were frequently released from its front scarp during the field visit (figure 2.15).

The altitudinal depression of the relict with respect to the active rock glacier unit amounts to ∼800 m. This suggests a temperature depression of about 5.5°C at the time of activity of the lowest relict unit. The modern regional MAAT of ∼7°C at 2630 m a. s. l. suggests even a greater thermal discrepancy. Consequently the position of the relict rock glacier probably corresponds to thermal conditions of the Late Glacial of possibly of the Last Glacial Temperature Minimum (Brenning, 2005a). For the latter, a temperature depression of 6–8°C in Central Chile has been derived from geomorphological and palynological findings (Garleff and Stingl, 1985; Heusser, 1983, 1990; Veit, 1991, 1993).

2.3.8 Remarks on periglacial microforms

While patterned ground and stone-banked gelifluction terraces are particularly well-developed in the high Arid Andes (Schröder, 1999, 2001; Schröder and Makki, 1998), these features are usually less prominent in the Andes of Santiago (cf. Lliboutry 1961). The following paragraphs present three examples of microform occurrences in this area.

Periglacial processes at low elevations on Cerro San Ramón

In the south-exposed cirque of Cerro San Ramón, stone-banked terraces and shallow sorted striped ground with between-stripe distances of about 10 cm can be observed. In addition, in March 2004 needle-ice (pipkrake) of about 2–3 cm of length was widespread within several meters from the cirque's lakes. It had formed overnight, and melted down very quickly as soon as the sun reached the place. Needle-ice formation is conditioned by the presence of fines and abundant soil moisture near the lakes, and it is apparently favored by topoclimatic conditions that allow for nocturnal frost at this altitude in late summer.

Patterned ground and earth hummocks at Cerro Catedral

The distribution of periglacial microforms at Cerro Catedral is restricted to relatively fine-grained morainic deposits. In addition to several forms of patterned ground and shallow stone-banked terraces, several earth hummocks are present at ∼3500 m a. s. l. (figure 2.17). The latter are found in an area with good availability of fine-grained, wet material, where a small meltwater creek originates diffusely. The earth hummocks are attributed to cryoturbation within the seasonally frozen ground layer.

Earthy and stony mounds in the Cerro La Parva area

In the study area of Cerro La Parva, a variety of stony to earthy mounds has developed on the surface of the lowest rock glacier unit (no. 164) at ∼3200 m a. s. l. (figure 2.17). These features are adjacent to the steepest part of a superimposed lateral rock glacier slope, inclined 46°. Only few, small features consist mainly of fines and pebbles, and contrast with the stony rock glacier surface. The mounds are ∼0.3–2 m high. Taking into account the presence of active creeping permafrost in the immediate surroundings, cryoturbation is made responsible for the development of the mounds (cf. Pollard 1988; Schunke and Zoltai 1988).

General remarks

In the Andes of Santiago, shallow periglacial microforms exist locally in south exposition above 3000 m and become more widespread above 3500 m a. s. l. The occurrences are restricted to finer-grained material and gentle slopes. Especially morainic material on cirque floors, and local weathering products on cols are suitable combinations of material and topography.

Figure 2.17: (Figure on the next page.)
a) Earthy patterned ground on morainic debris at 3500 m a. s. l. showing two nested patterns (Cerro Catedral area). The inner (unsorted) earth polygons are about 15–20 cm in diameter; sorting of stone nets reaches only about 5 cm of depth.
b) Earth hummocks at 3500 m a. s. l. just before the toe of rock glacier no. 185. Photographs: 5 Mar 2002.
c–d) Earthy and stony frost mounds west of rock glacier no. 164 at ∼3200 m a. s. l., and the lateral rock glacier slope with 46° of inclination (Cerro La Parva area). The mounds in photograph c) are up to 2 m high, the earth hummock on the d) about 30 cm. Photographs: 4 Apr 2002.

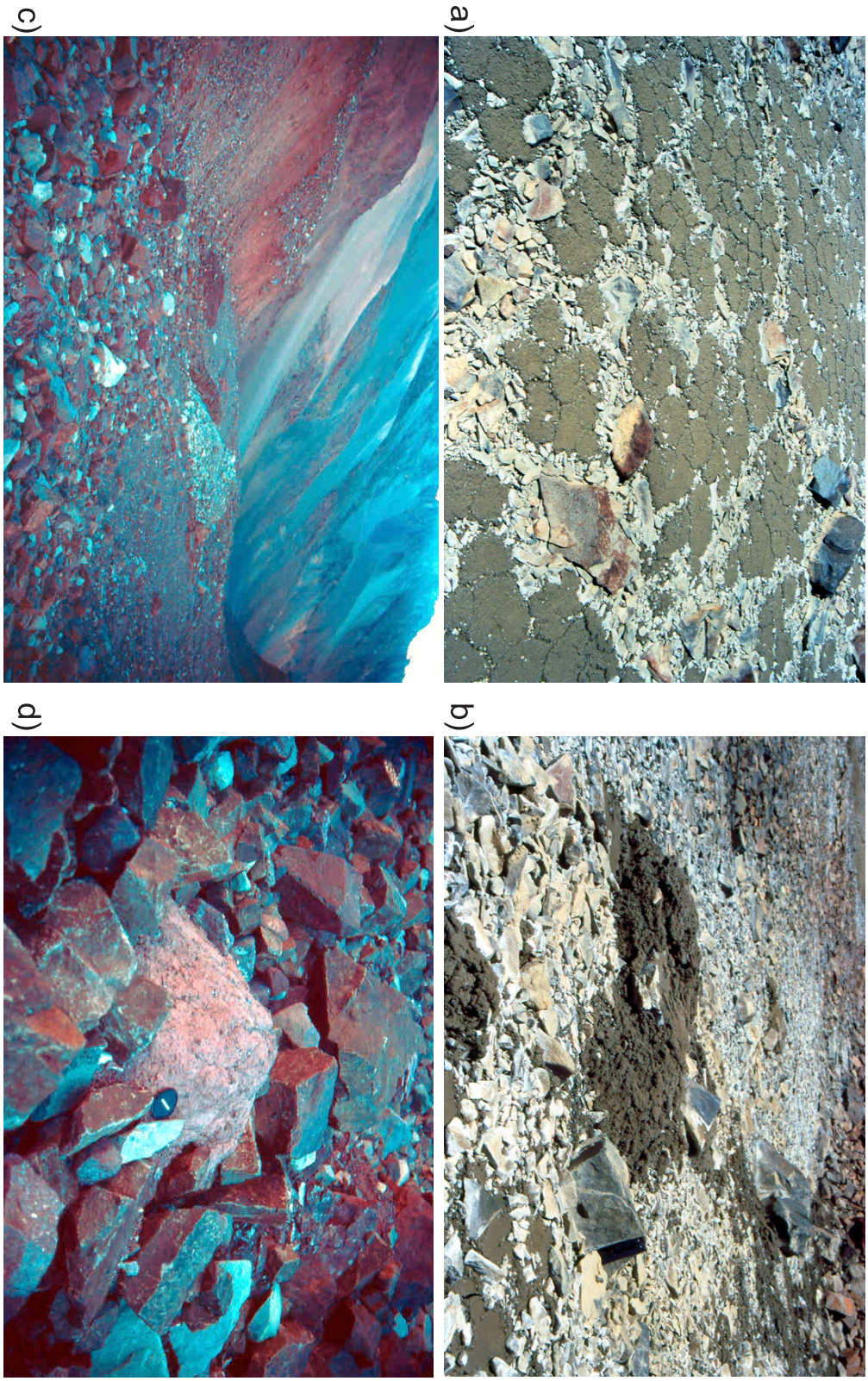

(Figure caption on previous page.)

2.4 South of Santiago

2.4.1 Cerro El Moño and Volcán Tinguiririca: rock glaciers on the defensive

As mentioned earlier, south of the Andes of Santiago summit elevations decrease, while climatic conditions become more favorable for glaciers, and volcanism becomes a more characteristic Holocene landforming process. The area of Volcán Tinguiririca (4280 m) and Cerro El Moño (4699 m a. s. l.) is a good example of both phenomena. Only few other mountains in the region reach altitudes that are comparable to those studied in the Andes of Santiago. The present section focuses on the Río de las Damas catchment, which runs parallel to the continental divide in southward direction.

The Tinguiririca Massif, which is built up by Quaternary and late Tertiary volcanic rocks, has had at least one eruption in historic times, and a solfatar on its west side is continuously active (González-Ferrán, 1994; Lankenau, 1958). Furthermore, a late-glacial volcanic debris flow (*lahar*) started at the west side of the volcano and strongly impacted upon the lower Tinguiririca valley (Abele, 1979, 1982; Marangunic et al., 1979).

In contrast to the volcanic complex in the western part of the Damas catchment, its eastern side exposes clastic marine sedimentary rocks and volcanic rocks of Jurassic age (Formación Río Damas; Charrier et al., 1996).

Glaciation and glacier retreat

The Damas valley hosts several glaciers, the largest of which are the southeast-exposed Palacios and Pincheira valley glaciers (*c.* 3.8 and 3.9 km^2, respectively) descending from the Tinguiririca Massif (figure C.8 on page 134). Both glaciers have retreated during the 20th century (Brüggen, 1929; Lankenau, 1958; Valdivia, 1984b). Fresh lateral and frontal moraines in the Damas and Palacios valleys indicate the extent of Holocene, presumably Little Ice Age glacier advances (table 2.11, figure 2.18).

The 2950 m moraine of the Pincheira glacier (or unified Damas glacier) divides the Damas valley in an upper part that is characterized by very dynamic modern paraglacial processes and moraines, and a lower part, where valley sides already present more regular talus slopes (figure 2.18). Therefore the 2950 m Damas moraine probably indicates the Holocene maximum glacier extent.

Rock glaciers on the defensive

As a consequence of the strong fluvioglacial and paraglacial activity in the upper Damas valley, rock glacier development is restricted to elevations above 3200 m a. s. l. (figure C.8). This lower limit is, according to air photo interpretation, also representative for the neighboring valleys. On the other hand, modern glaciers occupy potential morphographic rock glacier niches such as cirques and valley heads to a much greater extent than east of Santiago due to the lower snow-line in the Tinguiririca area.

Although the mentioned processes restrict rock glacier distribution macroscopically from above and from below, the most significant restriction of rock glacier distribution occurs in the potential altitudinal zone of rock glacier development itself: This zone is being "invaded" and fragmented. Rock glacier distribution is therefore limited to ap-

	Terminus altitude [m a. s. l.]				Volume loss	
	LIA?[a]	$\leq$ 1939[b]	1955[a,c]	1997[a]	Absolute[d] [km^3]	Relative[e]
Palacios	2600	2700	2900	3150	0.04	0.1
Pincheira	2950		3150	3400	0.06	0.2

Table 2.11: Retreat of the Palacios and Pincheira glaciers of Cerro Tinguiririca.
Remarks: [a] Own estimates; "LIA?" extent according to fresh, undated moraines. [b] Brüggen (1929); Lankenau (1958). [c] Valdivia (1984b). [d] Using the size–thickness relation of Chen and Ohmura (1990), and glacier sizes of Valdivia (1984b) for 1955, and own size estimates for 1997. [e] Expressed as proportion; the use of percentages is avoided since the actual precision does not justify the use of two digits.

a)

b)

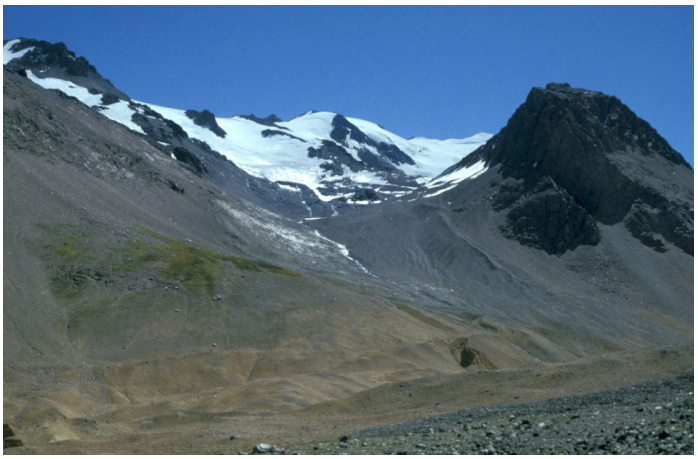

Figure 2.18: a) The glacial trough of the lower Damas valley, looking downvalley from the front slope of rock glacier no. 198. On the valley floor at the right hand side, the 2950 m Damas moraine is visible.
b) Lateral moraines on the eastern side of Volcán Tinguiririca, built up by an eastern (secondary) tongue of the Palacios glacier. In the main valley (Río de las Damas), the 2950 m moraine of the Pincheira glacier can be seen. Photographs: 20 Mar 2002.

	Number of features	Area [km^2]	[%]	Water equiv. [10^6 m^3]
Intact rock glaciers	7	1.0	2	14–21
Glaciers	12	12.9	22	455
Thermokarst areas	1	0.3	< 1	6

Table 2.12: Areas and water equivalence of intact rock glaciers, glaciers and thermokarst in the upper Río de las Damas catchment (59 km^2), Cerro El Moño area. Assumptions: See table 2.1.

a)

b)

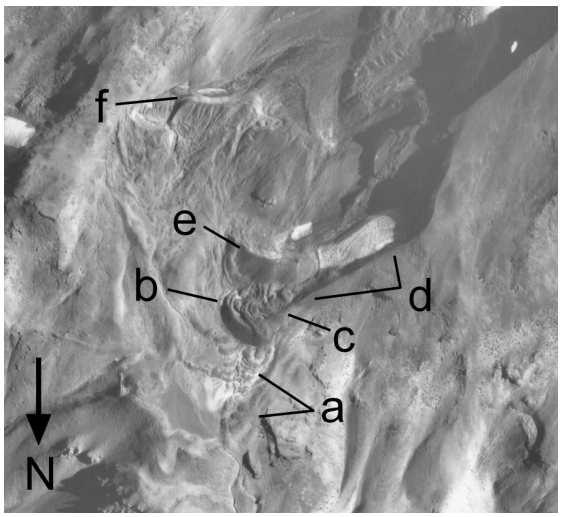

Figure 2.19: a) Volcán Planchón with the Lagunas del Teno seen from north. Photograph: 14 Feb 2002.
b) Glacial and periglacial geomorphology of the northern cirque of Volcán Planchón. a: relict rock glaciers; b: active rock glacier, toe at 3060 m a. s. l.; c: lateral moraine; d: ridge; e, f: frontal moraines. Aerial photograph: SAF, 1997.

propriate slopes and subcatchments (especially hanging valleys) with minor fluvioglacial, paraglacial and glacial influence.

2.4.2 Volcán Planchón: the southern limit of rock glacier distribution

The Planchón–Peteroa volcano complex is the southernmost study area considered in this work, since it constitutes the southern limit of intact rock glacier distribution in the Central Chilean Andes (figure 2.19). The complex has been built up during the Pleistocene on top of a tectonically deformed, stratified (sedimentary and volcanic) Mesozoic and Tertiary basement (Naranjo et al., 1999). While the southern Peteroa summit (35° 17′ S, 70° 35′ W, 4101 m), which has become inactive during the Pleistocene, has been strongly eroded by glaciers and presents an important modern glacierization, Volcán Planchón (35° 13′ S, 70° 34′ W, 3920 m) last erupted in 1991 and possesses only a small plateau glacier surrounding the craters south of the summit area (Naranjo and Haller, 2002; Naranjo et al., 1999).

Quaternary relief development in the area of the volcano complex is characterized not only by the direct impact of lava flows and ash eruptions. A Holocene (after 5000 BP; González-Ferrán, 1994) volcanic debris flow (*lahar*) originated in a collapse at Volcán Planchón and reached the Chilean Central Depression at 95 km of distance. Moreover, a prehistoric landslide has dammed the Lagunas del Teno north of Volcán Planchón within a glacial trough (Abele, 1981, 1984; Naranjo et al., 1999).

Modern glaciers at the volcanic complex extend down to ∼3000 m a. s. l. mainly on the west and south side of Volcán Peteroa and around the craters of Volcán Planchón (Naranjo et al., 1999). The north-exposed cirque of Volcán Planchón is currently not glacierized, but it presents significant firn fields above 3000 m a. s. l.

Two probably active rock glaciers exist on the Chilean side of Volcán Planchón, both on its northern slope: The lower one is a debris rock glaciers extending down to 3060 m a. s. l. (figure 2.19), and the other one an initial talus rock glacier at ∼3500 m a. s. l. Another active feature exists on the eastern, Argentinian slope of Volcán Planchón at ∼3250 m a. s. l. The rock glaciers on the northern side of Volcán Planchón are —according to thorough interpretation of aerial photographs of the surrounding areas— the southernmost active rock glaciers of Central Chile and most likely of the entire country (Brenning et al., 2005).

The presence of extended, thick perennial snow fields in the surroundings of the debris rock glacier suggests its coexistence with non-creeping discontinuous permafrost.

The unfavorable conditions for rock glacier development at the Planchón–Peteroa complex and in its surroundings are attributed to the following reasons (Brenning et al., 2005): Similar to the Cerro El Moño area (section 2.4.1), glaciofluvial processes become dominant on the glacierized west and south side of the volcano complex (but not at its north face). Furthermore, the area is to a great extent covered with young volcanics, which are relatively resistent to weathering in comparison to the Mesozoic and Cenozoic sedimentary and volcanic rocks that prevail in the Andes of Santiago. In addition, direct impact of frequent volcanic action (25 eruptions of Planchón–Peteroa, Descabezado Grande and Quizapu volcanoes during the last 200 years; González-Ferrán,

1994; Naranjo et al., 1999) and geothermal heating have to be taken into account as factors that may inhibit the development of creeping permafrost. Last but not least, potential rock glacier and permafrost areas become rather rare south of the Planchón–Peteroa complex, because only the highest summits in that area surpass an elevation of 3000 m a. s. l.

In the Argentinian Andes of El Sosneado and Malargüe between 35° 0′ S and 35° 30′ S, in contrast, the elevation of Volcán Planchón is surpassed by several peaks, among them Cerro Las Leñas (4234 m) and Cerro Serrucho (4173 m). Because of the generally higher elevation of this mountain range, the minor volcanic influence and lower precipitation, it is believed that rock glaciers in this area extend southward to 35° 25′ S (Brenning et al., 2005). South of this latitude, lower elevations and Holocene volcanism also impede the development of rock glaciers on the Argentinian side. On the eastern, leeward flank of the Patagonian Andes, active rock glaciers may appear again.

2.5 Discussion

2.5.1 Central Chile

On a supra-regional scale, rock glacier distribution is mainly controlled by the following factors related to climate, geomorphological processes and topography (figure 2.20):

Temperature. The lower limit of abundant active rock glacier distribution ("LRG" in figure 2.20) follows a slightly positive air isotherm in the semi-arid Andes, and shifts to clearly negative MAAT levels as aridity increases northward. The lowest intact occurrences are particularly lowered in the Andes of Santiago (next section).

Past glaciations. Glacial landforms, especially cirques, are appropriate morphographic niches for rock glacier development. Past glaciations have furthermore provided important amounts of source material for rock glacier development. Arid conditions during the late Quaternary constitute therefore a disadvantage especially near the South American Arid Diagonal.

Modern and subrecent glaciation. Glacial, fluvioglacial and paraglacial processes of modern and late Holocene glaciation restrict rock glacier development. These limiting factors are particularly important on the highest mountains of the Andes of Santiago, and south of 34.5° S towards the southern distributional limit.

Talus supply. Paraglacial denudation of steep glacial troughs and cirque walls provides a better talus supply than non-glacial, often rectilinear slopes of the arid Andes (compare Chapter 4).

Volcanism. Young volcanism restricts rock glacier development either directly through catastrophic mass movements, or indirectly due to the largely divergent topography of volcano cones, and weathering-resistant young rock. Volcanism plays a major role at the southern limit of the study area, and to a minor degree in the northern part.

In summary, the late Quaternary aridity is a major direct and indirect limiting factor for rock glacier development near the Arid Diagonal. The morphography of volcano cones and relatively low denudation rates may play an additional role.

At the southern limit, in contrast, the lowering topography implies by itself certain rarity of potential rock glacier niches. Active young volcanism and late Holocene glaciation impose further important limitations. The southern limit is not primarily a climatic one.

2.5.2 Andes of Santiago

Topography and modern glacierization are the dominant controls of rock glacier distribution in the Andes of Santiago. In general an asymmetric zonation of rock glaciers in south/southeast versus north/northwest exposition can be observed: In south-oriented valleys, rock glaciers are limited to low elevation sites often with particular topographic and topoclimatic conditions. In north exposition, in contrast, distribution is shifted upward and is not seriously restricted by glaciation.

Table 2.13 summarizes the vertical association of forms and processes in the Andes of Santiago and Mendoza. Based on the distribution of (especially small) rock glaciers, snow and firn fields

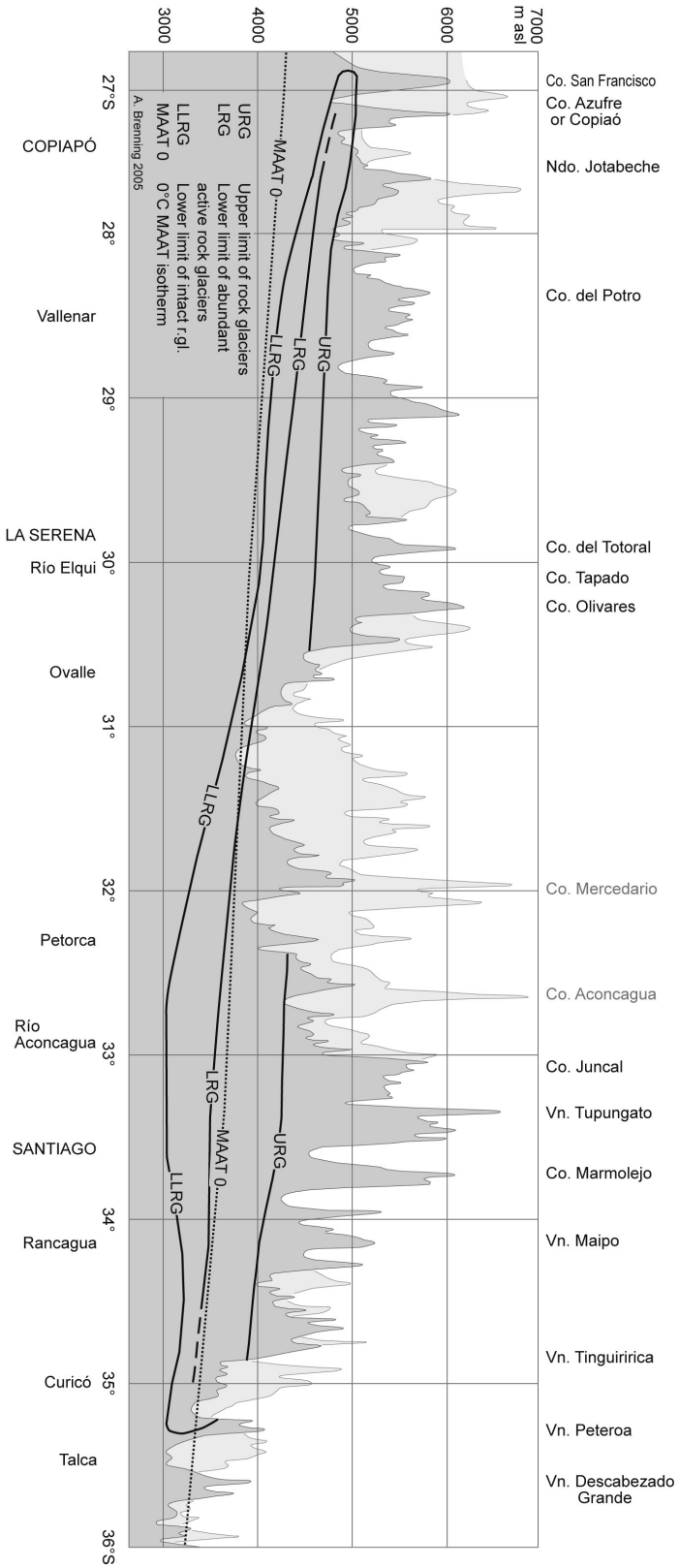

Figure 2.20: North–south profile of rock glacier distribution in Central Chile. The black and grey lines represent maximum elevation in the Chilean and Argentinian Andes, respectively.

Andes of Santiago	Andes of Mendoza	Phenomenon
3800–4000	4200–4400	Regional ELA
		Cols mostly snow-free up to 4200 m a. s. l.
3600–4000		ELA range of Echaurren glacier (mean: 3800 m)
4250	4500	Upper limit of active rock glaciers
∼3600		0°C isotherm
3500	3750	Lower limit of abundant active rock glaciers
3300–3500		Lower limit of the periglacial belt
3000	3100	Lower limit of patterned ground and needle ice
3000–3200	3200–3400	Lower limit of sporadic active rock glaciers
3000–3300/3500		Andean–periglacial transition zone
3000/3600		Lower limit of perennial snow in S/N exposure
∼2900		Lower limit of the Juncal Norte glacier
3000–3300		Upper limit of the Andean belt (steppe-like vegetation)

Table 2.13: Modern altitudinal zonation in the Andes of Santiago and Mendoza (32.5°–34.5° S). The Argentinian Precordillera is not included. Sources: Present work, Lliboutry (1956) and Ahumada (1992).

and other observations (see e. g. section 2.3.2), it is proposed that permafrost is discontinuous above 3500 m a. s. l. and sporadic down to 3000 m in south exposition. On north-facing slopes, in contrast, these zones may shift at least 200–300 m upwards according to rock glacier distribution, or by more than 500 m if firn fields are used as indicators.

Regarding rock glacier ages, intact rock glaciers can in most cases be assigned to the Holocene. The existence of hypsometric rock glacier sequences as well as the association with moraines of Holocene glacier advances indicate however that many active rock glaciers are much younger. The existence of active initial rock glaciers indicates a continuing development of new rock glaciers.

Inactive rock glaciers are situated about 100–200 m lower than nearby active features, suggesting a climate variability of ~ -1°C during the Holocene. Relict rock glaciers can in some cases be attributed to the Late Glacial, though Holocene ages may not be excluded at the moment.

Finally, the quantitative evaluation of rock glacier and glacier distribution as shown in figure 2.2 (page 27) and 2.10 (page 40) are characterized by a great variability depending on topographic conditions. They are therefore hardly suited for drawing quantitative conclusions on a regional scale and motivate the use of statistical methods to achieve more general results.

Chapter 3

Statistical modelling of rock glacier distribution in the Andes of Santiago

Turning from individual catchments to the regional scale, the fundamental difference between mapping and statistical approaches used in the present work should be recalled. The goal of the last Chapter was to derive geomorphological interpretations from observed and secondary information on rock glaciers and their environments. Especially the validity of quantitative results is restricted to the selected mapping areas. Therefore the interpretations on a regional scale were mainly qualitative.

In contrast to this, the present chapter covers a vast area —the Andes of Santiago (and Mendoza)— by means of a sample of surface locations and associated terrain parameters. This sample is used in the quantitative statistical estimation of total rock glacier, glacier and other areas (section 3.1), and in the analysis of rock glacier distribution with logistic regression (section 3.2). While these two methods focus on the areal distribution of rock glaciers, a third approach is applied to statistically analyze the population of rock glaciers and their morphographic site characteristics (section 3.3).

Though the present work focuses on the Chilean Andes of Santiago, the Argentinian Andes of Mendoza are included in the following analyses. This is due to two reasons: First, a trans-Andean analysis is of scientific interest since it follows a strong humidity gradient under otherwise comparable conditions. Second, the independent subsurveys on both sides of the Andes provide an opportunity for model validation.

3.1 Statistical estimation of the areal distribution

3.1.1 Method

The statistical land cover survey is based upon estimators of proportions for a stratified random sampling design. The corresponding theory of statistical sampling and estimation is fully explained e. g. by Raj (1968) or Thompson (2002).

Stratification was used in order to obtain uniform precision in different elevations and terrain orientations. It was implemented with respect to elevation and aspect classes based upon DEMs of 90 and 100 m of resolution[1]. Elevation classes comprise 250 m intervals between 2750 and 4250 m a. s. l., and one single class for elevations $\geq$4250 m. Aspect classes correspond to 90° sectors centered at the geographic main directions. The sampling area extends below the actual hypsometric range of intact rock glaciers because relict rock glaciers were also intended to be considered, and possible intact rock glacier occurrences below 3000 m a. s. l. should not be excluded in advance.

Independent surveys were executed for the Chilean and Argentinian part of the study area, the Argentinian area being situated 29 km further to the north due to different air photo availability[2] (table 3.1). The independent subsurveys were executed by the present author during summer 2003 for the Chilean area (Brenning, 2005a), and for the Argentinian part during a one-week stay in March 2004 at the Instituto Argentino de Nivología y Glaciología (Mendoza).

1105 and 823 sampling points were evaluated in the Chilean and Argentinian part of the study area, respectively. At the sampling points, land cover was examined by visual interpretation of aerial photographs, using SRTM DEMs and derived contour lines and in Chile also topographic maps for locating the points within the air photos (Appendix A).

The classes "intact rock glacier", "glacier" (including debris-covered glaciers), "thermokarst" (i. e. massive ice with well-developed thermokarst features), "debris" and "rock" were distinguished. No distinction was made between active and inactive rock glaciers due to the limitations inherent to air photo interpretation. Relict rock glaciers were not included in the final analyses since the recognition of these features is subject to great uncertainties at the given scale ($\sim$1:50,000). The differentiation of (debris-covered) glaciers and thermokarst areas has earlier been applied in Argentinian glacier inventories (Corte and Espizua, 1981). It appears to be useful since it is independent of a genetic interpretation or of a dynamic classification as a stagnant or active part of a glacier (Clayton 1964; compare section 1.4.2).

At 40 Chilean and 14 Argentinian sampling locations, an interpretation was not possible, mostly due to shadow in the air photo. These sampling points had to be excluded from further analyses. This may lead to a slight underestimation of rock glacier areas because typical rock glacier niches in cirques and below rock faces are more prone to receiving shadow than more exposed surfaces. A systematic analysis of shadow orientation or flight times has not been performed.

[1] An SRTM DEMs was used for the Argentinian side; in the Andes of Santiago, a contour line DEM of similar quality as SRTM data was originally used for stratified sampling. SRTM DEMs were used for any further analysis in the whole study area.

[2] This may account for a regional ELA shift of 70 m (compare figure 1.7 on p. 12).

	Andes of Santiago	Andes of Mendoza
Northern limit	6348 km / 33° 00′ S	6377 km / 32° 45′ S
Southern limit	6181 km / 34° 30′ S	6210 km / 34° 15′ S
Area [km^2]		
— above 4000 m	957	3167
— above 3000 m	4682	7254
— above 2750 m	5644	7860
Sampling points	1105	823
Sampled rock glaciers	58	32

Table 3.1: Descriptive data on the statistical modelling area and sample summary data. UTM coordinates refer to UTM Zone 19S, PSAD 1956.

At further 37 Chilean and 33 Argentinian locations, classification could not be made unambiguously because of positional or interpretative uncertainties. This concerns e. g. the rooting zones of rock glaciers, the differentiation of rock glaciers from thermokarst areas, and in general the borders between discrete features. A Monte Carlo approach was used in order to account for this uncertainty in the estimation of proportions, performing independent simulations with equal probabilities assigned to the different interpretative alternatives.

For an appropriate interpretation of the quantitative results it is anticipated that the recognition of rock glaciers smaller than 0.02 km^2 in the Andes of Santiago is clearly incomplete. This interpretation that is based upon a critical examination of the sample. A comparison of rock glacier size distributions on both sides of the Andes suggests that the Argentinian sample is less accurate, being substantially complete for rock glaciers larger than 0.1 km^2 and incomplete below this conservative (i. e. possibly too high) threshold. Note that glaciers are not affected by these problems because of their greater size (by definition $\geq$ 0.1 km^2 according to Haeberli 2000) and better recognition in aerial photographs.

For trans-Andean comparisons, rock glacier samples are therefore filtered with a size threshold of 0.1 km^2. Unfiltered data are used to obtain less conservative estimates of rock glacier areas in the Andes of Santiago.

In addition to area estimates, the water equivalent stored within rock glaciers was estimated based upon simple assumptions. For the ice-rich rock glacier permafrost, an ice content of 40–60 % and an ice density of 0.9 g/cm^3 were assumed (table 2.1 on p. 24; cf. Brenning 2005a). The thickness of this permafrost body was assumed to be 30 m on average; this value is in agreement with the mean value of the conservative size–thickness relationship from table 2.1 weighted according to the empirical size distribution of the rock glacier sample (described later in section 3.3).

The statistical confidence limits indicated in this section can be regarded as too wide (i. e. too pessimistic) since the sampled features have a spatial extent and therefore induce a spatial autocorrelation structure.

3.1.2 Results

Figure 3.1 shows the statistically estimated rock glacier, thermokarst and glacier distribution in the Andes of Santiago and Mendoza.

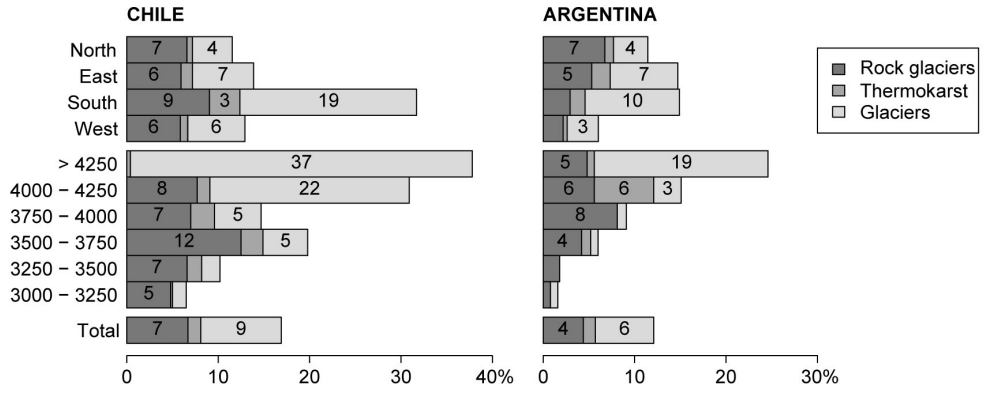

Figure 3.1: Distribution of rock glaciers, thermokarst areas and glaciers in the Andes of Santiago and Mendoza as related to altitude and aspect, without applying rock glacier size thresholds. For an estimation based on rock glaciers $\geq 0.1\,\mathrm{km}^2$ only, refer to the upper panels of figure 3.6 on p. 78. In the present figure, 90 % confidence intervals are in the order of ± 3 to ± 4 % within each elevation class, and ± 1 to ± 1.5 % for the totals.

Glaciers and thermokarst

In the Argentinian part of the study area, glaciers become abundant at least 250 m higher than in the Andes of Santiago. In addition, Chilean glaciers and thermokarst areas reach much lower altitudes than Argentinian ones, and they occupy greater areas at comparable altitudes. These observations clearly reflect the increasing aridity and the eastward rise of the ELA.

Glacier abundance is greatest in south exposure. Although solar radiation patterns may explain this distribution, it also has to be taken into account that valley geometry is anisotropic especially on the Chilean side. In particular, south-exposed Pleistocene cirques and geologically-induced southward draining valleys favor modern south-exposed glaciers.

Interestingly, in the Andes of Mendoza east exposure is more favorable for glacierization than west exposure. This is attributed to the fact that Argentina comprises only the eastern flank of the highly glacierized main chain of the Andes, which strongly contributes to the overall glacierization of the Andes of Mendoza. A complementary effect is not observed on the Chilean side, possibly because of the existence of an additional strongly glacierized area around Cerro Altar (5180 m) and a generally greater abundance of glaciers on the western side.

Rock glaciers

The hypsometric optimum zone of rock glacier abundance on the Chilean side is situated ∼250 m lower than in the Andes of Mendoza (figure 3.1). The difference in total rock glacier areas in Chile and Argentina is not significant for rock glaciers greater than $0.1\,\mathrm{km}^2$ (figure 3.6 on p. 78).

Rock glacier distribution as related to terrain aspect shows contradictory patterns on both side of the Andes. This may be due to topographic effects. Logistic regression analysis will give better insights into these patterns.

Regarding the altitudinal zonation of

the western and eastern Andes, both areas present a belt where rock glaciers predominate over glaciers, followed by a transition zone near the glacier ELA, and a belt where glaciers clearly prevail.

Rock glacier water equivalent

While rock glaciers cover almost the same total area as glaciers in the study area, the amount of water stored within them is much lower due to lower ice contents and smaller thicknesses. In total, water equivalence of rock glaciers in the Chilean and Argentinian part of the study area reach 3.4–5.1 and 3.5–5.2 km^3, respectively (90 % confidence intervals). If related to the total area above 3000 and 3250 m a. s. l., respectively, this corresponds to 0.7–1.1 and 0.5–0.8 km^3 per 1000 km^2 (Chile/Argentina). The actual values for the Andes of Mendoza will be approximately equal to the Chilean estimates because of the aforementioned incompleteness in the case of small Argentinian rock glaciers.

3.1.3 A brief discussion

The statistical land cover survey proved to be an efficient tool for providing quantitative data on the overall distribution of rock glaciers and other geomorphological features. Genetic interpretations of the estimated distribution are however very limited.

3.2 Logistic regression modelling with morphometric parameters

The goal of the present section is to find a statistical model that explains the observed distribution of rock glaciers in the Andes of Santiago and Mendoza in terms of morphometric and climatic variables. Such a model will be mainly of analytical value since it characterizes the geomorphological niche of rock glaciers. It should in addition be able to "predict" (in a statistical sense) potential areas of rock glacier development.

It is therefore intended to indentify morphographic and climatic controls on rock glacier distribution (Brenning, 2005b). It is not desired to determine a possible morphometric signature of these rock glaciers themselves within a DEM.

3.2.1 Introduction

Logistic regression models are special generalized linear models that can be used for analyzing and predicting binary outcome variables Y such as the presence ($Y = 1$) versus the absence ($Y = 0$) of rock glaciers (Brenning, 2004a), landslides (Ohlmacher and Davis, 2003) or other environmental phenomena (Keating and Cherry, 2004; Lewkowicz and Ednie, 2004; Luoto et al., 2004; Luoto and Hjort, 2004), although their main fields of application are in biostatistics and econometrics (Collett, 1991; Hosmer and Lemeshow, 2000; McCullagh and Nelder, 1990; Menard, 1995). These models can be used for statistically analyzing and predicting the conditional probability

$$\pi(\mathbf{x}) = P(Y = 1 \,|\, \mathbf{x})$$

given a set of p explanatory variables $\mathbf{x} = (x_1, \ldots, x_p)^T$. Instead of modelling $\pi(\mathbf{x})$ linearly, which could lead to meaningless probabilities greater than 1 or below 0, logistic regression uses the so-called *logits*:

$$\text{logit}(\mathbf{x}) := \ln\left(\frac{\pi(\mathbf{x})}{1 - \pi(\mathbf{x})}\right) \qquad (3.1)$$

for $\pi(\mathbf{x}) \in]0, 1[$. Logits are unbounded quantities. In logistic regression, logits are modelled linearly by

$$\text{logit}(\mathbf{x}) = \beta^T \mathbf{x},$$

where β is a coefficient vector determining the weight of each explanatory variable within the model.

Changes in the explanatory variables have a nonlinear effect on the conditional probability $\pi(\mathbf{x})$, which is best understood by looking at the odds instead of the probabilities. The quantity $\pi(\mathbf{x})/(1 - \pi(\mathbf{x}))$ in formula (3.1) is called the *odds* of $\pi(\mathbf{x})$. It may range between 0 (for $\pi(\mathbf{x}) = 0$) and $+\infty$ (for $\pi(\mathbf{x}) \to 1$). For the ith variable x_i, a coefficient of $\beta_i = 2$ would imply a change in the odds by the factor $\exp(2)$ per unit increase of the explanatory variable x_i.

The textbook of Hosmer and Lemeshow (2000) is a good reference for further technical and interpretative details.

3.2.2 Method

Separate logistic regression models were fitted for the presence–absence variables corresponding to rock glaciers, glaciers and exposed bedrock. Data from the Andes of Santiago and Mendoza were pooled in the analyses. The hierarchical relationship between the land cover classes was honored in the following way: Since rock glaciers cannot form on exposed bedrock or on glacierized

Local morphometry	
X	Easting [m]
Y	Northing [m]
Z	Elevation [m]
ARGENTINA	1, if located in Argentina, 0 otherwise
SLP	Slope [°]
NORTH	"Northexposedness": sin(aspect); aspect according to Zevenbergen and Thorne (1987)
WEST	"Westexposedness": $-\cos(90° - \text{aspect})$
CVX	Convergence index (Köthe and Lehmeier, 1994; negative: convergent; positive: divergent)
CPROF	Profile curvature (positive: convex)
CPLAN	Plan curvature (positive: divergent)
SOLRAD	Potential incoming solar radiation [kWh/m^2] for January and February as computed with SAGA
Characteristics of the contributing area	
CA.AREA	Size of the contributing area [m^2]
CA.SLP	Mean slope [°] of the contributing area
CA.NORTH	Mean "northexposedness" of the contributing area
CA.WEST	Mean "westexposedness" of the contributing area
CA.HGT	Maximum altitudinal difference within the contributing area
Variables from smoothed data	
SM4.*	As above, but computed for a smoothed DEM using a simple mean filter of radius 450 m
Transformed variables	
ctrY	Centered northing (see below) [10^{-4} m]
ctrSOLRAD	Centered SOLRAD variable (see below) [kWh/m^2]
CA.AREA.LL	ln(ln(CA.AREA))
SM4.CA.AREA.LL	ln(ln(SM4.CA.AREA))
MODZ5	Transformed elevation (see below), considering an eastward offset of 250 m per 60 km and a power transformation with exponent 0.25 in altitudinal direction (see below and in the text)
MODAREA	Transformed contributing area (see below)
MODSLP	Transformed mean slope of the contributing area (see below)
CA.HGT.P04	$\text{CA.HGT}^{0.4}$

where

$$
\begin{aligned}
\texttt{ctrSOLRAD} &= \texttt{SOLRAD} - 413, \\
\texttt{ctrY} &= (\texttt{Y} - 6275000)/10000, \\
\texttt{MODZ5} &= \left(\left| \texttt{Z} - 3000 - \frac{250}{60000}(\texttt{X} - 390000) \right| /100 \right)^{0.25}, \\
&\quad \text{if the base is positive, and 0 otherwise;} \\
\texttt{MODSLP} &= |\texttt{SM4.CA.SLP} - 20|, \\
\texttt{MODAREA} &= \begin{cases} 2.6 - \ln(\ln(\texttt{SM4.CA.AREA})) & \text{if } \ln(\ln(\texttt{SM4.CA.AREA})) \leq 2.6, \\ (\ln(\ln(\texttt{SM4.CA.AREA})) - 2.6)/2 & \text{otherwise.} \end{cases}
\end{aligned}
$$

Table 3.2: Variables used for logistic regression modelling. (Interaction terms are not listed here, but were also considered in model selection.)

surfaces, they were only discriminated against samples belonging to the class "debris". Glaciers were discriminated against the superset of "debris", "exposed bedrock" and "rock glacier" data, because they can form on top of any surface type. Consequently the rock distribution model was fitted only to glacier-free sampling points.

The models for glacier and rock distribution are intended to serve as simple "masks" for predicted rock glacier distribution without having to perform comprehensive analyses of remotely-sensed data. The glacier inventories of the area (Corte and Espizua, 1981; Marangunic, 1979) were not available as digital geodata; its limited precision and the methodological differences between Chilean and Argentinian inventories would have imposed serious constraints. The respective model fitting results will be discussed briefly.

The regression analysis was limited to rock glaciers of at least 0.1 km^2 in order to ensure homogeneous data in both parts of the study area (see section 3.1). Furthermore, ambiguous observations were excluded.

Thermokarst areas were not modelled because of their genetic particularities and the too small portion of presence data (cf. Whitemore 1981).

Explanatory variables

Only relief parameters —including potential solar radiation and several transformed parameters— were examined as possible covariates in the exploratory analysis and model selection process. Table 3.2 lists all variables considered, some of which were not established *a priori* but adjusted during exploratory data analysis and model fitting.

The set of variables contains parameters that were computed at the actual resolution of the projected SRTM DEM (90 m; compare Appendix A.3) as well as variables derived from a smoothed DEM, but also others corresponding to a DEM. This DEM was generated with a simple filter of radius 450 m in order to eliminate possible effects of medium-sized rock glaciers on the DEM and hence on the relief parameters. This step appears to be mandatory since the goal of this study consists of finding environmental controls on rock glacier distribution, not the morphographic representation of rock glaciers within the DEM.

Since the dependence of rock glacier distribution on elevation and easting is nonlinear (figure 3.1), a transform of elevation (`MODZ5`) was systematically designed in order to honor the mentioned relation. This was done by means of minimization of the Akaike Information Criterion (AIC) as a function of elevation and eastward gradient (figure 3.2, table 3.2). Other transforms (`MODSLP`, `MODAREA`, `[SM4.]CA.AREA.LL`) were adjusted by visual inspection of exploratory scatter plots and the comparison of model fit AIC for several alternative transformed variables.

Lithology was not included in the analysis because of the lack of adequate and homogeneous geological data for the study area. It also has to be pointed out that geological units generally extend in north–south direction, which leads to a great potential of confounding with other parameters, especially easting and, due to the north–south aligned main range, with elevation.

Model selection was performed interactively by hand. An automatic stepwise selection procedure was not fruitful because of the presence of strongly correlated pairs of explanatory variables (figure 3.3) and the need of carefully including meaningful interaction terms and transformed variables (figure 3.2).

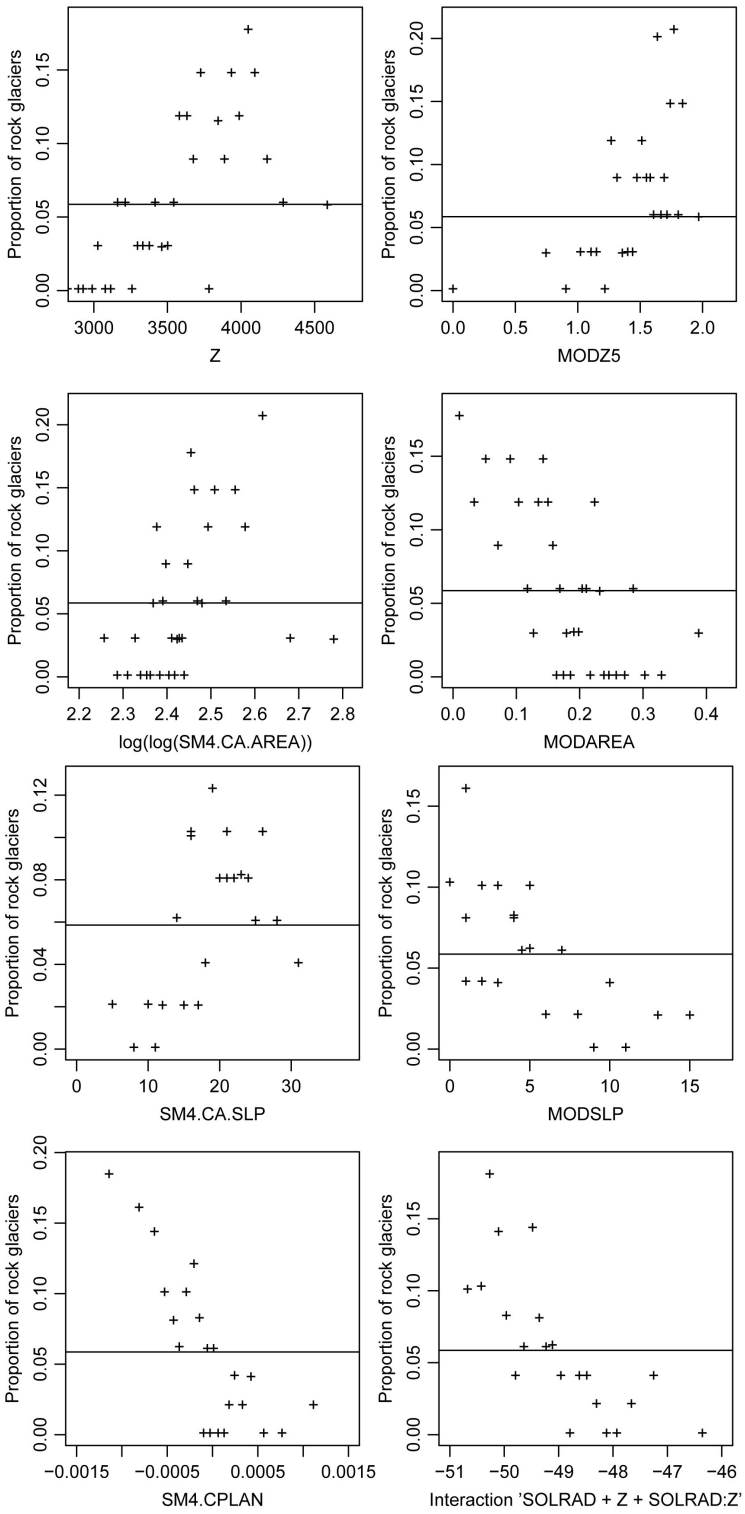

Figure 3.2: Selected plots from the exploratory data analysis relating rock glacier distribution to relief parameters and their transforms. Refer to table 3.2 for variable definitions.

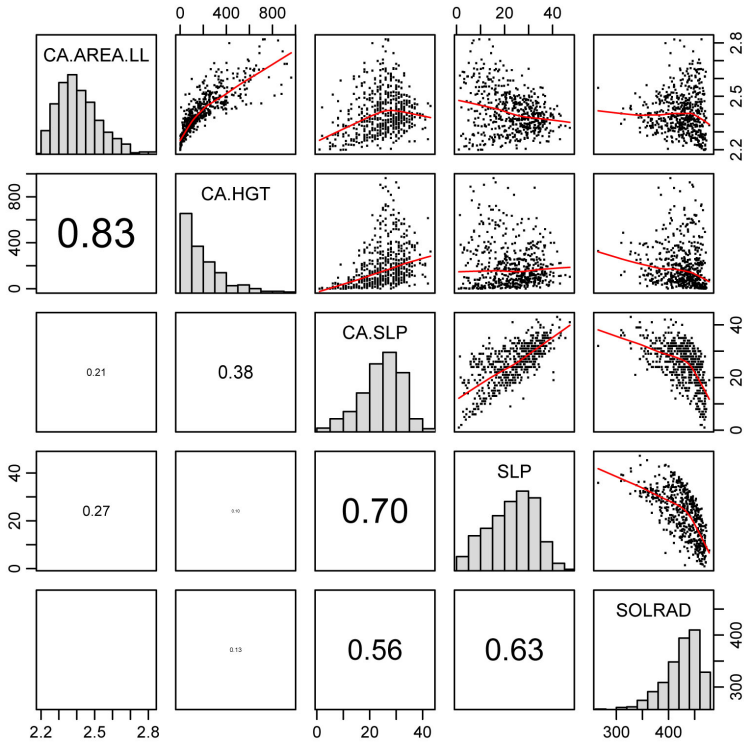

Figure 3.3: Scatter plots (upper right panels) and correlation coefficients (lower left panels) of selected groups of relief parameters for the stratified random sample. Font sizes of correlation coefficients are proportional to their values. Refer to table 3.2 for variable definitions.

The AIC, which "penalizes" for the addition of variables, was the main criterion for variable selection. Regarding the level of significance required for including variables in the model, a p-value of 0.05 was chosen.

Prediction and validation

The overall capability of discrimination of a model was measured by the area under the receiver operator characteristic (ROC) curve (Hosmer and Lemeshow, 2000), which is abbreviated as AUC value. The AUC can range between 0.5 (no separation) and 1.0 (complete separation).

In addition to classical parametric significance tests for explanatory variables, the final model variables were also tested using bootstrap techniques (Efron and Tibshirani, 1986, 1993). These are computationally intensive methods that are independent of distributional assumptions and more robust than standard methods. In the present work, the data were resampled 1000 times to get bootstrap samples.

After fitting the logistic regression models, these were used for the spatial prediction of rock glacier, glacier and rock probabilities based upon relief parameter grids. In order to obtain areas with "likely" occurrence of the mentioned features, probability thresholds were determined that comply with the condition of fitting the total areas as obtained from statistical estimation. Consistently with the already mentioned hierarchical relation between glacier, bedrock, and rock glacier surfaces, model calibration was performed in this order, predicted glacier and rock areas being masked in the calibration of rock glacier predictions. The probability

thresholds obtained will be referred to as area-preserving thresholds.

Model predictions are compared to mapping results in terms of ROC curves and AUC values, i. e. regarding the trade-off between sensitivity (probability of correctly predicting a rock glacier) and specificity (probability of correctly predicting the absence of a rock glacier).

3.2.3 Results

The following sections present and interpret the fitted models for rock glacier, glacier and rock distribution. Table 3.3 summarizes model structure, while table 3.4 and figure 3.5 give a less technical insight into the model results.

Glaciers

The model selected for the glacier occurrences (versus debris, rock and rock glacier samples) achieved an AUC value of 0.95, which is termed "outstanding" by Hosmer and Lemeshow (2000).

According to the model, which is summarized in tables 3.3 and 3.4, west-southwest-exposed high-elevation sites are most likely to be glacierized. Preferred contributing areas are large in vertical extent (and area; compare the relationship between both in figure 3.3) and show rather small average slope inclinations. These relations reflect the fact that the presence of a large (hence less steep), high-elevation accumulation area favors the extension of the glacier down to relatively low altitudes.

Regarding the regional distribution patterns, there is a decrease in glacier abundance towards the north (`ctrY`). The variable `ARGENTINA` reflects the contrast between the more oceanic and humid Chilean side and the drier and more continental Argentinian part of the study area. However, it does not represent this effect *ceteris paribus*, since for instance east-facing surfaces are more frequent on the Argentinian side.

Bootstrapping confirmed the significance of all selected explanatory variables as well as the AUC value.

Model calibration yielded a probability threshold of 0.86, which honors the statistically estimated total glacier area. The predicted glacier distribution fits the true pattern quite well (figures 3.4, 3.5, 3.6). However, high-elevation glacier occurrences are overestimated, and small low-elevation glaciers are not always predicted satisfactorily. Regarding the first issue, this is attributed to the relative small number of sampling points above the regional ELA, which is a consequence of the focus on rock glaciers between 3000 and 4000 m a. s. l. Small low-elevation glaciers such as the Echaurren glacier or the glaciers of Cerro Punta Negra are, in contrast, often subject to particular mass-balance conditions including the influence of avalanche accumulation or debris-covers reducing ablation. These effects are not appropriately reflected by the simple statistical model, which is not capable of predicting the Echaurren glacier and the glacier on the eastern side of Cerro Punta Negra, while the predicted glacier on the southern side of Cerro Punta Negra includes an actual thermokarst (dead-ice?) area and firn fields (figure 3.5, figure C.4, section 2.3.2).

Exposed bedrock

The overall fit of the bedrock distribution model turned out to be "excellent" (AUC = 0.85).

Since the presence of exposed bedrock is assumed to be mainly controlled and reflected by local morphometry, variables related to the contributing area and the smoothed variables `SM4.*` were

TA-1 — Rock glaciers — AUC 0.83		
Variable	Coefficient	Multiplicative change of the odds
`Intercept`	-4.5	
`MODZ5`	2.7	(In the western Andes:) 4250 vs. 3750 m: 1.83; 3250 vs. 3750 m: 0.34
`MODAREA`	-11	0.4 vs. 0.7 km^2: 0.62; 1.0 vs. 0.7 km^2: 0.56; 3 vs. 0.7 km^2: 0.1
`ARGENTINA`	-0.88	0.42 (Argentina vs. Chile)
TA-2 — Rock glaciers — AUC 0.84 [0.81–0.89] 95 % bootstrap confidence interval		
Variable	Coefficient	Multiplicative change of the odds
`Intercept`	$(-8.7 \cdot 10^2)$	(not significant, p-value > 0.9)
`Z`	$-2.7 \cdot 10^{-3}$	(See MODZ5)
`MODZ5`	5.5	Joint effect of `MODZ5` and `Z`, in the western Andes: 4250 vs. 3750 m: 0.91; 3250 vs. 3750 m: 0.43
`MODAREA`	-7.0	0.4 vs. 0.7 km^2: 0.74; 1.0 vs. 0.7 km^2: 0.70; 3.0 vs. 0.7 km^2: 0.24
`SM4.CPLAN`	$-9.9 \cdot 10^2$	0.59 per 1 std. dev. increase
`ctrSOLRAD`	$-9.6 \cdot 10^{-2}$	Joint effect of `ctrSOLRAD` and `ctrSOLRAD:Z` at 3500 m: 0.68 on average north-facing surfaces with respect to south-exposed surfaces
`ctrSOLRAD:Z`	$2.5 \cdot 10^{-5}$	The effect of `ctrSOLRAD` decreases as elevation increases.
TA-G2 — Glaciers — AUC 0.95		
Variable	Coefficient	Multiplicative change of the odds
`Intercept`	-19	
`Z`	$3.8 \cdot 10^{-3}$	0.68 per 100 m decrease
`ctrY`	$-5.9 \cdot 10^{-2}$	0.55 per 100 km toward the north
`ctrY:ARGENTINA`	-0.12	further 0.30 per 100 km toward the north in Argentina
`ARGENTINA`	-2.7	0.07 (Argentina vs. Chile)
`CA.SLP`	$-9.3 \cdot 10^{-2}$	0.63 per 5° increase
`CA.NORTH`	-0.92	0.16 (north vs. south exposed contrib. areas)
`CA.WEST`	1.6	0.04 (east vs. west exposed contrib. areas)
`CA.HGT.P04`	0.49	200 m vs. 500 m height of contrib. area: 0.16
TA-R2 — Exposed Bedrock — AUC 0.85		
Variable	Coefficient	Multiplicative change of the odds
`Intercept`	-7.854	
`Z`	$1.267 \cdot 10^{-3}$	0.88 per 100 m decrease
`SLP`	0.1013	0.60 per 5° decrease
`CVX`	$2.748 \cdot 10^{-2}$	0.59 per 1 std. dev. decrease
`CPROF`	$2.042 \cdot 10^2$	0.65 per 1 std. dev. decrease
`ARGENTINA`	-0.7728	0.46 (Argentina vs. Chile)
`ctrSOLRAD:ARGENTINA`	$-1.649 \cdot 10^{-2}$	0.51 per 1 std. dev. increase in Argentina

Table 3.3: Fitted logistic regression models for rock glacier, glacier and bedrock distribution. In the model formulas, "`A:B`" refers to the interaction term of variables `A` and `B`. Refer to table 3.4 for a less technical summary.

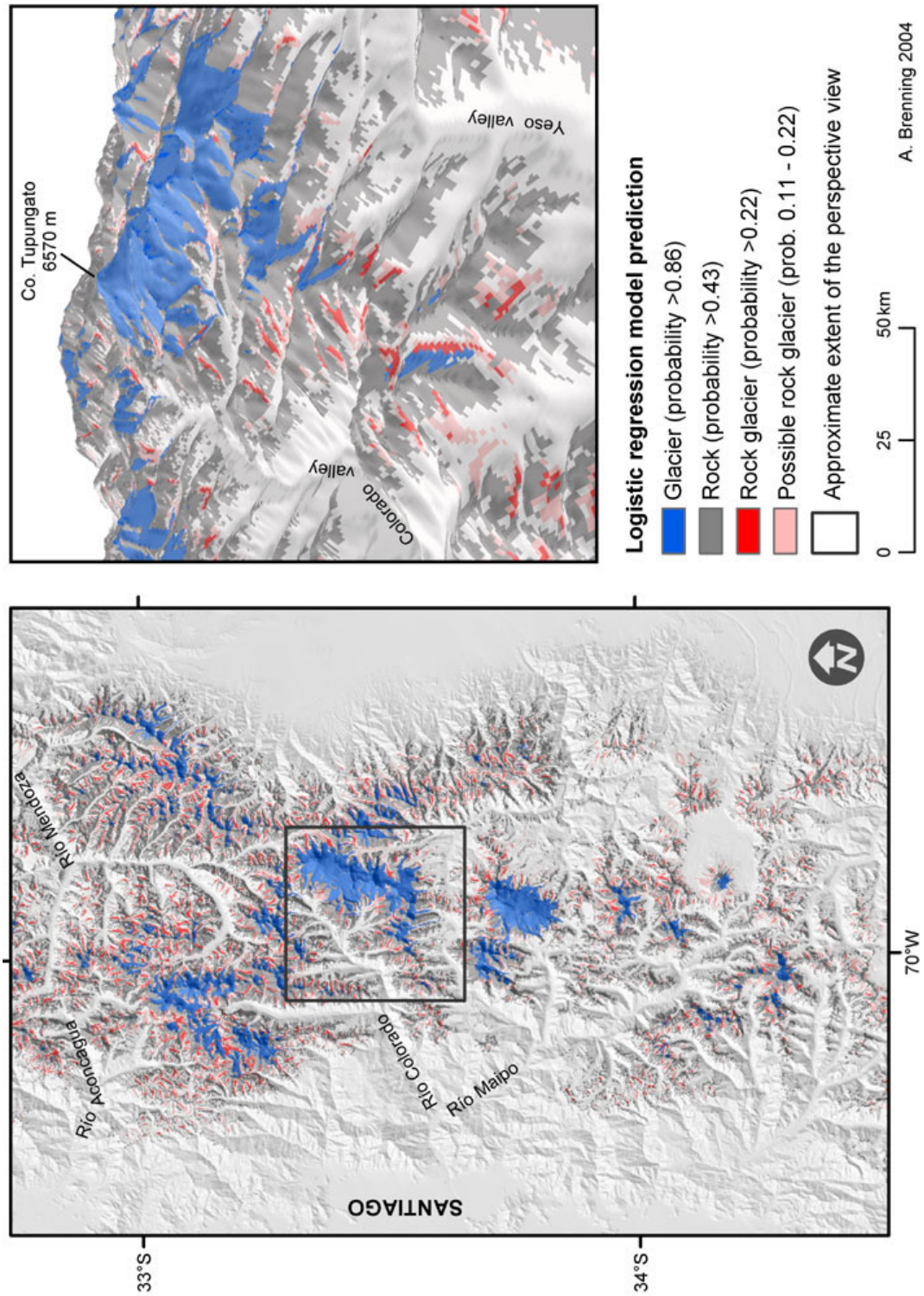

Figure 3.4: Statistical prediction of rockglacierized, glacierized and bedrock areas. Right: Overview and perspective view of the upper Río Yeso and Colorado catchments.

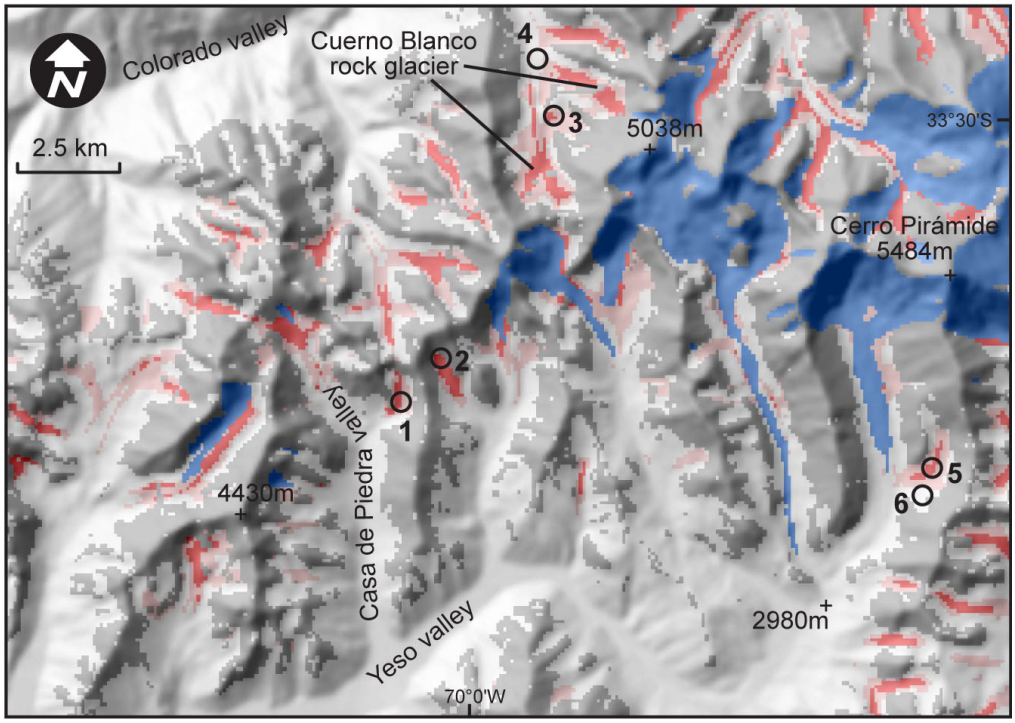

Site no. (see prediction map)	[1]	[2]	[3]	[4]	[5]	[6]
Site type	Cirque	Cirque	Huge r. gl.	Valley	Cirque	Slope
Terrain parameters[a]						
Elevation [m a. s. l.]	*3210*	**3500**	**3770**	**3420**	**3800**	**3770**
Contributing area	**Medium**	*Small*	**Medium**	*Large*	Medium	*Small*
— [km^2]	0.5	0.2	0.5	7.7	0.3	0.1
Potential solar radiation	**Very low**	**Very low**	High	*High*[b]	High	High
Plan curvature	**Strongly conv.**	**Strongly conv.**	Weakly conv.	**Convergent**	Weakly conv.	Weakly conv.
Logit-scale contribution of covariates						
Elevation (`MODZ5, Z`)	*−2.54*	**−1.41**	**−1.11**	**−1.59**	**−1.28**	**−1.30**
Contributing area (`MODAREA`)	**−0.16**	*−0.77*	**−0.22**	*−2.30*	−0.47	*−1.09*
Radiation (`ctrSOLRAD, ctrSOLRAD:Z`)	**0.62**	**0.28**	−0.02	*−0.27*[b]	−0.01	−0.03
Plan curvature (`SM4.CPLAN`)	**1.39**	**1.49**	0.40	**0.99**	0.59	0.30
Logit[c]	−0.77	−0.51	−1.04	−3.25	−1.26	−2.22
Probability	0.32	0.38	0.26	0.04	0.23	0.10
Predicted feature	Rock gl.	Rock gl.	Rock gl.	Debris	Rock gl.	Debris
Observed feature	Rock gl.	Debris	Rock gl.	Debris	Rock gl.	Debris

Figure 3.5: Map: Prediction of rockglacierized and glacierized areas and bedrock in the upper Río Yeso catchment based upon logistic regression models TA-2, TA-G2, and TA-R2 (table 3.3). A symbology is shown in figure 3.4.
Table: Predicted changes in the odds, logits, and rock glacier probabilities at example sites, according to model TA-2. Favorable characteristics are printed in bold type, unfavorable ones in italic.

Remarks: [a] Terrain parameters are shown in qualitative terms to facilitate interpretation. [b] In this case, high radiation is unfavorable due to the rather low elevation (interaction with `Z`). [c] The logits are the sum of the logit-scale contributions of covariates plus the constant intercept of −0.087 shown in table 3.3 for model TA-2.

ROCK GLACIERS	
Elevation	3500–3800 m a. s. l. in the western part, and $>$ 3750 m a. s. l. in the eastern part
Size of contributing area	0.5 – 1 km^2
Solar radiation	Low, if at low elevations
Plan curvature	Convergent
GLACIERS	
Elevation	As high as possible
Exposition	Westsouthwest
Slope within contributing area	Low inclination
Size of contributing area	As large as possible
Vertical difference within contrib. area	As large as possible
EXPOSED BEDROCK	
Elevation	As high as possible
Slope	High inclination
Curvature	Divergent and convex
Solar radiation	Low

Table 3.4: Qualitative summary of morphographic conditions that are best for the presence of rock glaciers, glaciers and exposed bedrock based upon logistic regression models.

not considered.

The distribution of exposed bedrock can be explained very well by slope, curvature, elevation, and, on the Argentinian side, potential solar radiation. The interaction of the latter with the variable `ARGENTINA` may be due to different climatic or geological conditions related to weathering.

The area-preserving threshold for discriminating rock and non-rock areas is 0.43. Predicted rock distribution showed an excellent agreement with field observations, aerial photographs and topographic maps. In the author's view, the representation of rock surfaces in Chilean topographic maps 1:50,000 is only slightly better than the model predictions.

Rock glaciers

Two alternative rock glacier distribution models will be presented here (table 3.3). The first one, TA-1, is very simple, but its adjustment to the data is close to the fit of the more complex model TA-2. In both cases, the AUC values of 0.83 and 0.84, respectively, are "excellent". All of the final model variables are significant at the 95 % level with respect to parametric and bootstrapped confidence limits. The bootstrapped AUC confidence limits of model TA-2 extend from 0.81 to 0.89 at the 95 % level).

Numeric examples that illustrate the functioning of model TA-2 in a predictive context are shown in figure 3.5.

The most difficult task in fitting an appropriate rock glacier model is that of finding a suitable representation of elevation that honors the eastward shift in the altitudinal distribution (figure 3.1; section 3.2.2). A comparison of several variable transformation approaches as well as the use of numerical optimization with respect to AIC have lead to the choice of a power transformation of a rescaled elevation parameter, which in addition is linearly shifted in

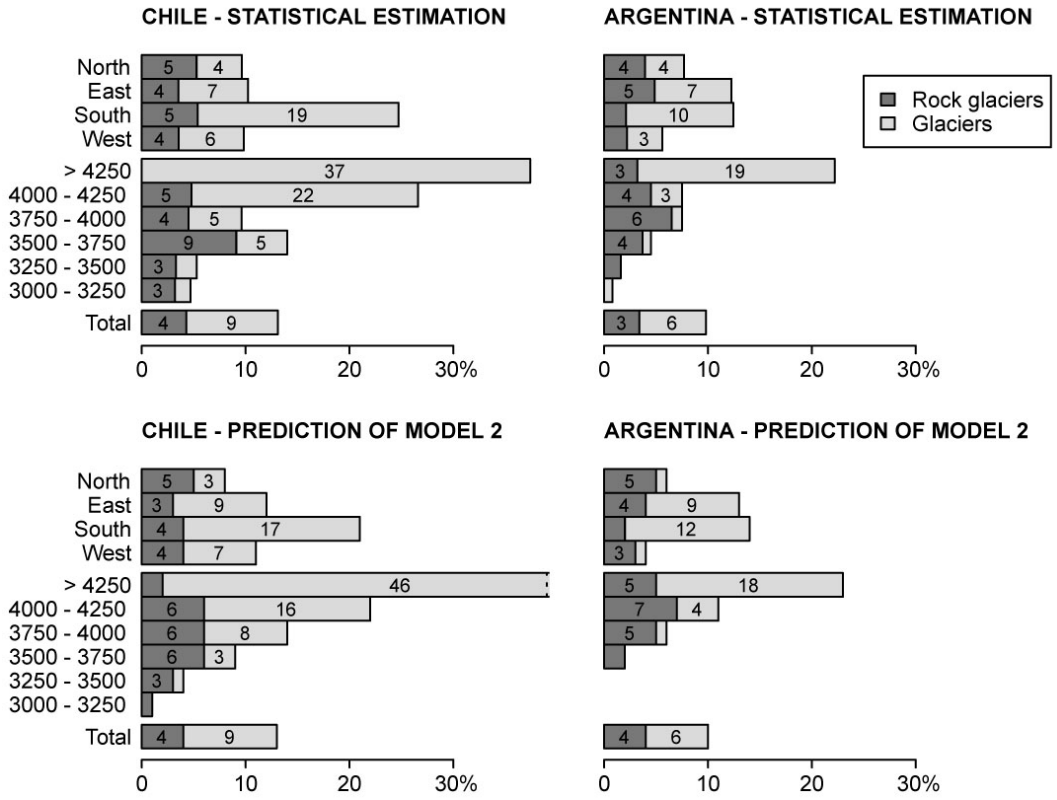

Figure 3.6: Comparison of rock glacier ($\geq$ 0.1 km^2) and glacier distribution in the Andes of Santiago and Mendoza according to statistical estimation and logistic regression model predictions (models TA-2 and TA-G2).

west–east direction. The resulting function is parabolic in vertical direction with a strong increase between its origin at 3000–3250 m a. s. l. and ~3500–3750 m a. s. l., and it presents a hypsometric 250 m-shift towards the east. This numerically fitted shift agrees with the one observed in the statistically estimated distribution pattern (figure 3.1). Model TA-2 adds a significant negative altitudinal trend, which leads to a more realistic, but still not completely satisfying decrease in rock glacier abundance at high elevations (figure 3.6).

According to exploratory data analysis and the fitted models, rock glaciers develop best within contributing areas of about 0.7 km^2 of size with convergent horizontal curvature (tables 3.3, 3.4).

Solar radiation becomes important at low elevations, where low radiation sums favor rock glacier development. Although expositional differences are not significant by themselves, they are represented up to certain degree by potential solar radiation (table 3.3). However, solar radiation and its interaction with elevation in model TA-2 may also be interpreted as a lumped topographic effect that includes other favorable geomorphological and topoclimatic conditions within south-exposed Pleistocene cirques at low elevations.

A mean slope angle of about 20° within the contributing area is an additional favorable characteristic, which however did not result in a significant variable in the final model. The rather

small size of optimum contributing areas reflects the predominance of rather small rock glaciers (cf. Brenning 2004a).

Rock glaciers versus glaciers

In general there is certain overlap between (true and predicted) glacierized areas and areas that topographically favor rock glacier formation. On one hand, this reflects the relative similarity of site conditions needed for glacier and rock glacier formation. On the other hand, it shows that glaciers occupy at high elevations most rock glacier niches and therefore strongly reduce the abundance of rock glaciers above ∼4000–4200 m a. s. l. (compare table 3.5 and sections 2.3.5 and 2.4.1).

In order to materialize this conflict between rock glacier and glacier formation, an attempt was made to include the predicted extent of glacierization within a contributing area as an explanatory variable into the rock glacier prediction model. Several alternative variables were tested:

- The portion of predicted glaciers within a contributing area;
- the sum of predicted glacier probabilities within a contributing area,
- the presence of a predicted glacier within the contributing area as a dichotomous variable,
- and other, similar variables or their transforms.

However, none of these alternatives led to results that were consistent with the above-mentioned observations.

Specifically, the presence or likely presence of a glacier in a contributing area appears to statistically favor rock glacier development. The following interpretation helps understand this problem: Many glacierized areas would topographically also favor rock glacier formation if glaciers were absent. Furthermore, glaciers exist in the catchments of some debris rock glaciers. Therefore the probability of the contributing area of a given place (especially between 3500 and 4000 m a. s. l.) being glacierized is at least a moderately good indicator for the favorability for rock glacier formation at this place. This relationship is stronger than the negative effect of glaciers occupying rock glacier niches or increasing fluvioglacial processes in glacierized catchments.

Rock glacier prediction

The area-preserving threshold for rock glacier prediction was determined to be 0.22. This takes into account the fact that rock glaciers cannot form in glacierized and rock areas, the predictions of which were therefore used as exclusion masks. Areas of predicted probabilities of occurrence between 0.11 and 0.22 were furthermore labelled “possible rock glaciers” (figure 3.4).

Model fit shows a uniformly good

Model area	Potential rock glacier area	
Andes of Santiago	66 km^2	1.4 %
Andes of Mendoza	78 km^2	1.2 %

Table 3.5: Estimation of potential rock glacier areas that are currently glacierized, based on logistic regression predictions. Percentages refer to areas above the regional lower limit of intact rock glaciers, i. e. 3000 and 3250 m a. s. l. in the Andes of Santiago and Mendoza, respectively.

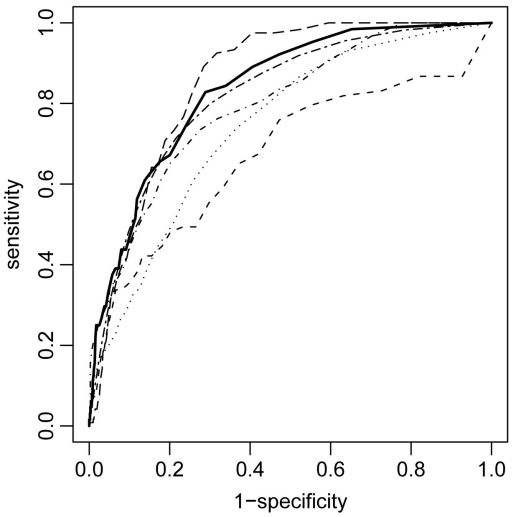

Data set	AUC	Line type
Training data	0.84	Solid
Cerro La Parva	0.80	Dot–dash
C. Picos Negros	0.67	Short dashes
Cerro Catedral	0.74	Dotted
Cerro Tinguiririca	0.86	Long dashes
Cordón del Plata[a]	0.82	Short & long dashes

Figure 3.7: ROC curves of rock glacier prediction with model TA-2 in different mapping areas (table 3.3).
Remark: [a] Argentinian Precordillera, 32° 50′–33° 20′ S.

quality if compared by means of ROC curves to mapping results even in marginal parts and outside the study area (figure 3.7). Furthermore, the predicted pattern of rock glacier probabilities is in general in good agreement with reality, though important differences can be recognized (figure 3.5).

The model's weakness lies in the extremes. Errors occur especially in areas adjacent to present and former glaciers, where modern and younger Holocene glacial and fluvioglacial processes have inhibited rock glacier formation. Furthermore, the prediction of isolated low-elevation occurrences of rock glaciers between 3000 and ∼3300 m a. s. l. is not satisfactory. This may be attributed to local topoclimatic conditions and to the fact that many low-elevation rock glaciers originate from morainic debris, which itself presents particular distribution patterns. In general, model predictions are more reliable for talus than for debris rock glaciers, and rock glaciers are often predicted in niches that have become glacier-free during the Late Holocene. These shortcomings are related to the complex glacial history of the Late Quaternary, which is not sufficiently reflected by the selected explanatory variables.

3.2.4 Discussion

With very good AUC values and an overall rate of correct classification of 69 %, the general pattern of intact rock glaciers $\geq$ 0.1 km^2, glaciers, rock and debris surfaces can be statistically explained quite well by logistic regression models.

Morphometric and climatic controls on a local scale were identified as well as regional-scale trends. In addition to a suitable morphographic niche that guarantees sufficient debris and water supply, favorable topoclimatic conditions including low solar radiation are required at lower elevations for rock glacier development.

Relief parameters present strong correlations even between variables that are semantically clearly distinct (figure 3.3). This may lead to the confounding of different effects and therefore affects the

interpretation of model results. The variables used in the final models of this study are only weakly correlated; this favorable circumstance may be attributed to the random sampling design and the regional spread of sampling points, which reduces local effects that are due to individual valley geometries or inadequate sampling designs.

When looking at the limited ability of predicting rock glaciers in rather unfavorable areas, especially at low elevations, the actual statistical scope of the model should be recalled: Logistic regression models predict conditional probabilities $\pi(\mathbf{x})$ by means of an estimated conditional expected value. Predictions are therefore much smoother than the actual probabilities since "error" terms (i. e. effects that are not explained by the model) cannot be predicted. This phenomenon is well-known in geostatistics, where more realistic spatial patterns are obtained for scalar data by means of stochastic simulation if compared to kriging (cf. Wackernagel 2003). Similar techniques might produce more realistic scenarios of rock glacier distribution at low elevations.

The semivariogram analysis of logit-scale model residuals indicates an autocorrelation range of $\sim$850 m. These autocorrelations are insignificant at the present sampling density, and independent replications may therefore be assumed (cf. Crawley 2002; Hurlbert 1984).

Scale issues as related to the DEM resolution and the signature of rock glaciers within DEMs have been dealt with in a pragmatic way by using original 90 m DEMs and smoothed DEMs to reduce the direct representation of rock glaciers within the elevation data. These issues deserve further research especially if higher-resolution DEMs are to be used.

3.3 Rock glacier and site characteristics: population analysis

The goal of this section is to determine the distribution of rock glacier and site characteristics and explore the relations between both. In contrast to the previous section, which focused on rock glaciers as areal surface properties, now the population of rock glaciers is studied.

While the present section is mainly descriptive, it provides fundamental data on rock glaciers in the Andes of Santiago, which is required for the application of sediment budget models in the following Chapter 4.

3.3.1 Methods

Data collection

For the random sample of rock glaciers in the Andes of Santiago, 34 variables representing rock glacier and site properties were examined using the SRTM DEM and aerial photographs. Data were also collected for most rock glaciers presented in Chapter 2, and a subset of parameters was also evaluated for the Argentinian random sample of rock glaciers. The database contains a total of 185 Chilean and 34 Argentinian rock glaciers. It will be submitted to the Frozen Ground Data Center at the National Snow and Ice Data Center[3] (NSIDC) at Boulder/Colorado.

The rock glacier attributes include size, length, width, complexity and source material (talus or morainic debris); site characteristics include the size of the contributing area, its vertical extent, mean slope and orientation (cf. Barsch 1987, 1996a; Parson 1987). The full list of attributes with corresponding operational definitions is presented in Appendix B. Attribute values were determined both manually and automatically or semi-automatically.

Statistical analysis

The statistical analysis of the rock glacier sample aims at reconstructing the frequency distributions of attributes for the entire rock glacier population in the study area. Of particular interest is rock glacier size distribution; its mean value is used to estimate the total number of rock glaciers in the study area.

The reconstruction of the statistical distribution of rock glacier and site characteristics for the given random sample is not straightforward, since large rock glaciers are more likely to be "hit" by a sampling point than small ones. More precisely, the probability of a rock glacier being hit is proportional to the inverse of its size. This effect and the stratified sampling design are honored by using an appropriate weighting scheme.

Since rock glaciers are essentially weighted with the inverse of their size, very small rock glaciers have a great influence on the estimated attribute distribution. This would result in statistically instable estimations as a consequence of the small number of small rock glaciers in the sample (5 rock glaciers smaller than $0.02\,km^2$ in the Andes of Santiago). Because of this and the aforementioned underrepresentation of small features (section 3.1.1), any analysis in this section will include only rock glaciers of at least $0.02\,km^2$, if not stated otherwise.

Statistical inference on differences between both genetic classes of rock glaciers will not be made because of the small number debris rock glaciers within the sample and uncertainties regarding the assignment to either of both classes.

[3] URL: `http://nsidc.org/fgdc/`

INTACT ROCK GLACIERS IN THE ANDES OF SANTIAGO

Genetic class[1]:	Talus:	83 %
	Debris:	10 %
	Both/uncertain:	7 %
Shape:	Tongue-shaped:	76 %
	Lobate:	2 %
	Transitional:	15 %
	Complex shape:	7 %
Complexity:	Singular:	69 %
	Multi-unit:	10 %
	Multi-lobe:	2 %
	Multi-root:	1 %
	Multi-part:	18 %
Size:	Median:	0.04 km^2
	Mean:	0.09 km^2
	Maximum:	2.0 km^2
Number:	Estimate:	$\sim$3500
Maximum length:	Minimum:	100 m
	Median:	300 m
	Mean:	425 m
	Maximum:	2800 m
Mean width:	Minimum:	55 m
	Median:	100 m
	Mean:	130 m
	Maximum:	650 m
Position:	Valley head, cirque:	50 %
	Valley side:	35 %
	Valley floor:	15 %
Mean ridge crest height above rooting zone:	Minimum:	50 m
	Median:	170 m
	Mean:	226 m
	Maximum:	1000 m
Size of contributing area[2]:	Minimum:	0.02 km^2
	Median:	0.10 km^2
	Mean:	0.26 km^2
	Maximum:	4.65 km^2
Ratio rock glacier size : contributing area:	Minimum:	0.06
	Median:	0.37
	Mean:	0.50
	Maximum:	1.6
Ratio max. length : mean width:	Minimum:	0.5
	Median:	3.2
	Mean:	3.6
	Maximum:	16.7

Table 3.6: Rock glacier and site characteristics in the Andes of Santiago. Estimates are based upon the random sample of rock glaciers ($n = 53$). Only rock glaciers $\geq 0.02\,km^2$ are considered; missing values are disregarded.

Remarks: [1] The true percentage of debris rock glaciers is probably underestimated. [2] Note that this is not a contradiction to the "optimum" 0.5–1 km^2 contributing areas indicated in table 3.4: The latter refers to rock glaciers "by area", the present table to the population of rock glaciers independently of their size.

3.3.2 Results

Table 3.6 gives a summary of selected rock glacier attributes. Histograms of empirical distributions are shown in figures 3.8, 3.9 and 3.10.

Size and number of rock glaciers

The rock glacier size distribution in the Andes of Santiago and Mendoza is strongly skewed even on a logarithmic scale (figure 3.8). Maximum observed rock glacier sizes reach 2.0 and 2.5 km^2 in the Andes of Santiago and Mendoza, respectively.

Based on estimated average rock glacier sizes and total rock glacier areas in the Andes of Santiago and Mendoza, the estimated total number of intact rock glaciers is of about 3500 in the Andes of Santiago and of a similar order in the Andes of Mendoza (table 3.6). As a conservative rule of thumb, there is at least one intact rock glacier per 2 km^2 of mountain area above the lower limit of rock glacier distribution.

The relationship between rock glacier size and contributing area

There is a non-linear relationship between rock glacier size a and the size of the contributing area s (figure 3.11). The $s : a$ ratio generally varies around 2–3 for medium-sized rock glacier and drops below 2 for rock glaciers greater than 0.4 km^2. There seems to be no strong influence of the genetic class on this ratio.

Observed $s : a$ ratios will later be compared to ratios from sediment budget models (Chapter 4).

Rock glacier shape

Rock glaciers in the Andes of Santiago are mainly tongue-shaped. Furthermore, large rock glaciers within the sample tend to be more elongated than smaller ones.

There is no relation between the length : width ratio of a rock glacier and its surface slope or the valley slope below its toe.

3.3.3 Discussion

Basic numeric results on the distribution of rock glacier attributes have been obtained. The rock glacier size distribution reveals the enormous number of rock glaciers in the study area, a great majority of which is sized smaller than 0.1 km^2.

Though large rock glaciers have larger contributing areas, the ratio of contributing areas to rock glacier sizes decreases linearly with increasing rock glacier (or contributing area) size. If large rock glaciers are assumed to be older than small ones, the following hypothesis may be derived: Large, old rock glaciers are closer to "saturating" their contributing area, i. e. to reaching the maximum possible rock glacier size that may be nourished from that area.

3.4 Conclusions

Statistical estimation based upon point observations proved to be an efficient tool for the quantification of surface characteristics on a regional scale. It has for the first time yielded trans-Andean estimates of rock glacier surfaces, glaciers and thermokarst areas, revealing the great abundance of rock glaciers and a pronounced west–east trend.

Geomorphometric and climatic con-

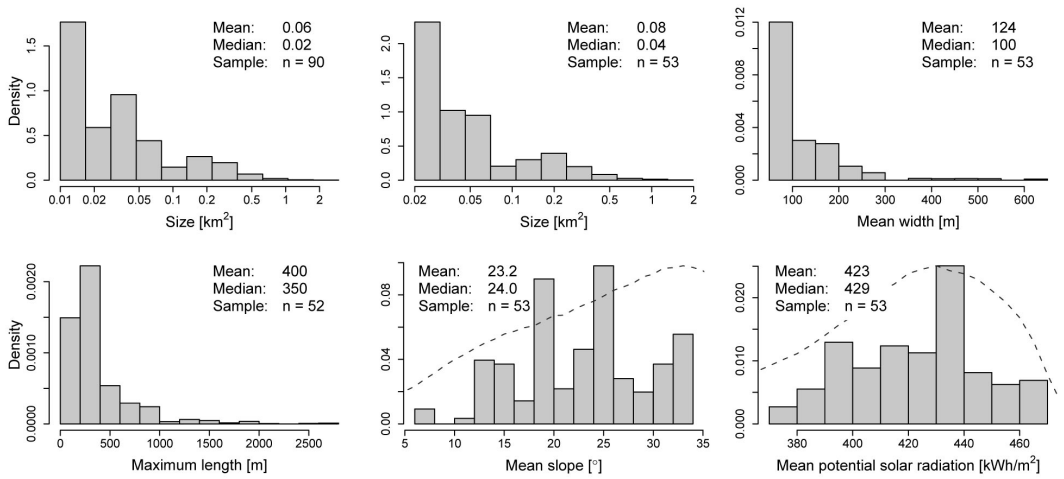

Figure 3.8: Morphometric characteristics of rock glaciers in the Andes of Santiago based upon the random sample. The y-axes represent dimensionless densities.
Remarks: The upper left panel refers to both sides of the Andes and includes all rock glaciers greater or equal 0.01 km^2; all other figures consider only rock glaciers of at least 0.02 km^2 of size in the Andes of Santiago. The dashed lines represent, respectively, the overall distribution of slope and potential solar radiation above 2750 m a. s. l. The indicated sample sizes vary between the plots because of partially missing values.

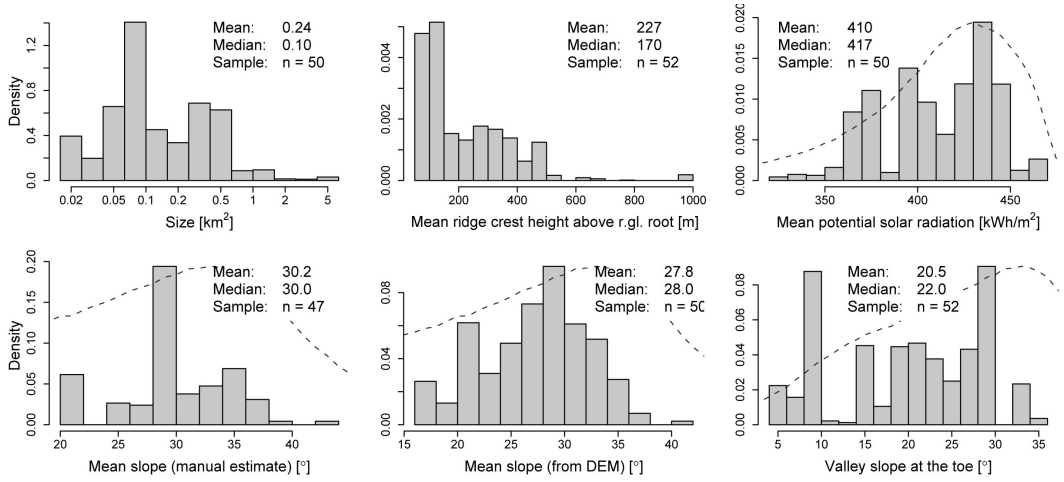

Figure 3.9: Morphometric characteristics of rock glacier contributing areas in the Andes of Santiago based upon the random sample.
Remarks: Only rock glaciers of at least 0.02 km^2 of size are considered. The dashed lines represent the overall distribution of slope and potential solar radiation above 2750 m a. s. l. The indicated sample sizes vary between the plots because of partially missing values.

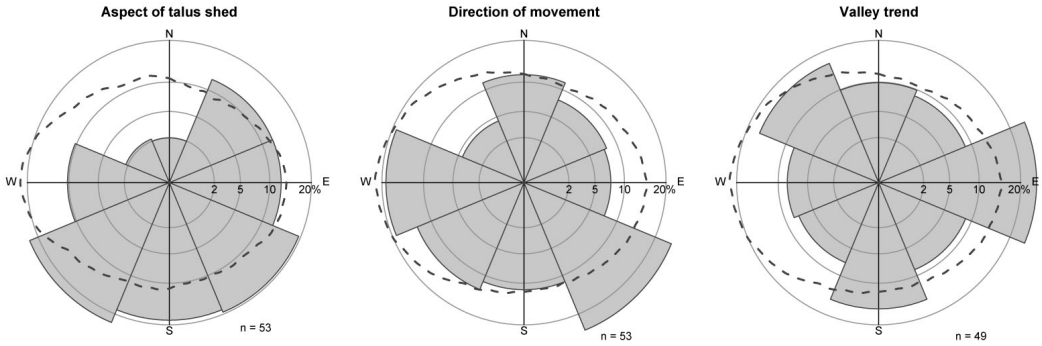

Figure 3.10: Orientational characteristics of rock glaciers in the Andes of Santiago derived from the random sample.

Remarks: Only rock glaciers of at least 0.02 km^2 of size are considered. Note the nonlinear axis; percentages are represented linearly by sector areas. The dashed lines represent the overall distribution of catchment aspect (left panel) and local aspect (middle and right panels) above 2750 m a. s. l. as dimensionless densities.

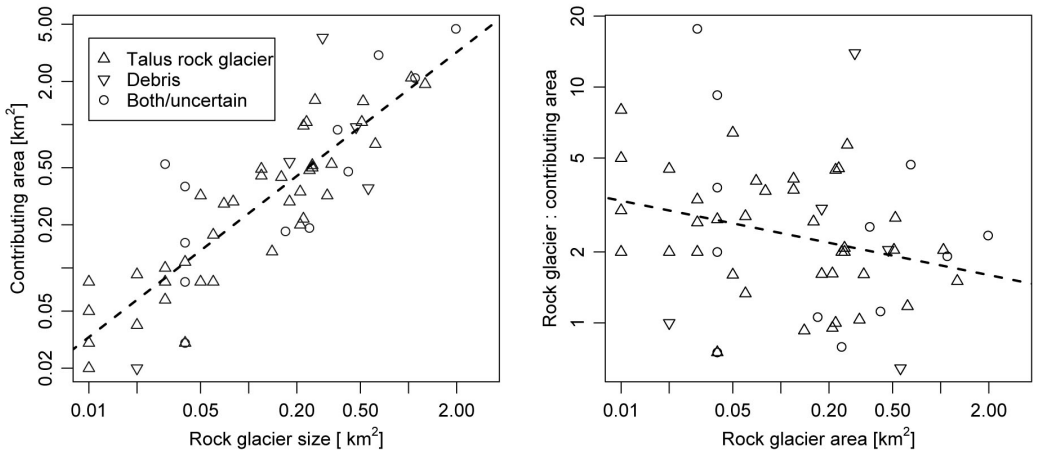

Figure 3.11: The relationship between rock glacier size and contributing area.

trols on rock glaciers (and glaciers) on a regional and local scale have been successfully inferred using logistic regression analysis. Results confirm the importance of topoclimatic and local topographic factors for low-elevation occurrences of rock glaciers. Furthermore, model predictions are able to reproduce the "rock glacier pattern" observed in the region.

A population-oriented analysis of rock glacier and site characteristics has provided a large database, which is the base for the analysis of sediment budgets in the following chapter.

Chapter 4

Modelling rock glacier sediment budgets and advance

Sediment budgets are often used for inferring process rates based upon, for example, the debris volume of rock glaciers, alluvial cones or talus cones (André, 2003; Barsch, 1977c,d; Barsch and Jakob, 1998; Caine, 1976; Curry and Morris, 2004; Hoffmann and Schrott, 2002; Humlum, 2000; Müller, 1999; Schrott and Adams, 2002). While alluvial cones are temporary sediment stores within an open system, rock glaciers are particularly suited for such approaches since they are good approximations of closed sediment traps. Rock glacier sediment budgets have been applied to individual rock glaciers (Barsch and Jakob, 1998; Schrott, 1994), and also to an entire inventory (on an averaged basis; Barsch, 1977c). A combination of individual calculations with a sample of rock glaciers as available within the present work may in contrast yield both robust average values and information on the variability within a population of rock glaciers and contributing areas.

In addition to rock glacier sediment budgets, the length of a rock glacier in the direction of flow may be used to estimate its age from the mean advance rate, or vice versa. This approach has been applied by (Frauenfelder and Kääb, 2000) based upon photogrammetrically-derived modern creep rates of a small number of rock glaciers. The present work follows a much simpler approach, but uses a large sample of rock glaciers, and is combined with the mentioned sediment budget approach.

In an attempt to model post-glacial rock glacier development in a study area in the Swiss Alps, Frauenfelder (2004) combined a talus production model with a physically-motivated model of rock glacier palaeo-creep. Her model is a forward model with non-deterministic model components, which would require great effort if it was to be "fitted" to the data.

In this section, simple models of rock glacier sediment budgets and rock glacier growth are presented and applied to the assessment of process rates within the Andean debris-transport system. They require prior knowledge of simple morphometric parameters as analyzed in the last section.

Modelling will only be performed for rock glaciers that were classified as active, singular, talus-derived features, and for which the required morphometric data is available. In total, 28 rock gla-

ciers from the Andes of Santiago (including 16 features from the random sample) and 37 rock glaciers from the Tapado and Potro areas in the arid North are considered.

4.1 Model formulation

For any singular talus rock glacier, the following morphometric rock glacier characteristics are considered:

- l Maximum horizontal rock glacier length,
- w Width in the upper part,
- a Rock glacier area,
- t Mean thickness,
- p Volumetric talus content (assumed constant),
- s Planimetric size of the contributing area.

The following quantities shall be modelled:

- A Rock glacier age,
- C Horizontal advance rate,
- D Denudation rate in the contributing area,

where the denudation rate D is defined as a vertical lowering rate.

Using these symbols, sD is the total amount of denudation per unit time within the talus shed of rock glacier, and $v = pta$ is the total amount of talus stored within a rock glacier in the present. The quantity $ptwC$ is the talus volume needed per unit of time to nourish a rock glacier with an upper width of w advancing at the rate C.

For each rock glaciers, the following equations relate rock glacier age A to advance rate C and denudation rate D:

$$C = l/A, \quad (4.1)$$

$$pta = sDA, \quad (4.2)$$

$$ptwC = sD. \quad (4.3)$$

Equation (4.1) expresses the average rock glacier advance rate as the ratio of its length and age; it shall be called the *longitudinal growth approach*. The second equation (4.2) represents the mass balance of the closed rock glacier–talus shed debris-transport system as an integrated sediment budget and is therefore referred to as the *sediment budget approach*. The last equation (4.3) models the sediment transfer from the talus shed to the rock glacier and shall be called the *talus supply approach*. While the last two approaches model the rock glacier's mass balance, the first equation is based on simple dynamic considerations. All involved parameters and process rates are assumed to remain constant over time (or to vary without temporal trend around a constant mean).

If the morphometric rock glacier and site properties are given and one out of the three parameters D, C and A is known, then the remaining two parameters may be obtained from any two of the three equations (4.1–4.3).

Values of l, a, s, and w can easily be obtained from aerial photographs and topographic maps and are available for the rock glaciers used here (Appendix B). Average rock glacier thicknesses t, however, have to be estimated. Based on field data from this study and a rule-of-thumb given by Barsch (1977c) for the Swiss Alps, rock glacier thickness is modelled empirically as

$$t[\mathrm{m}] = 50 \cdot (a[\mathrm{km}^2])^{0.2},$$

where both the multiplicative parameter and the exponent were manually adjusted. The volumetric talus content p was assumed to be 50 %.

To obtain estimates of process rates, it shall be assumed that "most" (75 %)

of the rock glacier sample are not older than 10 ka. The rather low percentage of 75 % was chosen since model and data uncertainties may produce unreliable results in some cases as confirmed by inspection of outliers. Some of these were found to present much wider cross-sections that connect them with the source area than suggested by the morphometric "upper width" parameter determined in this work. The use of the median (instead of the mean) and quartiles is however rather robust with respect to outliers.

4.2 Results

The sediment budget and talus supply approaches were first used to estimate rock glacier ages for given denudation rates in the Andes of Santiago and in the arid North separately. For this estimation, constant denudation rates were used for all contributing areas, and denudation rates were allowed to vary between rock glaciers (figures 4.1 and 4.2).

The age constraint yields estimated denudation rates of $\sim 0.75\,\mathrm{mm\,a^{-1}}$ for the Andes of Santiago, and lower values for Northern Chile ($\sim 0.5\,\mathrm{mm\,a^{-1}}$). The corresponding age ranges cover almost the entire Holocene, which is not surprising and consistent with earlier observations (section 2). Age medians are in the order of 6–7 ka. In a similar fashion, advance rates of rock glaciers were estimated to be in the order of several centimeters per year.

Further results are presented in figures 4.1 and 4.2 and summarized in table 4.1.

Figure 4.4 (left panel) shows that, according to model results, elongated rock glaciers are older than more compact ones (note the logarithmic scale), as suggested in section 3.3. Furthermore, $s : a$ ratios computed from measured s and a values are in good agreement with values obtained from the sediment budget model of equation 4.2 (figure 4.4, right side).

4.3 Discussion

The different models built from equations (4.1)–(4.3) yield similar results (figures 4.1, 4.2, 4.3). While denudation and rock glacier advance rates could be estimated in a very stable way, modelled rock glacier ages show a greater variability suggesting that the beginning of their development is spread over a longer time period. This may be due to Holocene climate variability, the different initial material availability, and/or differential paraglacial activity.

The higher denudation rates in the Andes of Santiago compared to the Tapado and Potro areas are attributed to the following reasons:

1. The stronger Pleistocene glaciation of the Andes of Santiago produced greater morainic deposits and more intensive paraglacial activity.

2. Holocene denudation processes on high-elevation slopes are less intensive in the Arid Andes because of the limited availability of water.

Possibly different rates of tectonic uplift may also have an influence, as well as the different distribution of lithologic units within both study areas.

The calculated denudation rates are

	Andes of Santiago	Arid Andes
Age [ka]	6–7	6–7
Advance rate [cm a^{-1}]	6–7	3
Denudation rate [mm a^{-1}]	0.75–1	0.5 (–0.75)

Table 4.1: Median modelled rock glacier ages, advance rates, and denudation rates in the Andes of Central Chile, based upon the assumption that "most" (75 %) rock glaciers are not older than ∼10 ka. (Parameter ranges are depicted in figures 4.1 and 4.2.)

at the lower end of the range of values determined by Barsch (1977c) based upon rock glaciers in the Swiss Alps. The above given climate-related arguments may also apply to this comparison with a temperate and more humid mountain area. Barsch's estimation includes debris rock glaciers and may therefore suffer from a reservoir effect produced by a greater availability of older debris.

Regarding the estimated average advance rates, the values are comparable to those estimated on centennial to millennial scales in different mountain areas (cf. Bachrach et al. 2004 for a recent review).

The longitudinal growth approach yields lower rock glacier ages than the sediment budget approach, given a fixed denudation rate (figure 4.3). This is attributed to a significant offset between the beginning of sediment accumulation (including a possible reservoir effect due to morainic material) and rock glacier creep. This implies that the age parameter has different meanings in equation (4.1) compared to equations (4.2) and (4.3).

In general, the results of the different modelling approaches have shown to be largely consistent with each other, which is encouraging in spite of their simplicity. There is however still much room for improvements regarding (among others) the following issues:

- Time-dependent denudation rates may be introduced in order to take into account paraglacial activity and the post-glacial (exponential?) decay of denudation rates. This would produce a non-linear adjustment of the time scale and reduce the scatter among the older rock glaciers.
- The simplistic model of talus production used in the present work could be improved by taking into account the effects of topography and especially surface roughness.
- Geology-dependent rates of talus production have been used in an alpine area by Frauenfelder et al. (2003); the available geological information from the present study area is however not sufficient for applying similar approaches.
- An offset term differentiating the beginning of rock glacier development from the beginning of talus supply might be useful. This would however introduce additional degrees of freedom into the underdetermined models.
- A meaningful mathematical measure of model misfit would help adjust model parameters. This is not trivial since the magnitude of the deviation from the mean or median depends on these. An unsuitable measure of misfit leads to biased parameter estimation or to the divergence of fitting algorithms.

4.4 Conclusions

To conclude, the approaches used for modelling rock glacier sediment budgets give further insight into rock glacier development and provide information on Holocene denudation rates in a semi-arid to arid high-mountain region at an active plate margin. Arid Andean environments are characterized by lower denudation rates than semi-arid ones, thus being less favorable for rock glacier development. The lower denudation rates may be explained by a less intensive paraglacial activity in the arid Andes, and to less effective water-dependent gravitational processes on desert slopes compared to non-vegetated talus slopes of semi-arid high mountains (cf. Abrahams et al. (1994)). The effects of lithology and differential tectonic uplift on denudation rates are however unknown.

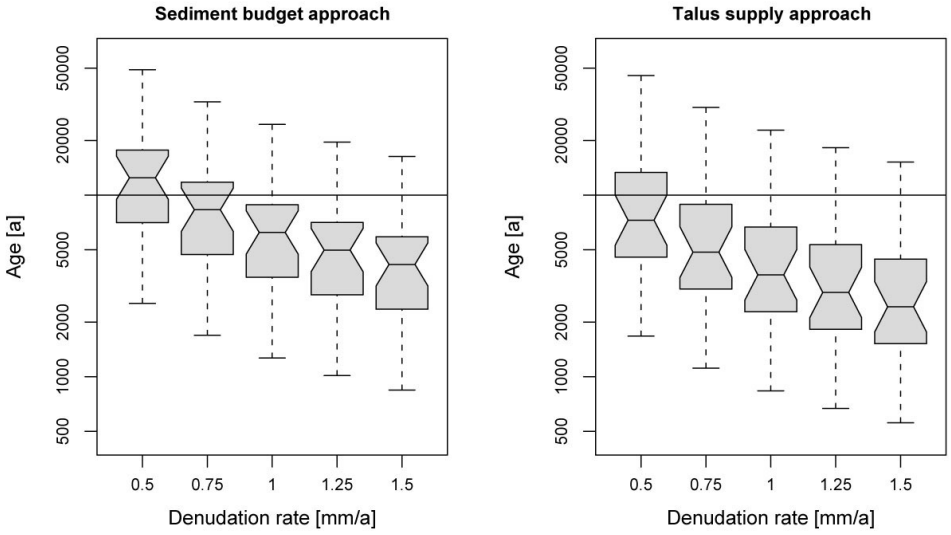

Figure 4.1: Rock glacier ages in the Andes of Santiago, estimated for fixed denudation rates: Application of equations (4.1)–(4.3) to a set of 28 active singular talus rock glaciers.

The plots show the distribution of an estimated parameter for different assumed values of a given variable. Boxes around the median represent the quartiles, their incised part the notches, and the bars outside the boxes are the hinges. Refer to Chambers et al. (1983) for technical details.

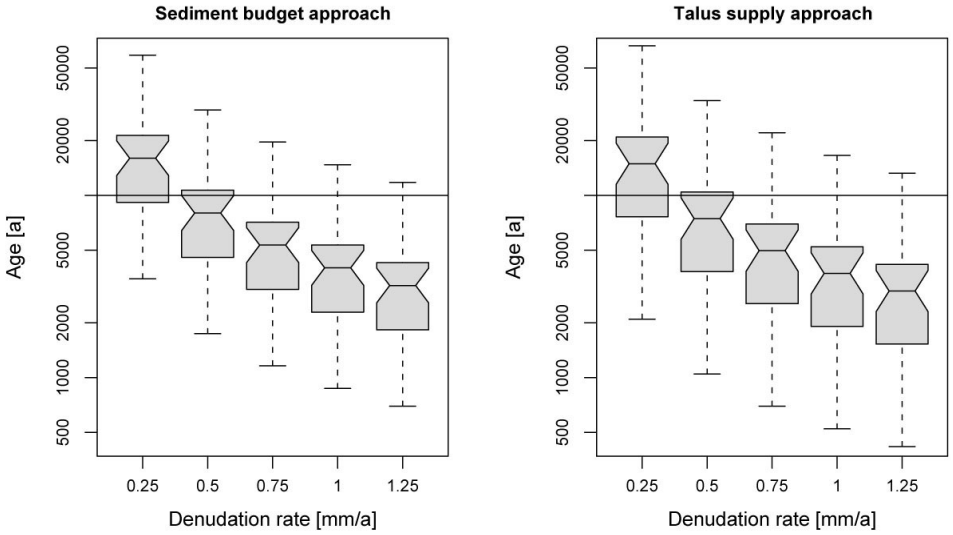

Figure 4.2: Rock glacier ages in the Arid Andes (Tapado and Potro areas), estimated for fixed denudation rates : Application of equations (4.1)–(4.3) to a set of 37 active singular talus rock glaciers.

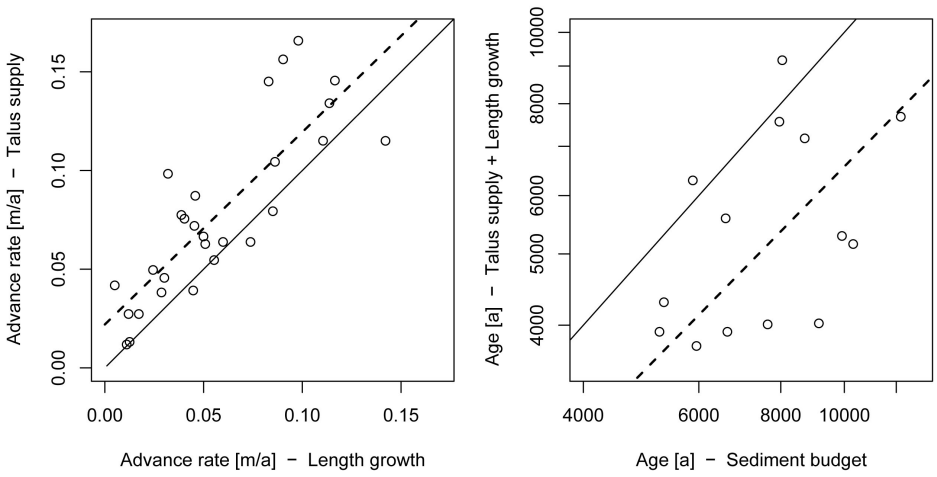

Figure 4.3: Comparison of modelled advance rates and rock glacier ages (partial view, extremes omitted) in the Andes of Santiago for given $D = 0.75\,\mathrm{mm/a}$. Dashed lines: linear trend (for the full data set); solid lines: perfect match.

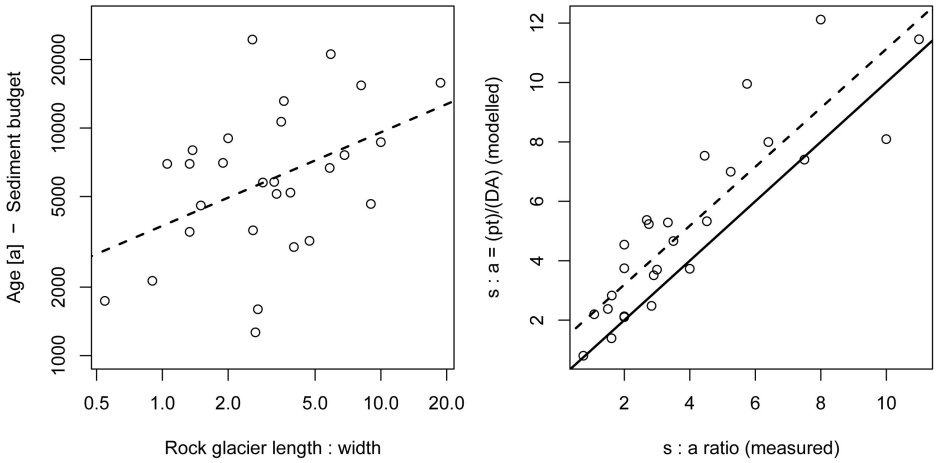

Figure 4.4: Left: Relationship between rock glacier elongation and modelled age according to the sediment budget approach. Right: Measured $s : a$ ratios compared to ratios derived from the sediment budget model of equation (4.2). Dashed lines: linear fit; solid line: perfect match.

Chapter 5

Conclusions

The distribution and significance of rock glaciers is controlled by climatic and topographic factors and glacial history. The differential importance of corresponding process-related parameters on different scales will be synoptically presented in the following concluding sections. Furthermore, the geomorphological and hydrological significance of rock glaciers within their environment shall be highlighted.

5.1 Methodological considerations

Statistical methods have shown to be efficient and reliable instruments for quantitative analyses of landform distribution on a regional scale based upon digital elevation models.

Qualitative field observations on distribution patterns as related to topographic and climatic factors were confirmed and enhanced using logistic regression analysis. In this way, a numeric characterization of rock glacier niches was achieved.

The statistical random sample of rock glaciers has shown to be a valuable data set for further geomorphological studies. Used as an input to sediment budget models, it allowed to infer regionally representative process rates within the Andean debris-transport system.

5.2 Controls of the supra-regional distribution of rock glaciers

Intact rock glaciers exist in the Central Chilean Andes between 27° and 35.25° S. In this area of predominant winter rainfall, annual precipitation ranges between ~200 and 2000 mm, covering almost the entire humidity range that is suitable for rock glacier development (cf. Haeberli, 1975).

Aridity is the main force that impedes rock glacier formation at the northern distributional limit as it reduces talus supply both directly and by means reduced glacial and paraglacial activity. This interpretation is supported by regional sediment budget models of rock glaciers.

At the southern limit, in contrast, lowering topography, active volcanism and strong Holocene glaciation coincide as limiting factors for rock glacier development. According to predictions of the logistic regression model, which ignores direct influence of volcanism and precipitation, the effects of topography suffice to explain this southern limit, but model and mapping results both confirm that modern glacierization is also a significant limiting factor south of 34.5° S. Volcanism becomes particularly important from the southern distributional limit on southward.

Excellent conditions for rock glacier formation in the study area prevail from the Arid North at 28.5° S to the Andes of Santiago (33°–34.5° S). In the latter area of topographic culmination, glaciers enter into competition, but they also act as important past and present suppliers of debris. Topoclimatic conditions within deep glacial troughs and cirques play an additional role in the Andes of Santiago, where the lower limit of sporadic intact rock glaciers is significantly depressed.

5.3 Local environmental controls on rock glacier development

Greatest rock glacier abundance in the Andes of Santiago is found between the modern regional -1 and $+1$°C isotherms and the regional ELA of glaciers. The optimum morphographic niche is, according to statistical analyses, a contributing area of 0.5–1 km^2 with convergent slopes enhancing talus supply.

Furthermore, low radiation is favorable at low altitudes, while medium to high radiation is preferred towards the upper limit as it limits glacierization. These findings are consistent with the morphographic position of low-elevation rock glaciers in south-exposed (and convergent) cirques and glacial troughs, and with huge, north-facing ones occurring at higher elevations in clear opposition to south-exposed glaciers. Thus, an asymmetric hypsometric pattern is characteristic of the distribution of rock glaciers in the semi-arid Andes.

5.4 Thermal controls on relict and intact rock glaciers

The altitudinal zonation of relict, inactive and active rock glaciers reflects both past and present thermal conditions.

The lowest significant relict rock glaciers are found in geomorphological and altitudinal positions that correspond to the late-glacial period or to the LGM. They are attributed to thermal depressions of at least 4.5–5.5°C.

Inactive rock glaciers in the study area generally occur about 100–200 m lower than active ones in similar topographic position. They indicate therefore colder phases in the Holocene.

Active and inactive rock glaciers especially in the Andes of Santiago exist far within the zone of positive regional MAAT. Moderately positive regional MAAT at active rock glacier fronts is rather the rule than the exception. The following effects are made responsible for these discrepancies between ground and air temperatures:

1. Rock glaciers react with a delay

of decades to centuries to climate warming. In Central Chile, a temperature increase of 1–2°C during the 20th century (Rosenblüth et al., 1997).

2. Coarse debris on the surface of rock glaciers allows the penetration of cold air at night and in autumn. This effect might be of particular importance in the semi-arid Andes, where a snow cover forms late in autumn and is less stable than in the European Alps.
3. In some cases local topoclimatic effects such as shading and local wind systems may have a significant cooling effect.

Detailed research on the thermal regime of rock glaciers in the semi-arid Andes is however needed to fully understand these phenomenona.

5.5 The importance of rock glaciers and permafrost within the Andean hydrological system

The specific density and hence the amount of water stored within intact rock glaciers in the Central Andes is by one order of magnitude higher than in the Swiss Alps, and still several times greater than in the Zailijskiy Alatau of Central Asia (table 5.1).

A numeric comparison with glacier volumes is subject to great uncertainties. Nevertheless, the estimated ratio of rock glacier and glacier ice contents in the arid and semi-arid Andes clearly demonstrates the great relative importance of rock glaciers as stores of water in the study area. This will become increasingly important if the 20th century glacier retreat in the study area (Casassa, 1995) —a consequence of regional climate change (Rosenblüth et al., 1997)— is projected into the future. Even today, rock glaciers are the most important stores of water in many medium-sized high Andean catchments in the Andes of Santiago and especially further to the north (table 5.1).

At least one fifth of the total land surface of the Andes of Santiago above 3000 m a. s. l. is drained through rock glaciers. The active layer of rock glaciers and the permafrost-free ground below rock glaciers are therefore important (seasonal) aquifers (section 1.4.2, figure 1.10; Burger et al., 1999). Since ice-rich permafrost acts as a barrier for water percolation, rock glaciers furthermore accelerate the drainage of meltwater from their contributing areas.

5.6 Rock glaciers as key element of the Andean debris transport system

The talus produced in at least one fifth of the land surface above 3000 m a. s. l. in the Andes of Santiago has been trapped by intact rock glaciers during great part of the Holocene. The slow mass-movement process of rock glacier creep advances at average rates of less than $0.1\,\mathrm{m\,a^{-1}}$. Permafrost degradation due to climate warming may however destabilize rock glaciers, slopes and rock walls, and enhance fast gravitational processes.

Rock glaciers contain valuable information about Holocene denudation

Area	Specific density [%]	Ratio of ice volumes Glaciers : Rock glaciers
Dry Andes	∼4	< 3 : 1
— Potro	3	3 : 1
— Tapado	5	1 : 1.4
— Agua Negra[2]	4	1.4 : 1
Andes of Santiago[1]	6.7 ± 1.3	7 : 1
— La Parva (Laguna del Inca)	7	1 : 2
— Casa de Piedra valley	5	1 : 3
— Catedral (Río Blanco)	9	0
South of Santiago		
— El Moño (Río de las Damas)	2	26 : 1
Andes of Mendoza	5.0 ± 1.5	
Swiss Alps[3]	0.3	83 : 1
— Turtmanntal, Wallis[4]	4	
Zailijskiy Alatau[5]	1.7	
— Issyk river basin[5]	5	

Table 5.1: Specific density of rock glaciers in high mountains of the world. The specific density of intact rock glaciers in the sense of the rockglacierized portion of area above the regional lower limit of rock glaciers; cf. Gorbunov (1983).
Remarks: Data from the present work, except where indicated otherwise. [1] Present work and Marangunic (1979); optimistic glacier volumes estimated by the latter were divided by 2 (!) to comply with area–thickness relationships used in the Swiss Alps and in other areas; cf. Marangunic (1979, pp. 22–23), Chen and Ohmura (1990); Schneeberger (1994). Thermokarst-affected massive ice is not included. [2] Schrott (1994). [3] Müller et al. (1976), Barsch (1977b), Barsch (1977d), Gorbunov (1983). [4] Nyenhuis (in press). [5] Gorbunov (1983), corrected to include the 15 % inactive rock glaciers present in the area.

rates (in the sense of uniform lowering rates) within their contributing areas. These are in the order of 0.75 mm a^{-1} on a regional scale in the Andes of Santiago and lower in the Arid Andes (0.5 mm a^{-1}).

5.7 Applied aspects of Andean rock glaciers

In addition to the hydrological significance of rock glaciers (section 5.5), several other applied aspects of Andean rock glaciers emerged while the present work was in progress.

The destruction and degradation of rock glaciers by mining activities in Central Chile and the associated potential hazards should constitute a major concern (Brenning, 2004b). Especially copper mining activities of Codelco División Andina and Los Bronces (Disputada de Las Condes) in the Andes of Santiago have to be mentioned in this context (section 2.3.6). Mining in the periglacial environment of Nevado Jotabeche (Compañía Minera Casale, gold) and Cerro Catedral (dormant project of Compañía Minera Catedral, limestone) may become an issue in the next years.

In the future, tourism will increasingly reach rockglacierized areas such as the cirque of Cerro San Ramón, Santiago's landmark mountain. While hiking trails have just recently been marked, in 2004 the idea of building a cable car to the summit area and corresponding leisure facilities in the surroundings

came up and was soon abandoned (Ertel 2004, and Protege[1], Dec. 2004). Ski resorts in other parts of the study area have not yet reached rockglacierized areas (in contrast to the Italian Alps; Cannone et al., 2003), but they are likely to do so in the future.

While a modern environmental legislation exists in Chile (cf. Carruthers 2001), an effective protection of rock glaciers or the mitigation of human impact also requires a better knowledge of the existence and importance of rock glaciers in the public and in the governmental institutions involved in environmental decision-making processes in the Andes. Hopefully, the present dissertation will contribute to the familiarity of Chileans with rock glaciers.

[1]URL: `http://www.protege.cl/protege.asp?seccion=bicentenario`

Bibliography

G. Abele. Schnelle Massenselbstbewegungen, ein dominanter morphodynamischer Faktor in den chilenischen Anden. *Innsbrucker Geogr. Studien*, 5:21–38, 1979.

G. Abele. Trockene Massenbewegungen, Schlammströme und rasche Abflüsse, dominante morphologische Vorgänge in den chilenischen Anden. *Mainzer Geogr. Studien*, 23, 1981.

G. Abele. El lahar Tinguiririca: su significado entre los lahares chilenos. *Inform. geogr. Chile*, 29:21–34, 1982.

G. Abele. Derrumbes de montaña y morrenas en los Andes chilenos. *Revista de Geografía Norte Grande*, 11:17–30, 1984.

A. D. Abrahams, A. D. Howard, and A. J. Parsons. *Rock-mantled slopes*, pages 173–212. In Abrahams and Parsons, 1994.

A. D. Abrahams and A. J. Parsons, editors. *Geomorphology of desert environments*. Chapman & Hall, London, 1994.

A. L. Ahumada. Periglacial climatic conditions and vertical form associations in Quebrada Benjamín Matienzo, Mendoza, Argentina. *Permafrost Periglac. Process.*, 3:221–224, 1992.

C. Ammann. Climate Change in den trockenen Anden: Aktuelle Niederschlagsmuster. *Geographica Bernensia*, G46:81–127, 1996.

M. E. Andía, G. E. Lagos, and L. J. Danielson. The challenges posed by mine closure in Chile. In *Proc. of the Copper 99 Conference*, Phoenix, Arizona, 1999.

M.-F. André. Do periglacial landscapes evolve under periglacial conditions? *Geomorphology*, 52:149–164, 2003.

Arcadis Geotécnica. Estudio de impacto ambiental Proyecto de Expansión División Andina. Santiago, 2001.

L. Arenson, M. Hoelzle, and S. Springman. Borehole deformation measurements and internal structure of some rock glaciers in Switzerland. *Permafrost Periglac. Process.*, 13: 117–135, 2002.

Ayala, Cabrera y Asociados Ltda. *Modelo de simulación hidrológico operacional cuencas de los ríos Maipo y Mapocho*. Ministerio de Obras Públicas, Dirección General de Aguas, Santiago, 2000.

T. Bachrach, K. Jakobsen, J. Kinney, P. Nishimura, A. Reyes, C. P. Laroque, and D. J. Smith. Dendrogeomorphological assessment of movement at Hilda rock glacier, Banff National Park, Canadian Rocky Mountains. *Geografiska Annaler*, 86A:1–9, 2004.

C. K. Ballantyne. Paraglacial geomorphology. *Quat. Sc. Rev.*, 21:1935–2017, 2002.

C. K. Ballantyne and D. I. Benn. Paraglacial slope adjustment and resedimentation following recent glacier retreat, Fabergstolsdalen, Norway. *Arct. Antarct. Alp. Res.*, 26:255–269, 1994.

D. Barsch. Alpiner Permafrost: ein Beitrag zur Verbreitung, zum Charakter und zur Ökologie am Beispiel der Schweizer Alpen. *Akad. Wiss. Göttingen Math.-Phys. Kl. Folge 3*, 31: 118–141, 1977a.

D. Barsch. Ein Permafrostprofil aus Graubünden, Schweizer Alpen. *Z. Geomorph. NF*, 21: 79–86, 1977b.

D. Barsch. Eine Abschätzung von Schuttproduktion und Schutttransport im Bereich aktiver Blockgletscher der Schweizer Alpen. *Z. Geomorph. Suppl.-Bd.*, 28:148–160, 1977c.

D. Barsch. Nature and importance of mass-wasting by rock glaciers in alpine permafrost environments. *Earth Surf. Process.*, 2:231–245, 1977d.

D. Barsch. Active rock glaciers as indicators for discontinuous alpine permafrost. An example from the Swiss Alps. In *Proc. of the Third International Conference on Permafrost, Vol. 1*, pages 349–353, 1978.

D. Barsch. Problems of the delimitation of geomorphic belts on the East slope of the Cordillera Frontal. *Acta Geocriogénica*, 1:18–21, 1983.

D. Barsch. Probleme der Abgrenzung der periglazialen Höhenstufe in semi-ariden Hochgebirgen; am Beispiel der Mendozinischen Anden (Argentinien). *Geoökodynamik*, 7:215–228, 1986.

D. Barsch. *Rock glaciers: an approach to their systematics*, pages 41–44. In Giardino et al., 1987.

D. Barsch. *Rockglaciers*, pages 69–90. In Clark, 1988.

D. Barsch. *Rockglaciers*. Springer, Berlin, 1996a.

D. Barsch. Welche geoökologischen und klimatischen Aussagen erlauben aktive, inaktive und fossile Blockgletscher? *Heidelberger Geogr. Arb.*, 100:32–39, 1996b.

D. Barsch and N. Caine. The nature of mountain geomorphology. *Mountain Res. Dev.*, 4(4): 287–298, 1984.

D. Barsch and H. Happoldt. Blockgletscherbildung und holozäne Höhenstufengliederung in den mendozinischen Anden, Argentinien. *Zbl. Geol. Paläont. T. I*, 11/12:1625–1632, 1985.

D. Barsch, H. Happoldt, R. Mäusbacher, L. Schrott, and G. Schukraft. *Discharge and fluvial sediment transport in a semi-arid high mountain catchment, Agua Negra, San Juan, Argentina*, pages 213–224. In Ergenzinger and Schmidt, 1994.

D. Barsch and G. Hell. Photogrammetrische Bewegungsmessungen am Blockgletscher Murtèl I, Oberengadin, Schweizer Alpen. *Z. Gletscherk. Glazialgeol.*, 11:111–142, 1975.

D. Barsch and M. Jakob. Mass transport by active rockglaciers in the Khumbu Himalaya. *Geomorphology*, 26:215–222, 1998.

D. Barsch and L. King. Origin and geoelectrical resistivity of rock glaciers in semi-arid subtropical mountains (Andes of Mendoza, Argentina). *Z. Geomorph.*, 33:151–163, 1989.

M. P. Bishop, R. G. Barry, A. B. G. Bush, L. Copeland, J. L. Dwyer, A. G. Fountain, W. Haeberli, D. K. Hall, A. Kääb, J. S. Kargel, B. F. Molnia, J. A. Olsenholler, F. Paul, B. H. Raup, J. F. Shroder, D. C. Trabant, and R. Wessels. Global Land Ice Measurements from Space (GLIMS): Remote sensing and GIS investigations of the Earth's cryosphere. *Geocarto International*, 19(2):57–85, 2004.

R. S. Bivand. Using the R statistical data analysis language on GRASS 5.0 GIS data base files. *Computers & Geosciences*, 26:1043–1052, 2000.

T. Bolch and H. Schröder. Geomorphologische Kartierung und Diversitätsbestimmung der Periglazialformen am Cerro Sillajhuay (Chile/Bolivien). *Erlanger Geogr. Arbeiten, Sonderband*, 28, 2001.

J. Borde. *Les Andes de Santiago et leur avant-pays: étude de géomorphologie*. Thèse de Doctorat. Union Française d'Impression, Bordeaux, 1966.

A. Brenning. La importancia de los glaciares de escombros en los sistemas geomorfológico e hidrológico de la Cordillera de Santiago: fundamentos y primeros resultados. *Revista de Geografía Norte Grande*, 30:7–22, 2003.

A. Brenning. Statistical estimation and logistic regression modelling of rock glacier distribution in the Andes of Santiago, Central Chile. *Geophys. Res. Abstracts*, 6:01032, 2004a.

A. Brenning. The impact of opencast mining on rock glaciers: examples from Central Chile. In *Abstracts of the Wengen Workshop 2004 "Mountain Glaciers and Society", 6–8 October 2004*, Wengen/Switzerland, 2004b.

A. Brenning. Geomorphological, hydrological and climatic significance of rock glaciers in the Andes of Central Chile (33–35° S). *Permafrost Periglac. Process.*, 16(3):231–240, 2005a.

A. Brenning. Morphographic and climatic controls on rock glaciers in the semiarid Andes: a logistic regression approach. In *Abstracts of the 9th Alpine Glaciological Meeting, 24–25 February 2005*, Milan/Italy, 2005b.

A. Brenning, D. Trombotto, and H. Schröder. Zur Verbreitung von Blockgletschern in den semiariden Anden (Chile/Argentinien, 32–35°S): Bedeutung, regionale Trends und der Einfluss des Reliefs. *Berliner Geogr. Arb.*, 100:19–27, 2005.

A. Brenning and K. G. van den Boogaart. Geostatistics without stationarity assumptions within GIS. In *Proc. of the 7th Annual Conference of the International Association for Mathematical Geology*, Cancún, 2001.

J. Brüggen. *Texto de geología. Tomo 1.* El Globo, Santiago, 1929.

J. Brüggen. La cronología de las épocas glaciales de Chile. Revista Universitaria, Santiago, 1946. 36 pp.

E. Buk. Glaciares de escombros y su significación hidrológica. *Acta Geocriogénica*, 1:22–38, 1983.

K. C. Burger, J. J. Degenhardt Jr., and J. R. Giardino. Engineering geomorphology of rock glaciers. *Geomorphology*, 31:93–132, 1999.

K. C. Burger, J. R. Giardino, G. Ridenour, and J. D. Vitek. A thermodynamic approach to rock glacier development. In *Abstracts and Program, Annual Meeting, The Geological Society of America, Salt Lake City, Utah*, 1997.

N. Caine. A uniform measure of subaerial erosion. *Geol. Soc. Amer. Bull.*, 87:137–140, 1976.

N. Cannone, M. Guglielmin, C. Hauck, and D. Vonder Mühll. The impact of recent glacier fluctuation and human activities on permafrost distribution, Stelvio Pass (Italian Central-Eastern Alps). In *Proc. of the Eighth International Conference on Permafrost*, pages 125–130, Zürich, 2003.

D. Carruthers. Environmental politics in Chile: legacies of dictatorship and democracy. *Third World Quarterly*, 22(3):343–358, 2001.

G. Casassa. Glacier inventory in Chile: current status and recent glacier variations. *Ann. Glaciol.*, 21:317–322, 1995.

G. Casassa and C. Marangunic. The 1987 Río Colorado rockslide and debris flow, Central Andes, Chile. *Bull. Assoc. Engineering Geologists*, XXX:321–330, 1993.

C. Caviedes. *Quartärgeomorphologie des Aconcagua-Tales*. Doctoral thesis, Universität Freiburg, 1969.

C. Caviedes. Geomorfología del cuaternario del valle del Aconcagua, Chile Central. *Freiburger Geogr. Hefte*, 11, 1972.

C. Caviedes and R. Paskoff. Quaternary glaciations in the Andes of North Central Chile. *J. Glaciol.*, 14:155–169, 1975.

C. Caviedes and R. Waylen. Chapters for a climatic history of South America. *Freiburger Geogr. Hefte*, 32:149–211, 1991.

J. M. Chambers, W. S. Cleveland, B. Kleiner, and P. A. Tukey. *Graphical methods for data analysis*. Wadsworth & Brooks/Cole, 1983.

R. Charrier, A. R. Wyss, J. J. Flynn, C. C. Swisher, M. A. Norell, F. Zapatta, M. C. McKenna, and M. J. Novacek. New evidence for Late Mesozoic–Early Cenozoic evolution of the Chilean Andes in the upper Tinguiririca valley (35°S), Central Chile. *J. Sth. Amer. Earth Sci.*, 9:393–422, 1996.

J. Chen and A. Ohmura. *Estimation of Alpine glacier water resources and their change since 1870s*, pages 172–135. In Lang and Musy, 1990.

M. Church and J. M. Ryder. Paraglacial sedimentation: consideration of fluvial processes conditioned by glaciation. *Bull. Geol. Soc. Am.*, 83:3059–3071, 1972.

M. A. Cioccale. Climatic fluctuations in the central region of Argentina in the last 1000 years. *Quat. Int.*, 62:35–47, 1999.

M. J. Clark, editor. *Advances in Periglacial Geomorphology*. Wiley, Chichester, 1988.

L. Clayton. Karst topography on stagnant glaciers. *J. Glaciol.*, 5:107–112, 1964.

D. Collett. *Modelling binary data*. Chapman & Hall, London, 1991.

A. Contreras and J. L. Illanes. Depósito de lastre glaciar Infiernillo Sur Mina Los Bronces. In *43a Convención del Instituto de Ingenieros de Minas de Chile, La Serena, October 1992*, 1992.

R. U. Cooke, A. Warren, and A. S. Goudie. *Desert geomorphology*. UCL Press, London, 1993.

J. G. Corripio and R. S. Purves. The influence of penitentes on the energy balance of high altitude glaciers in the dry Central Andes. *Geophys. Res. Abstracts*, 5:12738, 2003.

A. E. Corte. The hydrological significance of rock glaciers. *J. Glaciol.*, 17:157–158, 1976a.

A. E. Corte. Rock glaciers. *Biul. Periglacjalny*, 26:175–197, 1976b.

A. E. Corte. Rock glaciers as permafrost bodies with a debris cover as an active layer. A hydrological approach. Andes of Mendoza, Argentine. In *Proc. of the Third International Conference on Permafrost, NRC, Ottawa*, pages 262–269, 1978.

A. E. Corte. Glaciers and glaciolithic systems of the Central Andes. In *Proc. of the Riederalp Workshop, September 1978*, pages 11–22, Discussion: 22–24, 1980. IAHS-AISH Publ. no. 126.

A. E. Corte and L. E. Espizua. Inventario de glaciares de la cuenca del Río Mendoza. Technical report, CONICET–IANIGLA, Mendoza, 1981.

N. Corvalán, I. Kovacic, and O. Muñoz. Quebrada de Macul: el aluvión del 3 de mayo 1993. Causas y consecuencias. *Terra Australis*, 42:139–167, 1997.

M. J. Crawley. *Statistical computing: an introduction to data analysis using S-Plus*. Wiley, New York, 2002.

F. A. Croce and J. P. Milana. Internal structure and behaviour of a rock glacier in the Arid Andes of Argentina. *Permafrost Periglac. Process.*, 13:289–299, 2002.

A. M. Curry and C. J. Morris. Lateglacial and Holocene talus slope development and rock-wall retreat on Mynydd Du, UK. *Geomorphology*, 58:86–106, 2004.

R. Delaloye, E. Reynard, C. Lambiel, L. Marescot, and R. Monnet. Thermal anomaly in a cold scree slope (Creux du Van, Switzerland). In *Proc. of the Eighth International Conference on Permafrost*, pages 175–180, Zürich, 2003.

J. Dessens and A. Bücher. A critial examination of the precipitation record at the Pic du Midi observatory, Pyrenees, France. *Climatic Change*, 36:345–353, 1997.

J. C. Dixon and A. D. Abrahams, editors. *Periglacial geomorphology. Proc. of the 22nd Annual Binghamton Symposium in Geomorphology*. Wiley, Chichester, 1992.

F. Dramis, M. Govi, M. Guglielmin, and G. Mortara. Mountain permafrost and slope instability in the Italian Alps: the Val Pola Landslide. *Permafrost Periglac. Process.*, 6:73–81, 1995.

Editec. *Compendio de la minería chilena*. Editec, Santiago, 2000.

B. Efron and R. Tibshirani. The bootstrap method for standard errors, confidence intervals, and other measures of statistical accuracy. *Statistical Science*, 1(1):1–35, 1986.

B. Efron and R. Tibshirani. *An introduction to the bootstrap*. Chapman and Hall, New York, London, 1993.

D. B. Enfield. El Niño, past and present. *Review of Geophysics*, 27:159–187, 1989.

EPA. *Abandoned mine site characterization and cleanup handbook*. United States Environmental Protection Agency, 2001. EPA 530-C-01-001.

C. Ereño and J. Hoffmann. El régimen pluvial en la Cordillera central. Series Cuadernos de Geografía, No. 5. Instituto de Geografía, Facultad de Filosofía y Letras, Universidad de Buenos Aires, 1978.

P. Ergenzinger and K.-H. Schmidt, editors. *Dynamics and geomorphology of mountain rivers*, volume 52 of *Lecture Notes in Earth Sciences*. Springer, Berlin Heidelberg, 1994.

M. Ertel. Projektentwicklungsstudien Erschließung des Cerro San Ramon bei Santiago de Chile. Diplomarbeit, Fakultät für Architektur und Stadtplanung, Universität Stuttgart, 2004.

F. Escobar, G. Casassa, and C. Garín. 25 year record of mass balance of Echaurren glacier, central Chile, and its relation with ENSO events. In *Proc. of the Sixth International Conference on Southern Hemisphere Meteorology and Oceanography, Santiago de Chile, 3–7 April 2000*, pages 118–119, 2000.

F. Escobar, V. Pozo, A. Salazar, and M. Oyarzo. Balance de masa en el glaciar Echaurren Norte 1975 a 1992: resultados preliminares. Technical report, Dirección General de Aguas, Santiago, 1995.

A. N. Fox and M. R. Strecker. Pleistocene and modern snowlines in the Central Andes (24–28°S). *Bamberger Geogr. Schriften*, 11:169–182, 1991.

R. Frauenfelder. *Regional-scale modelling of the occurrence and dynamics of rockglaciers and the distribution of plaeopermafrost*. Doctoral thesis, Universität Zürich, 2004.

R. Frauenfelder, W. Haeberli, and M. Hoelzle. Rockglacier occurrence and related terrain parameters in a study area of the Eastern Swiss Alps. In *Proc. of the Eighth International Conference on Permafrost*, pages 253–258, Zürich, 2003.

R. Frauenfelder and A. Kääb. Towards a palaeoclimatic model of rock-glacier formation in the Swiss Alps. *Ann. Glaciol.*, 31:281–286, 2000.

H. M. French. *The periglacial environment*. Longman, London, 1976.

G. Furrer and P. Fitze. Beitrag zum Permafrostproblem in den Alpen. *Vierteljahresschrift der Naturforschenden Gesellschaft in Zürich*, 115:353–368, 1970.

J. S. Gardner and I. Bajewsky. *Hilda rock glacier stream discharge and sediment load characteristics, Sunwapta pass area, Canadian Rocky Mountains*, pages 161–175. In Giardino et al., 1987.

C. Garín. Inventario de los glaciares de los Andes Chilenos desde los 18° a los 32° de latitud Sur. *Revista de Geografía Norte Grande*, 14:35–48, 1987.

K. Garleff. Höhenstufen der argentinischen Anden in Cuyo, Patagonien und Feuerland. *Göttinger Geogr. Abh.*, 68, 1977.

K. Garleff and H. Stingl. Hangformen und Hangformung in der periglazialen Höhenstufe der argentinischen Anden zwischen 27° und 55° südlicher Breite. *Abh. Akad. Wiss. Göttingen, Math.-Phys. Kl., 3. Folge*, 35:425–434, 1983.

K. Garleff and H. Stingl. Höhenstufen und ihre raumzeitlichen Veränderungen in den argentinischen Anden. *Zbl. Geol. Paläont. T. I*, 1984(11/12):1701–1707, 1985.

K. Garleff and H. Stingl. Geomorphologische Aspekte aktuellen und vorzeitlichen Permafrostes in Argentinien. *Zbl. Geol. Paläont. T. I*, 1985(9/10):1367–1374, 1986.

Geotécnica Consultores. Estudio de impacto ambiental Compañía Minera Disputada de Las Condes, Proyecto de Epansión–2, mina Los Bronces. 1996.

J. R. Giardino, J. F. Shroder, and J. J. D. Vitek, editors. *Rock glaciers*. Allen & Unwin, Boston, 1987.

J. R. Giardino, J. D. Vitek, and J. L. DeMorett. *A model of water movement in rock glaciers and associated water characteristics*, pages 159–184. In Dixon and Abrahams, 1992.

O. González-Ferrán. *Volcanes de Chile*. Editorial Instituto Geográfico Militar, Santiago, 1994.

A. P. Gorbunov. Permafrost investigations in high-mountain regions. *Arct. Alp. Res.*, 10: 283–294, 1978.

A. P. Gorbunov. Rock glaciers of the mountains of middle Asia. In *Proc. of the Fourth International Conference on Permafrost, Fairbanks, Alaska*, pages 359–362, Washington, 1983. National Academic Press.

V. I. Grebenets, A. G.-O. Kerimov, and S. N. Titkov. Dangerous movement of an anthropogenic "rock glacier", Norilsk region, northern Siberia. In *Proc. of the Seventh International Conference on Permafrost*, pages 347–350, Yellowknife, Canada, 1998.

S. Gruber, M. Hoelzle, and W. Haeberli. Permafrost thaw and destabilization of Alpine rock walls in the hot summer of 2003. *Geophys. Res. Letters*, 31(L13504):4 pp., 2004.

E. C. Grunsky. R: a data analysis and statistical programming environment — an emerging tool for the geosciences. *Computers & Geosciences*, 28:1219–1222, 2002.

M. Gude, S. Dietrich, R. Mäusbacher, C. Hauck, R. Molenda, V. Ruzicka, and M. Zacharda. Probable occurrence of sporadic permafrost in non-alpine scree slopes in central Europe. In *Proc. of the Eighth International Conference on Permafrost*, pages 331–336, Zürich, 2003.

M. Guglielmin, M. Camusso, S. Polesello, and S. Valsecchi. An old relict glacier body preserved in permafrost environment: the Foscagno rock glacier ice core (Upper Valtellina, Italian Central Alps). *Arct. Antarct. Alp. Res.*, 36(1):108–116, 2004.

W. Haeberli. Die Basis-Temperatur der winterlichen Schneedecke als möglicher Indikator für die Verbreitung von Permafrost. *Z. Gletscherk. Glazialgeol.*, 9:221–227, 1973.

W. Haeberli. Untersuchungen zur Verbreitung von Permafrost zwischen Flüelapass und Piz Grialetsch (Graubünden). *Mitteilungen der Versuchsanstalt für Wasserbau, Hydrologie und Glaziologie, ETH Zürich*, 17, 1975.

W. Haeberli. Creep of mountain permafrost: internal structure and flow of alpine rock glaciers. *Mitteilungen der Versuchsanstalt für Wasserbau, Hydrologie und Glaziologie, ETH Zürich*, 77, 1985.

W. Haeberli. Modern research perspectives relating to permafrost creep and rock glaciers: a discussion. *Permafrost Periglac. Process.*, 11:290–293, 2000.

W. Haeberli, M. Hoelzle, A. Kääb, F. Keller, D. Vonder Mühll, and S. Wagner. Ten years after drilling through the permafrost of the active rock glacier Murtèl, Eastern Swiss Alps: answered questions and new perspectives. In *Proc. of the Seventh International Conference on Permafrost*, pages 403–410, Yellowknife, Canada, 1998.

H. Happoldt and L. Schrott. A note on ground thermal regimes and global solar radiation at 4720 m a.s.l., High Andes of Argentina. *Permafrost Periglac. Process.*, 3:241–245, 1992.

S. A. Harris and A. E. Corte. Interactions and relations between mountain permafrost, glaciers, snow and water. *Permafrost Periglac. Process.*, 3:103–110, 1992.

S. A. Harris and D. E. Pedersen. Thermal regimes beneath coarse blocky materials. *Permafrost Periglac. Process.*, 9:107–120, 1998.

S. Hastenrath. On the Pleistocene snow-line depression in the arid regions of the South American Andes. *J. Glaciol.*, 3:255–267, 1971.

C. J. Heusser. Quaternary pollen record from Laguna Tagua-Tagua, Chile. *Science*, 219: 1429–1432, 1983.

C. J. Heusser. Paleoclimatic setting of the last glaciation in the South Chilean Andes. In *2. Bamberger Symposium Südamerika – Geomorphologie und Paläoökologie im jüngeren Quartär, July 6–8, 1990*, 1990.

H. Hintermayr. Die periglaziale Höhenstufung an der Westseite der nordchilenischen Hochanden zwischen 22°S und 27°S. Unpublished thesis (Examensarbeit), Institut für Geographie, Unversität Erlangen, 1997.

M. Hoelzle. *Permafrost und Gletscher im Oberengadin. Grundlagen und Anwendungsbeispiele für automatisierte Schätzverfahren*. Doctoral thesis, ETH Zürich, 1994.

M. Hoelzle, S. Wagner, A. Kääb, and D. Vonder Mühll. Surface movement and internal deformation of ice–rock mixtures within rock glaciers at Pontresina–Schafberg, Upper Engadin, Switzerland. In *Proc. of the Seventh International Conference on Permafrost*, pages 465–471, Yellowknife, Canada, 1998.

T. Hoffmann and L. Schrott. Modelling sediment thickness and rockwall retreat in an Alpine valley using 2D-seismic refraction (Reintal, Bavarian Alps). *Z. Geomorph. NF Suppl.-Bd.*, 127:153–173, 2002.

P. Höllermann. Verbreitung und Typisierung von Glatthängen. *Abh. Akad. Wiss. Göttingen, Math.-Phys. Kl., 3. Folge*, 35:241–260, 1983.

C. Holmgren and I. Vela. Visita a la mina Los Bronces. *Actas Congreso Geol. Chileno*, 6, 1991. Guía de Excursión, IC–5.

D. W. Hosmer and S. Lemeshow. *Applied logistic regression*. Wiley, New York, 2000.

O. Humlum. The geomorphic significance of rock glaciers: estimates of rock glacier debris volumes and headwall recession rates in West Greenland. *Geomorphology*, 35:41–67, 2000.

S. H. Hurlbert. Pseudoreplication and the design of ecological field experiments. *Ecological Monographs*, 54:187–211, 1984.

Y. Iijima and K. Fukui. The effect of surface nocturnal cooling on maintaining the mountain permafrost in central Japan. In *Proc. of the Eighth International Conference on Permafrost*, pages 449–454, Zürich, 2003.

A. Ikeda and N. Matsuoka. Degradation of Talus-derived Rock Glaciers in the Upper Engadin, Swiss Alps. *Permafrost Periglac. Process.*, 13:145–161, 2002.

M. Ishikawa, K. Fukui, M. Aoyama, A. Ikeda, Y. Sawada, and N. Matsuoka. Mountain permafrost in Japan: distribution, landforms and thermal regimes. *Z. Geomorph. NF Suppl.-Bd.*, 130:99–116, 2003.

J. D. Ives. *Permafrost*, pages 159–194. In Ives and Barry, 1974.

J. D. Ives and R. G. Barry, editors. *Arctic and alpine environments*. Methuen, London, 1974.

J. R. Janke. The occurrence of alpine permafrost in the Front Range of Colorado. *Geomorphology*, 67(3–4):375–389, 2005.

B. Jenny and K. Kammer. Climate Change in den trockenen Anden: Jungquartäre Vergletscherung. *Geographica Bernensia*, G46:1–80, 1996.

B. Jenny, B. L. Valero-Garcés, R. Urrutia, K. Kelts, H. Veit, P. G. Appleby, and M. Geyh. Moisture changes and fluctuations of the Westerlies in Mediterranean Central Chile during the last 2000 years: The Laguna Aculeo record (33° 50′S). *Quat. Int.*, 87:3–18, 2002.

H. Jin, S. Li, G. Cheng, W. Shaoling, and X. Li. Permafrost and climatic change in China. *Global and Planetary Change*, 26:387–404, 2002.

K. Kammer. Rock glaciers, Western Andes, Chile. National Snow and Ice Data Center / World Data Center for Glaciology, Boulder/Colorado. Digital Media, 1998.

J. Karte. Räumliche Abgrenzung und vertikale Differenzierung des Periglazials. *Bochumer Geogr. Arb.*, 35, 1979.

J. Karte and H. Liedtke. The theoretical and practical definition of the term periglacial in the geographical and geological meaning. *Biuletyn Periglacjalny*, 28:123–135, 1981.

K. A. Keating and S. Cherry. Use and interpretation of logistic regression in habitat–selection studies. *J. Wildl. Manage.*, 68(4):774–789, 2004.

F. Keller. Interaktionen zwischen Schnee und Permafrost: Eine Grundlagenstudie im Oberengadin. *Mitteilungen der Versuchsanstalt für Wasserbau, Hydrologie und Glaziologie, ETH Zürich*, 127, 1994.

F. Keller and M. Tamás. Enhanced ground cooling in periods with thin snow cover in the Swiss National Park. In *Proc. of the Eighth International Conference on Permafrost*, pages 531–536, Zürich, 2003.

C. Klohn. *Geología de la Cordillera de los Andes de Chile Central. Provincias de Santiago, O'Higgins, Colchagua y Curicó*. Instituto de Investigaciones Geológicas de Chile, Boletín No. 8, Santiago, 1960.

C. Kneisel, C. Hauck, and D. Vonder Mühll. Permafrost below the timerline confirmed and characterized by geoelectrical resistivity measurements, Bever valley, Eastern Swiss Alps. *Permafrost Periglac. Process.*, 11:295–304, 2000.

C. Kneisel, F. Lehmkuhl, S. Winkler, E. Tressel, and H. Schröder. Legende für geomorphologische Kartierungen in Hochgebirgen (GMK Hochgebirge). *Trierer Geogr. Studien*, 18, 1998.

R. Köthe and F. Lehmeier. SARA-Benutzerhandbuch, Morphometrie-Programm. 1994.

C. Kull, M. Grosjean, and H. Veit. Modeling modern and Late Pleistocene glacio-climatological conditions in the North Chilean Andes (29–30°S). *Climatic Change*, 52: 359–381, 2002.

H. Lang and A. Musy, editors. *Hydrology in mountainous regions I—Hydrological measurements; The water cycle. Proc. of two symposia held at Lausanne*. IAHS Press, 1990. IAHS Publication no. 192.

E. Lankenau. Tinguiririca, Vulkanismus und Vereisung als formende Elemente der mittelchilenischen Hochkordillere. *Petermanns Geogr. Mitt.*, Erg.-H. 267, 1958.

J. C. Leiva, L. E. Lenzano, G. A. Cabrera, and J. A. Suarez. *Variations of Río Plomo glaciers, Andes Centrales Argentinos*, pages 143–151. In Oerlemans, 1989.

A. G. Lewkowicz. *Slope processes*, pages 325–368. In Clark, 1988.

A. G. Lewkowicz and M. Ednie. Probability mapping of mountain permafrost using the BTS method, Wolf Creek, Yukon Territory, Canada. *Permafrost Periglac. Process.*, 15:67–80, 2004.

L. Lliboutry. Internal moraines and rock glaciers. *J. Glaciol.*, 2(14):296, 1953.

L. Lliboutry. The origin of penitentes. *J. Glaciol.*, 2:331–338, 1954.

L. Lliboutry. Origine et évolution des glaciers rocheux. *Comptes rendus des séances de l'Académie des Sciences, Paris*, 240:1913–1915, 1955.

L. Lliboutry. *Nieves y glaciares de Chile: fundamentos de glaciología*. Editorial Universitaria, Santiago, 1956.

L. Lliboutry. Phénomènes cryoniveaux dans les Andes de Santiago (Chili). *Biul. Peryglacjalny*, 10:209–224, 1961.

L. Lliboutry. Rock glaciers in the dry Andes. In *Proc. of the International Symposium "Glacier mass balance, fluctuations and runoff", Alma-Ata, Sept. 30 – October 5, 1985*, pages 18–24, 139–144, 1986.

L. Lliboutry. *Glaciers of Chile and Argentina*, pages I109–I206. In Williams Jr. and Ferrigno, 1999.

M. Luetscher, P.-Y. Jeannin, and W. Haeberli. Energy fluxes in an ice cave of sporadic permafrost in the Swiss Jura mountains – concept and first observational results. In *Proc. of the Eighth International Conference on Permafrost*, pages 691–696, Zürich, 2003.

M. Luoto, S. Fronzek, and F. S. Zuidhoff. Spatial modelling of palsa mires in relation to climate in Northern Europe. *Earth Surf. Process. Landforms*, 29:1373–1387, 2004.

M. Luoto and J. Hjort. Generalized linear modelling in periglacial studies: terrain parameters and patterned ground. *Permafrost Periglac. Process.*, 15:327–338, 2004.

C. Marangunic. El glaciar de roca Pedregoso, río Colorado, V Región. *Actas Congreso Geol. Chileno*, 1:D71–D80, 1976.

C. Marangunic. Inventario de glaciares. Hoya del río Maipo. Technical report, Dirección General de Aguas, Santiago, 1979.

C. Marangunic, H. Moreno, and J. Varela. Observaciones sobre los depósitos de relleno de la depresión longitudinal de Chile entre los ríos Tinguiririca y Maule. *Actas Congreso Geológico Chileno, Arica*, 2:I29–I39, 1979.

P. McCullagh and J. A. Nelder. *Generalized linear models*. Chapman & Hall, London, 1990.

S. Menard. *Applied logistic regression analysis*. Series on Quantitative Applications in the Social Sciences, vol. 106. Sage Publ., Thousand Oaks, CA, 1995.

B. Messerli, M. Grosjean, and K. Graf. Die Veränderungen von Klima und Umwelt in der Region Atacama (Nordchile) seit der letzten Kaltzeit. *Erdkunde*, 46:257–272, 1992.

Minería Chilena. Disputada de Las Condes: De los capachos a una faena que se proyecta al nuevo siglo. *Minería Chilena*, 145:43–47, 1993.

C. Mpodozis, P. Cornejo, S. M. Kay, and A. Tittler. La Franja de Maricunga: síntesis de la evolución del Frente Volcánico Oligoceno–Mioceno de la zona sur de los Andes Centrales. *Rev. geol. Chile*, 21:273–313, 1995.

B. U. Müller. Paraglacial sedimentation and denudation processes in an Alpine valley of Switzerland. An approach to the quantification of sediment budgets. *Geodinamica Acta*, 12:291–301, 1999.

F. Müller, T. Calfisch, and G. Müller. Firn und Eis der Schweizer Alpen (Gletscherinventar). Geographisches Institut Publ. Nr. 57, 1976.

S. W. Muller. *Permafrost or perennially frozen ground and related engineering problems*. Edwards Bros., Ann Arbor, 1947.

M. Muñoz, A. Moreira, C. Villagrán, and F. Luebert. Caracterización florística y pisos de vegetación en los Andes de Santiago, Chile central. *Boletín del Museo Nacional de Historia Natural*, 49:9–50, 2000.

J. A. Naranjo and M. J. Haller. Erupciones holocenas principalmente explosivas del volcán Planchón, Andes del sur (35°15′S). *Rev. geol. Chile*, 29(1):93–113, 2002.

J. A. Naranjo, M. J. Haller, H. A. Ostera, A. H. Pesce, and P. Struoga. *Geología y peligros del complejo volcánico Planchón–Peteroa, Andes del Sur (25°15′S), Región del Maule, Chile, Provincia de Mendoza, Argentina*. Sernageomin, Boletín No. 52, 1999.

M. Nyenhuis. *Permafrost und Sedimenthaushalt in einem alpinen Geosystem*. Doctoral thesis, Universität Bonn, in press.

J. Oerlemans, editor. *Glacier fluctuations and climatic change*. Kluwer Academic Publ., Dordrecht, 1989.

G. C. Ohlmacher and J. C. Davis. Using multiple logistic regression and GIS technology to predict landslide hazard in northeast Kansas, USA. *Eng. Geol.*, 69:331–343, 2003.

V. Olaya. A gentle introduction to SAGA GIS. Edition 0.90, 2004.

C. G. Parson. *Rock glaciers and site characteristics on the Blanca Massif, Colorado, U.S.A.*, pages 127–143. In Giardino et al., 1987.

R. Paskoff. Notes de morphologie glaciaire dans la haute vallée du Rio Elqui (Provence de Coquimbo, Chili). *Bull. Ass. Géog. français*, 350/351:44–55, 1967.

R. Paskoff. *Le Chili semi-aride, recherches géomorphologiques*. Biscaye, Bordeaux, 1970.

W. S. B. Paterson. *The physics of glaciers*. Pergamon, Oxford, 3rd edition, 1994.

D. Payne. Climatic implications of rock glaciers in the arid Western Cordillera of the Central Andes. *Glacial Geology and Geomorphology*, rp03, 1998.

W. H. Pollard. *Seasonal frost mounds*, pages 201–229. In Clark, 1988.

A. Puig and P. Valdivia. Estudio geomorfológico y glaciológico en la zona de la Laguna Negra. Univ. de Chile, Departamento de Geología, Taller de Título GL 697, GL 698. 93 pp., 1977.

R Development Core Team. *R: a language and environment for statistical computing*. R Foundation for Statistical Computing, Vienna, Austria, 2005. `http://www.R-project.org/`.

D. Raj. *Sampling theory*. McGraw-Hill series in probability and statistics. McGraw-Hill, New York, 1968.

F. Reichert. Die Penitentesschneefelder im Gebiet zwischen Aconcagua und Tupungato. *Z. Gletscherkunde*, 4:343–350, 1910.

M. Richter and D. Schmidt. Cordillera de la Atacama – das trockenste Hochgebirge der Welt. *Petermanns Geogr. Mitt.*, 146(4):48–57, 2002.

M. Richter and H. Schröder. Remarks on the paleocology of the Atacama based on the distribution of recent geomorphological and phytogeographical patterns. *Bamberger Geogr. Schriften*, 15:57–70, 1996.

E. A. Ripley, R. E. Redman, and A. A. Crowder. *Environmental effects of mining*. St. Lucie Press, Delray Beach, Florida, 1995.

A. Rivera and G. Casassa. Volume changes on Pio XI glacier, Patagonia: 1975–1995. *Global and Planetary Change*, 22:233–244, 1999.

I. Roer. Rock glacier kinematics in the Turtmanntal, Valais, Switzerland – observational concept, first results and research perspectives. In *Proc. of the Eighth International Conference on Permafrost*, pages 971–975, Zürich, 2003.

H. Romero. *Geografía de los climas*, volume XI of *Colección Geografía de Chile*. Instituto Geográfico Militar, Santiago, 1985.

B. Rosenblüth, H. A. Fuenzalida, and P. Aceituno. Recent temperature variations in southern South America. *Int. J. Climatol.*, 17:67–85, 1997.

F. Röthlisberger. *10 000 Jahre Gletschergeschichte der Erde*. Sauerländer, Aarau, 1986.

G. R. Rumney. *Climatology and the world's climates*. Macmillan, New York, 1968.

C. Schneeberger. *Glaciers and climate change: a numerical model study*. Doctoral thesis no. 14743, ETH Zürich, 1994.

K.-H. Scholl. Geomorphologische Kartierung im Einzugsgebiet des oberen Agua Negra, cuyanische Hochkordillere, Argentinien. Diplomarbeit, Geographisches Institut, Universität Heidelberg, 1992.

K.-H. Scholl. *Mapeo geomorfológico del piso periglacial en los Andes semiáridos*, pages 89–92. In Trombotto and Villalba, 2002.

H. Schröder. Vergleichende Periglazialmorphologie im Sommerregengebiet der Atacama. *Erdkunde*, 53:119–135, 1999.

H. Schröder. Vergleichende Periglazialmorphologie im Winterregengebiet der Atacama. *Erdkunde*, 55:311–326, 2001.

H. Schröder and M. Makki. Das Periglazial des Llullaillaco (Chile/Argentinien). *Petermanns Geogr. Mitt.*, 142:67–84, 1998.

H. Schröder and D. Schmidt. Klimamorphologie und Morphogenese des Llullaillaco (Chile/Argentinien). *Mitt. Fränk. Geogr. Ges.*, 44:225–258, 1997.

L. Schrott. Global solar radiation, soil temperature and permafrost in the Central Andes, Argentina: a progress report. *Permafrost Periglac. Process.*, 2:59–66, 1991.

L. Schrott. Die Solarstrahlung als steuernder Faktor im Geosystem der subtropischen semiariden Hochanden (Agua Negra, San Juan, Argentinien). *Heidelberger Geogr. Arb.*, 94, 1994.

L. Schrott. Some geomorphological–hydrological aspects of rock glaciers in the Andes (San Juan, Argentina). *Z. Geomorph. NF Suppl.-Bd.*, 104:161–173, 1996.

L. Schrott. The hydrological significance of high mountain permafrost and its relation to solar radiation. A case study in the high Andes of San Juan, Argentina. *Bamberger Geogr. Schriften*, 15:71–84, 1998.

L. Schrott and T. Adams. Quantifying sediment storage and Holocene denudation in an Alpine basin, Dolomites, Italy. *Z. Geomorph. NF Suppl.-Bd.*, 128:129–145, 2002.

E. Schunke and S. C. Zoltai. *Earth hummocks (thufur)*, pages 231–245. In Clark, 1988.

M. W. Smith. Microclimatic influences on ground temperatures and permafrost distribution, Mackenzie Delta, Northwest Territories. *Can. J. Earth Sci.*, 12:1421–1438, 1975.

K. J. V. Steenstrup. Bidrag til Kjendskab til Bræerne og Bræ-Isen i Nord-Grønland. *Meddelelser om Grønland*, 4(2):69–112, 1883.

H. Stingl and K. Garleff. Beobachtungen zur Hang- und Wandentwicklung in der Periglazialstufe der subtropisch-semiariden Hochanden Argentiniens. *Abh. Akad. Wiss. Göttingen, Math.-Phys. Kl., 3. Folge*, 35:199–213, 1983.

S. K. Thompson. *Sampling*. Wiley, New York, 2nd edition, 2002.

X. Toledo and E. Zapater. *Geografía general y regional de Chile*. Editorial Universitaria, Santiago, 1991.

C. Troll. Die Formen der Solifluktion und die periglaziale Bodenabtragung. *Erdkunde*, 1: 162–175, 1947.

D. Trombotto. Untersuchungen zum periglazialen Formenschatz und zu periglazialen Sedimenten in der Lagunita del Plata, Mendoza, Argentinien. *Heidelberger Geogr. Arb.*, 90, 1991.

D. Trombotto. Survey of cryogenic processes, periglacial forms and permafrost conditions in South America. *Rev. do Instituto Geológico, São Paulo*, 21 (1/2):33–55, 2000.

D. Trombotto, E. Buk, and J. Hernández. Monitoring of mountain permafrost in the Central Andes, Cordón del Plata, Mendoza, Argentina. *Permafrost Periglac. Process.*, 8:123–129, 1997.

D. Trombotto, E. Buk, and J. Hernández. Rock glaciers in the Southern Central Andes (approx. 33°–34° S), Cordillera Frontal, Mendoza, Argentina. *Bamberger Geogr. Schriften*, 19:145–173, 1999.

D. Trombotto and R. Villalba. *IANIGLA, 30 años de investigación básica y aplicada en Ciencias Ambientales*. Instituto Argentino de Nivología, Glaciología y Ciencias Ambientales, Mendoza, Argentina, 2002.

P. Valdivia. Inventario de glaciares en la hoya del Río Cachapoal y predicción de la escorrentía del deshielo. Technical report, Universidad de Chile, Departamento de Geología, Santiago, 1979.

P. Valdivia. Inventario de glaciares. Andes de Chile Central (32°–35° lat. S.). Hoyas de los rios Aconcagua, Maipo, Cachapoal y Tinguiririca. Technical report, Dirección General de Aguas, Santiago, 1984a.

P. Valdivia. Inventario de glaciares. Hoya del Río Tinguiririca, VI Región. Technical report, Dirección General de Aguas, Santiago, 1984b.

R. O. van Everdingen. Multi-language glossary of permafrost and related ground-ice terms. Technical report, National Snow and Ice Data Center / World Data Center for Glaciology, Boulder, Colorado, 2002.

H. Veit. Jungquartäre Relief- und Bodenentwicklung in der Hochkordillere im Einzugsgebiet des Rio Elqui (Nordchile, 30°S). *Bamberger Geogr. Schriften*, 11:81–97, 1991.

H. Veit. Jungquartäre Landschafts- und Bodenentwicklung im chilenischen Andenvorland zwischen 27–33° S. *Bonner Geogr. Abh.*, 85:196–208, 1992.

H. Veit. Upper Quaternary landscape and climate evolution in the Norte Chico (Northern Chile): an overview. *Mountain Res. Dev.*, 13/2:139–144, 1993.

J. Vergara and F. Escobar. The interannual variability of the Echaurren glacier mass balance: Chilean Andes. In *Symposium on Mass Balance of Andean Glaciers, 12–14 March 2003*, page 31, CECS, Valdivia, Chile, 2003.

C. Villagrán and J. Varela. Palynological evidence for increased aridity on the central Chilean coast during the Holocene. *Quat. Res.*, 34:198–207, 1990.

R. Villalba. Fluctuaciones climáticas en latitudes medias de América del Sur durante los últimos 1000 años: sus relaciones con la Oscilación del Sur. *Revista Chilena de Historia Natural*, 67:453–461, 1994a.

R. Villalba. Tree-ring and glacial evidence for the medieval warm epoch and the little ice age in southern South America. *Climatic Change*, 26(2):183–197, 1994b.

M. Vuille. Zur raumzeitlichen Dynamik von Schneefall un Ausaperung im Bereich des südlichen Altiplano, Südamerika. *Geographica Bernensia*, G45, 1996.

H. Wackernagel. *Multivariate Geostatistics: an introduction with applications*. Springer, Berlin, 3rd edition, 2003.

W. B. Wahrhaftig and A. Cox. Rock glaciers in the Alaska Range. *Geol. Soc. Am. Bull.*, 70: 383–436, 1959.

H. Wakonigg. Unterkühlte Schutthalden. *Arb. Inst. Geogr. (Graz)*, 33:209–223, 1996.

A. L. Washburn. *Periglacial processes and environments*. Arnold, London, 1973.

R. Waylen and C. Caviedes. Annual and seasonal fluctuations of precipitation and streamflow in the Aconcagua river basin. *J. Hydrol.*, 120:79–102, 1990.

W. J. Wayne. Ice segregation as an origin for lenses of non-glacial ice in "ice-cemented" rock glaciers. *J. Glaciol.*, 27:506–510, 1981.

W. Weischet. Zur Geomorphologie des Glatthangreliefs in der ariden Subtropenzone des Kleinen Norderns von Chile. *Z. Geomorph.*, 13:1–21, 1969.

W. Weischet. *Chile, seine länderkundliche Individualität und Struktur*. Wissenschaftliche Buchgesellschaft, Darmstadt, 1970.

W. Weischet. *Regionale Klimatologie – Teil 1, Die Neue Welt: Amerika, Neuseeland, Australien*. Teubner, Stuttgart, 1996.

O. R. Weise. *Das Periglazial*. Bornträger, Berlin, Stuttgart, 1983.

W. B. Whalley. Rock glaciers and their formation as part of a glacier debris-transport system. Geographic Papers, No. 27, University Reading, England, 1974.

W. B. Whalley, C. F. Palmer, S. J. Hamilton, and J. E. Gordon. Ice exposures in rock glaciers. *J. Glaciol.*, 40:427, 1994.

A. S. Whitemore. Sample size for logistic regression with small response probability. *J. Am. Stat. Assoc.*, 76:27–32, 1981.

R. S. Williams Jr. and J. G. Ferrigno, editors. *Satellite image atlas of glaciers of the world; South America*. U. S. Geological Survey Professional Paper, P 1386-I, Reston, VA, USA, 1999.

W. Zeil. *Geologie von Chile*. Bornträger, Berlin, 1964.

W. Zeil. *Südamerika*, volume 1 of *Geologie der Erde*. Enke, Stuttgart, 1986.

L. W. Zevenbergen and C. R. Thorne. Quantitative analysis of land surface topography. *Earth Surf. Process. Landforms*, 12:47–56, 1987.

Appendix A

Data, maps and software used

A.1 Aerial photographs

Aerial photographs from the Andes of Central Chile are in most parts of the study area only available for 1955/56 (Hycon flights) and 1996–99 (Geotec flights).

Hycon (1955/56)

Aerial photographs of the Hycon flights (1955/56) are the photogrammetric base of most Chilean topographic maps 1:50,000 of mountain areas. They were furthermore used for preparing the glacier inventories (Marangunic 1979 and others) and were therefore made available to the author by the Centro de Información de Recursos Hídricos (DGA).

Hycon photographs are monochrome and are scaled ∼1:50,000. There was no cloud cover in any of the photographs used in this work.

The following aerial photographs were used by the author on paper and as digital images scanned at 600 dpi (approximate resolution: 2.5 m):

M7 (8 Jan 1955): 1107–1116
M12 (22 Jan 1955): 1767–1768, 1809–1811
M25 (21 Feb 1955): 4065–4081
M26 (23 Feb 1955): 4185–4207, 4215–4221, 4225–4257, 4259–4294, 4274, 4299–4300, 4306–4321
M27 (24 Feb 1955): 4341–4352, 4355, 4357, 4359, 4368–4409, 4413–4416, 4418–4439
M147 (29 Feb 1956): 24870–24871
M148 (1 Mar 1956): 24903–24912, 24915–24922, 24924–24965
M157 (4 Apr 1955): 26141–26143

Geotec (1996–1999)

Selected Geotec photographs were obtained from the Servicio Aerofotogramétrico de la Fuerza Aérea (SAF, Santiago) in order to support geomorphological mapping. Nominal scale is 1:50,000, although the author estimated an approximate scale of 1:60,000. The monochrome photographs were scanned at 600 dpi (approximate res-

olution: 2.5–3 m). Geotec photographs show slightly better contrast and sharpness than Hycon photographs.

Juncal (1996) : S30 L06 2604–2607, S30 L06 2614–2622

Río del Carmen (1996) : S27 L10 1032–1036, S27 L10 1041–1042, S27 L09 1123–1124, S27 L14 1238–1241

El Palomo (1997) : S31 L03 3316–3318 (24 Jan 1997), S31 L03 3322–3326 (24 Jan 1997), S31 L03 3333–3334 (24 Jan 1997), S31 L05 4664–4677 (25 Feb 1997), S31 L04 4736–4740 (25 Feb 1997), S31 L04 4754–4756 (25 Feb 1997), S31 L02 4764–4766 (25 Feb 1997), S31 L03 5549–5557 (24 Jan 1997)

Juncal (1997) : S30 L01 4693–4694 (25 Feb 1997), S30 L03 5526–5528 (15 Apr 1997), S30 L03 5543–5546 (15 Apr 1997), S30 L04A 5584–5587

Laguna del Negro Francisco (1999) : S26 L15 14976–14977

Conama–Conaf (2001)

In 2001, flights were conducted in most parts of Central Chile in order to obtain color imagery for Comisión Nacional del Medio Ambiente (Conama) and Corporación Nacional Forestal (Conaf). The aerial photographs are available to the public[1] as digital orthophotos at an approximate resolution of 13 m. The following images from the Andes of Santiago were used for mapping and visualization purposes: 27875, 27884–27890, 27901–27904.

A.2 Satellite imagery

Satellite imagery was used in this work mainly in the qualitative assessment of seasonal snow cover evolution (especially in the case of Cerro San Ramón; section 2.3.1) and for visualizing remote areas.

Landsat TM and ETM+ imagery with a resolution of 30 m in the visible channels was available from the Global Land Cover Facility[2] at the University of Maryland for 17 Mar 1989 (TM) and 26 Dec 1999 (ETM+).

ASTER is a 14 band multi-spectral sensor aboard the Terra satellite. It offers three visible and near infrared channels at a resolution of 15 m. ASTER data of different processing levels (L1A/L1B) was retrieved from the EOS Data Gateway[3] at the USGS–NASA Distributed Active Archive Center. It was mainly used in the analysis of snow conditions on Cerro San Ramón and in the Cajón de la Casa de Piedra:

- 18 May 2000, 2 Oct 2000, 9 Oct 2000, 19 Nov 2000, 13 Jan 2001, 22 Sep 2002, 1 Mar 2003, 24 Mar 2003, 18 Apr 2003, 16 Sep 2003, 11 Oct 2003, 12 Nov 2003, 6 Jan 2004, 7 Feb 2004, 19 Mar 2004, 26 Mar 2004, 11 Apr 2004, 22 Feb 2005.

[1] URL: `http://www.sinia.cl`
[2] URL: `http://glcf.umiacs.umd.edu/`
[3] URL: `http://edcimswww.cr.usgs.gov/pub/imswelcome/`

A.3 Digital terrain data

During the Shuttle Radar Topography Mission (SRTM) in February 2000, radar data was acquired in order to produce elevation data for more than 80 % of Earth's land mass. Although the final goal is to produce interferometric DEMs of 1″ (or about 30 m) of resolution, currently only 3″ data is available for South America at the USGS Seamless Data Distribution Center[4] (SDDS). The 3″ DEMs from the study area are of a similar quality as the topographic information represented by contour lines in Chilean topographic maps 1:50,000. Gaps occur only locally mainly on lake surfaces and steep rock faces. Horizontal and vertical accuracy of SRTM DEMs is in general of 10–16 m (root mean-squared error; source: USGS SDDS), but lower accuracy has to be expected in high mountains.

The downloaded SRTM DEMs of the study area were processed with the terrain analysis software SAGA: Gaps were filled by a spline-type interpolation technique (function "Close gaps"), yielding reliable results except in some high parts of the Juncal and Aconcagua massifs. DEMs were then projected from World Geodetic System 1984 (WGS84) to an UTM projection, zone 19S, with respect to Provisional South American Datum 1956 (UTM 19S PSAD56), the system officially used in Chile. Target resolution was 90 m.

A digital elevation model was furthermore interpolated from digitized Chilean 1:50,000 contour lines for the Andes of Santiago but later replaced in all analyses by SRTM data because of its availability for the entire Andes.

A.4 Other material

Topographic maps 1:50,000 and 1:250,000 of the Chilean Instituto Geográfico Militar were available for the entire Andes of Santiago and most parts of the other study areas. They were used both as paper maps and as georeferenced GIS layers for geomorphological mapping and for finding the random sampling locations within aerial photographs.

Glacier inventories are available since the 1970s and 1980s for most parts of the Central Chilean Andes (Garín, 1987; Marangunic, 1979; Valdivia, 1979, 1984a) and the Andes of Mendoza (Corte and Espizua, 1981). The data were made available by the CIRH–DGA (Santiago) and IANIGLA (Mendoza) in printed form. The Chilean inventories do not distinguish between rock glaciers and debris-covered glaciers and are incomplete in the case of rock glaciers.

Geological maps of the Andes of Santiago are available at a scale of 1:250,000 (Ayala, Cabrera y Asociados Ltda., 2000; Klohn, 1960).

Meteorological data was provided by Aguas Andinas/Ondeo (R. Bernardin; Embalse El Yeso station), Compañía Minera Disputada de Las Condes (A. Contreras; Los Bronces) and the DGA.

Miscellaneous GIS data for map production was obtained from the Digital Chart of the World[5] and ESRI's World Basemap Data[6].

[4] URL: `http://seamless.usgs.gov`
[5] URL: `http://www.maproom.psu.edu/dcw/`
[6] URL: `http://www.esri.com/data/download/basemap/`

Appendix B

Samples and databases

B.1 Random sample

The statistical random sample that was generated and evaluated within this work is not printed here due to size limitations. Figure B.1 shows the samples from Andes of Santiago and Mendoza, which were drawn independently.

For each sample point, the class membership (rock glacier, glacier, etc.; compare section 3.1) as well as the terrain parameters listed in table 3.2 were compiled within a database. This database will be submitted to the Frozen Ground Data Center at the National Snow and Ice Data Center[1] (Boulder/Colorado), where it will be available for download.

[1] URL: `http://nsidc.org/fgdc/`

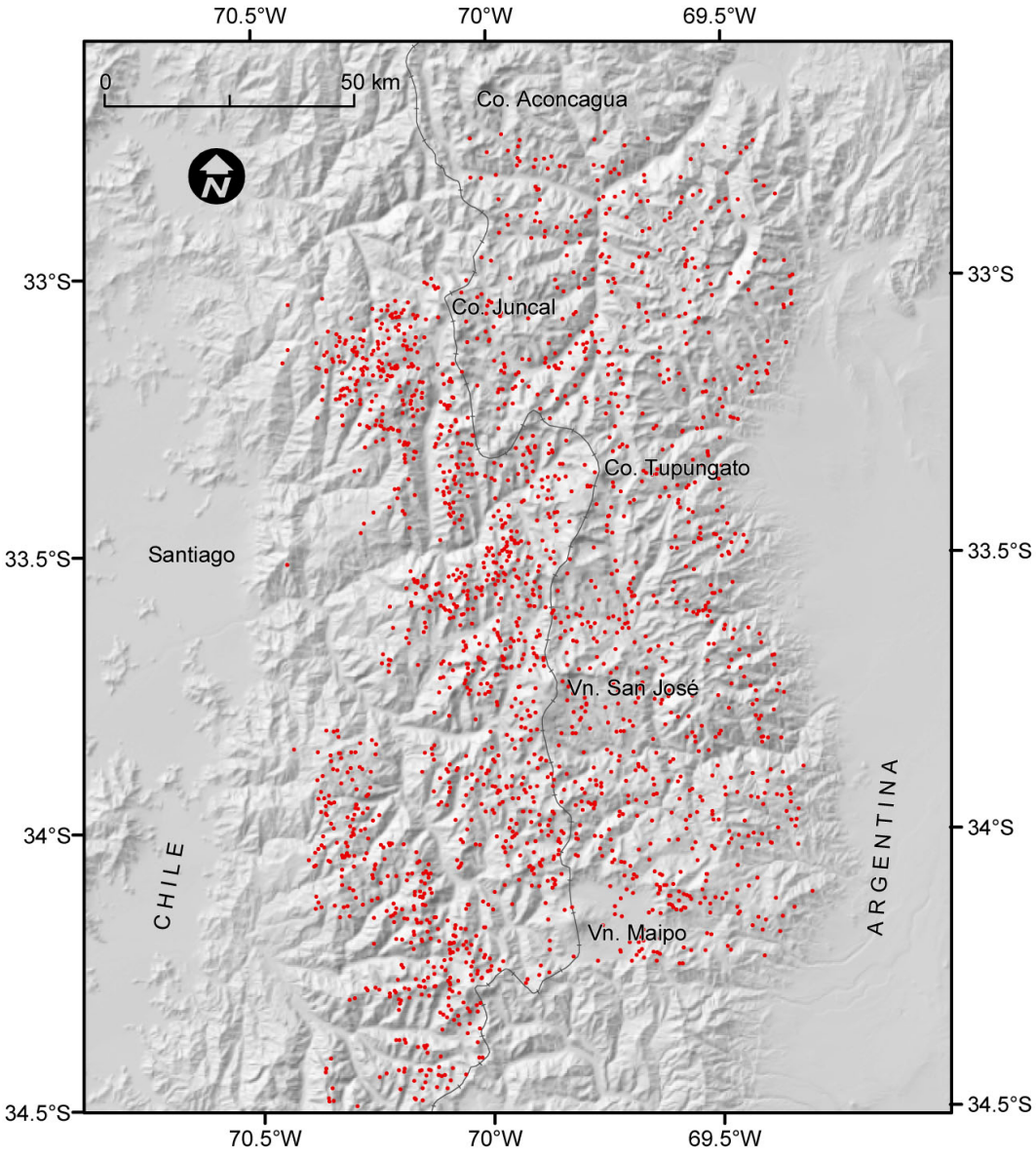

Figure B.1: Random sampling locations in the Andes of Santiago and Mendoza.

B.2 Rock glacier and site characteristics

For the rock glaciers from the statistical random sample and those mapped in the study areas, a comprehensive set of geomorphological characteristics and parameters was compiled as described below. These data will be submitted to the Frozen Ground Data Center at the NSIDC.

The tables on pages 121–123 define the attributes of the database with rock glacier and site characteristics as used in this work. Most parameters have been suggested either by Parson (1987) or Barsch (1987, 1996a). The definitions given here are operational in the sense that the computational or measuring method is indicated rather than a theoretical definition. An operational definition is needed since it represents the methodological and numeric uncertainties that are inherent to these estimates. Knowledge of these uncertainties is required if a comparison with data from other sources is to be made.

All DEM-dependent calculations and estimations are based upon the processed SRTM DEM with 90 m of resolution as described in section A.3. Terrain parameters were computed with SAGA. Coordinates refer to the UTM projection, zone 19S, Provisional South American Datum 1956. The aerial photographs used are listed in section A.1.

Rock glacier identification:	
Identifier:	A unique number identifying the rock glacier.
Rock glacier name:	An official or unofficial name for the rock glacier.
Sample identifier(s):	If applicable, identifiers of random sampling points that "hit" the rock glacier.
Catchment:	Branch within the tree of catchments the rock glacier belongs to. E. g.: "Río Maipo : Río Yeso : Cajón de la Casa de Piedra".
Aerial photographs:	Number and year of air photos used for the analysis.
Topographic map sheet(s) 1:50,000:	Names of map sheets used.

(Continued on the next pages.)

Rock glacier characteristics:	
UTM coordinates at the toe [m, m]:	UTM coordinates at the center of the rock glacier's toe.
Altitude at the toe [m a. s. l.]:	Altitude at the center of the toe.
Height of front above toe [m]:	Mean relative height of the rock glacier's front above its toe as measured in the field.
Front slope angle [°]:	Front slope angle as determined in the field with a hand-held clinometer. If possible, mean value of several measurements along the front.
Height of back above front [m]:	Mean relative height of the rooting zone above the front scarp.
Planimetric area [km^2]:	Planimetric area of the rock glacier including its front slope.
Lower width [m]:	Mean planimetric width of the lower third of the rock glacier, excluding lateral slopes.
Middle width [m]:	Mean width of the middle third.
Upper width [m]:	Mean width of the upper third.
Mean width [m]:	Total mean planimetric width of the rock glacier, excluding lateral slopes.
Maximum length [m]:	Maximum planimetric rock glacier surface length, excluding the front slope; measured along the assumed flow path.
Direction of rock glacier movement [octant]:	As derived from rock glacier surface structure and topography.
Genetic classification:	Talus/debris/uncertain. Cf. Barsch (1996a).
Surface relief:	1 = Very well developed; 2 = subdued to well-developed; 3 = no furrows and ridges. Cf. Barsch (1996a).
Shape:	1 = Lobate (length $<$ width); 2 = transitional; 3 = tongue-shaped; 4 = complex. Cf. Parson (1987).
Activity:	Intact / active / inactive / relict; derived from rock glacier appearance, e. g.: (1) Exposed fines in the upper part of the front slope (light, striped texture in the aerial photographs) indicate activity. (2) A smooth transition between front slope and rock glacier surface indicates inactivity. (3) An irregular, but smoothed surface relief and a decayed appearance indicate that a rock glacier is relict. If no distinction can be made between activity and inactivity, which is often the case for the interpretation of aerial photographs, "intact" indicates that the feature is not relict. Activity should be confirmed by photogrammetric measurements, intactness by geophysical field research.
Mean slope:	Mean slope of the rock glacier as computed by ArcGIS zonal statistics for rock glacier polygons; slope calculated with SAGA with the algorithm of Zevenbergen and Thorne (1987).
Mean radiation [kWh/m^2]:	Potential direct solar radiation for January plus February averaged over the rock glacier. Computed with SAGA using the following settings: Solar constant 1367 W/m^2, transmittance of the atmosphere 0.8, time step 5 days.

(Continued on the next page.)

Site characteristics of rock glaciers:

Position:	1 = Valley head including cirques; 2 = valley side; 3 = valley floor. Cf. Barsch (1996a); Parson (1987).
Connection to the source area:	Direct / not direct. Cf. Barsch (1996a).
Connection to moraines:	1 = None; 2 = frontal moraine; 3 = lateral moraine; 4 = morainic debris, not differentiated.
Relation to glaciers and thermokarst:	1 = Absence of glaciers or thermokarst-affected massive-ice in the talus shed. 2 = Connected to a glacier or thermokarst area. 3 = Presence of glaciers or thermokarst in the talus shed, but no connection.
Mean ridge crest height above back of rock glacier [m]:	Manual estimate from the DEM.
Area of talus shed [km^2]:	Planimetric area of the contributing area as computed from polygons digitized on-screen; does not include the rock glacier's area itself; was not determined for most debris rock glaciers.
Mean slope of talus shed (automated) [°]:	As computed by ArcGIS ("zonal statistics") from a slope model calculated with the algorithm of Zevenbergen and Thorne (1987).
Mean slope of talus shed (manual) [°]:	Manual estimation based on topographic data.
Mean radiation within talus shed [kWh/m^2]:	Potential solar radiation for January plus February averaged over the talus shed. See above for details.
Aspect of middle or main face of talus shed [octant]:	Determined manually.
Valley trend [octant]:	Downstream orientation of the cirque or valley axis.
Valley slope angle below toe [°]:	Determined manually from contour lines below the rock glacier's toe.
Windward landform type:	Indicates that the rock glacier is situated in the lee of one of the following landform types: *Peak:* A significant high point, all slopes trending downward from the point. *Divide:* A drainage divide not formed by a peak (i. e. shoulder, arête or col). *Open:* A point with no landform upwind, often a west-trend valley side.
Leeward landform type:	Compare "windward landform type" above.
Valley-side slope tendency:	Opening; straight; closing.
Main stratigraphic unit in the talus shed:	As derived from the geologic map 1:250,000 of Ayala, Cabrera y Asociados Ltda. (2000); Klohn (1960).

Comments:

Any other relevant information on the rock glacier or concerning data quality.

Appendix C

Geomorphological maps

The location of the following geomorphological maps on a regional scale is indicated in the overview map on page 3 (figure 1.2).

In the maps, ridge lines represent larger topographic features in parent bedrock, while crests refer to smaller structures in unconsolidated material. The symbology is based upon the one presented by Kneisel et al. (1998).

Map coordinates refer to UTM Zone 19S, PSAD 1956.

The geomorphological sketch map of Cerro San Ramón is displayed as a figure in the text on page 33.

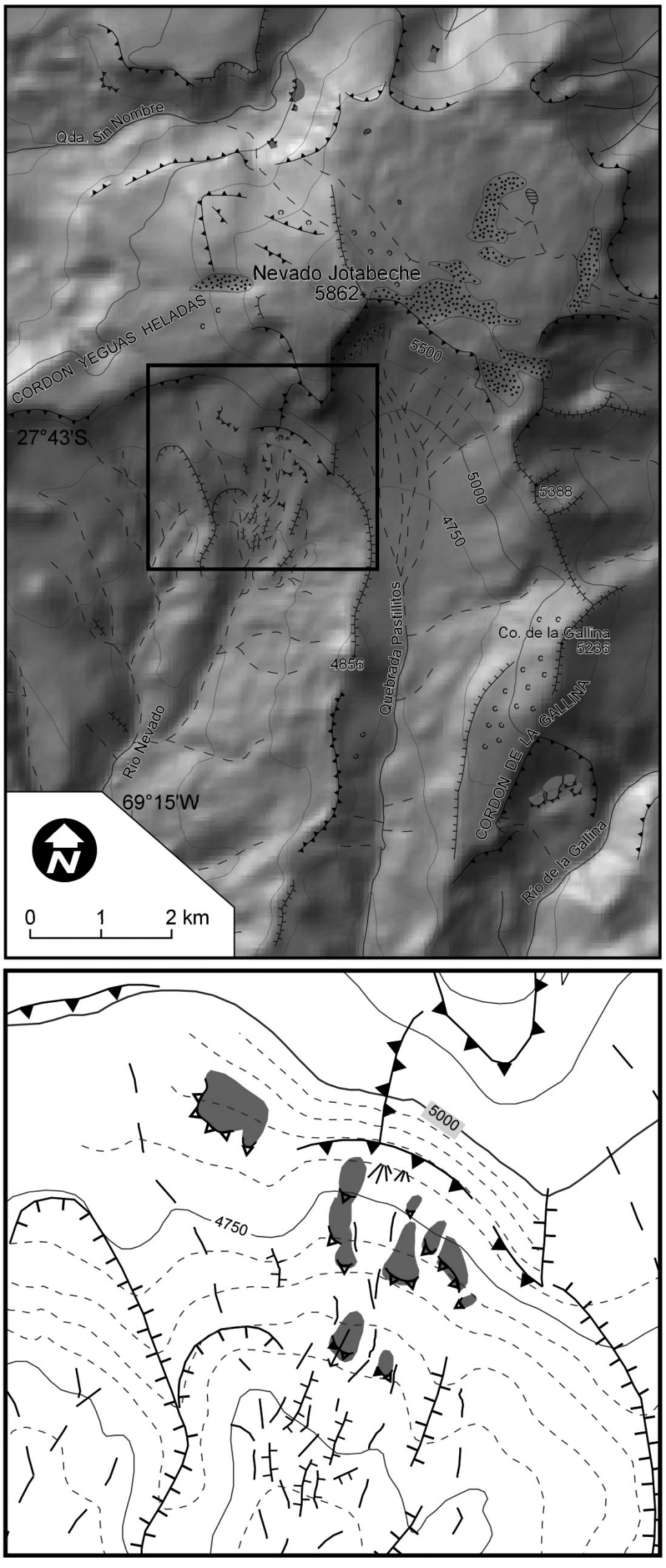

Symbology

- Crest (unconsol. material)
- Cliff (in bedrock)
- Scarp (unconsol. material)
- Talus cone
- Linear erosion
- Lake
- Firn
- Contour line, 250 m equidistance
- 50 m equidistance

Periglacial geomorphology

- Active rock glacier
- Inactive rock glacier
- Relict rock glacier
- Stone-banked terrace

Topography: Derived from SRTM data, 90 m resolution

Thematic layers: Derived from aerial photographs Geotec Laguna del Negro Francisco S26 L15 #14976-14977 (SAF, Santiago, January 1999) and field observations

A. Brenning 2005

Figure C.1: Geomorphological map of Nevado Jotabeche (27° 42′ S).

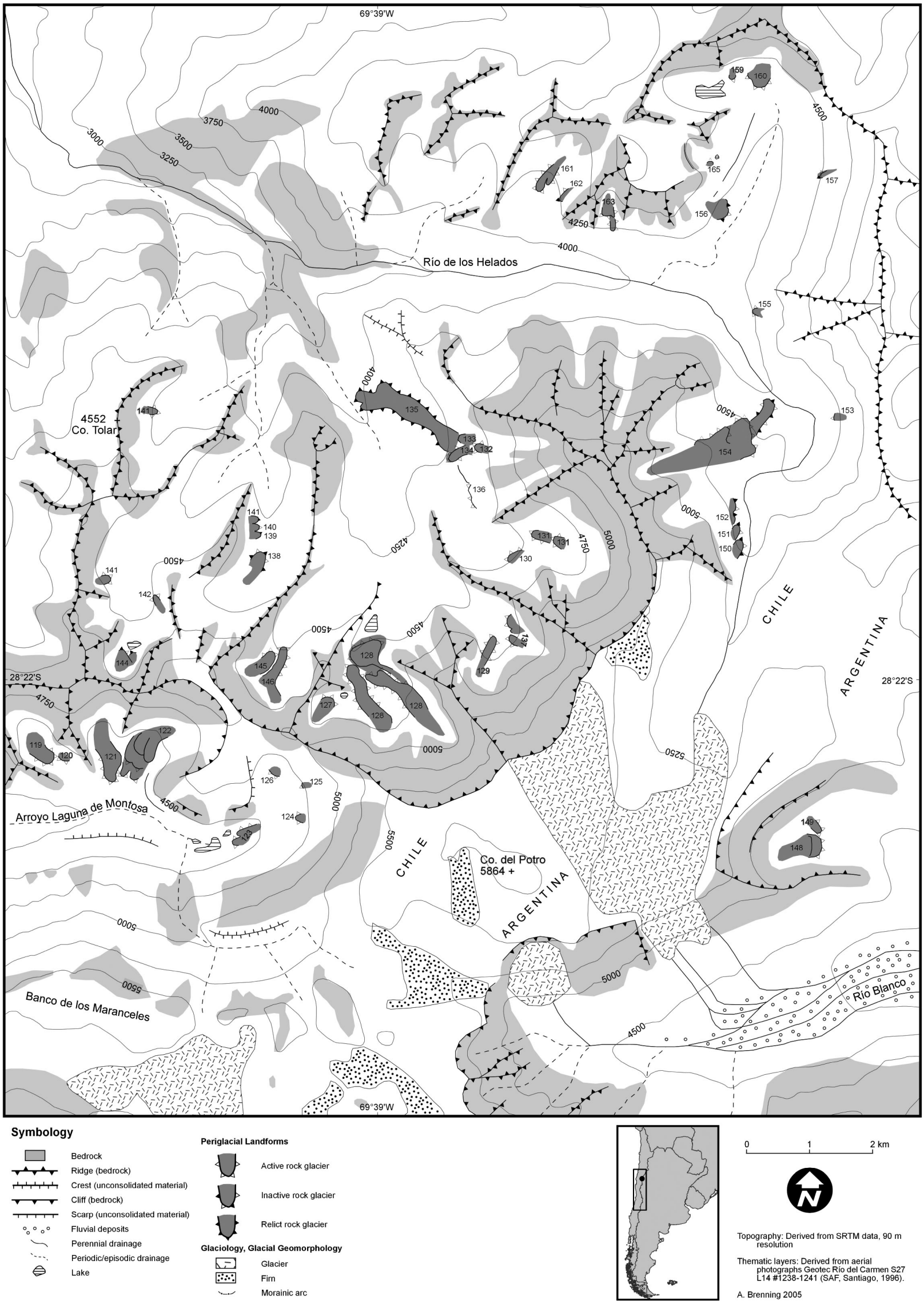

Figure C.2: Geomorphological map of Cerro del Potro (28° 23′ S).

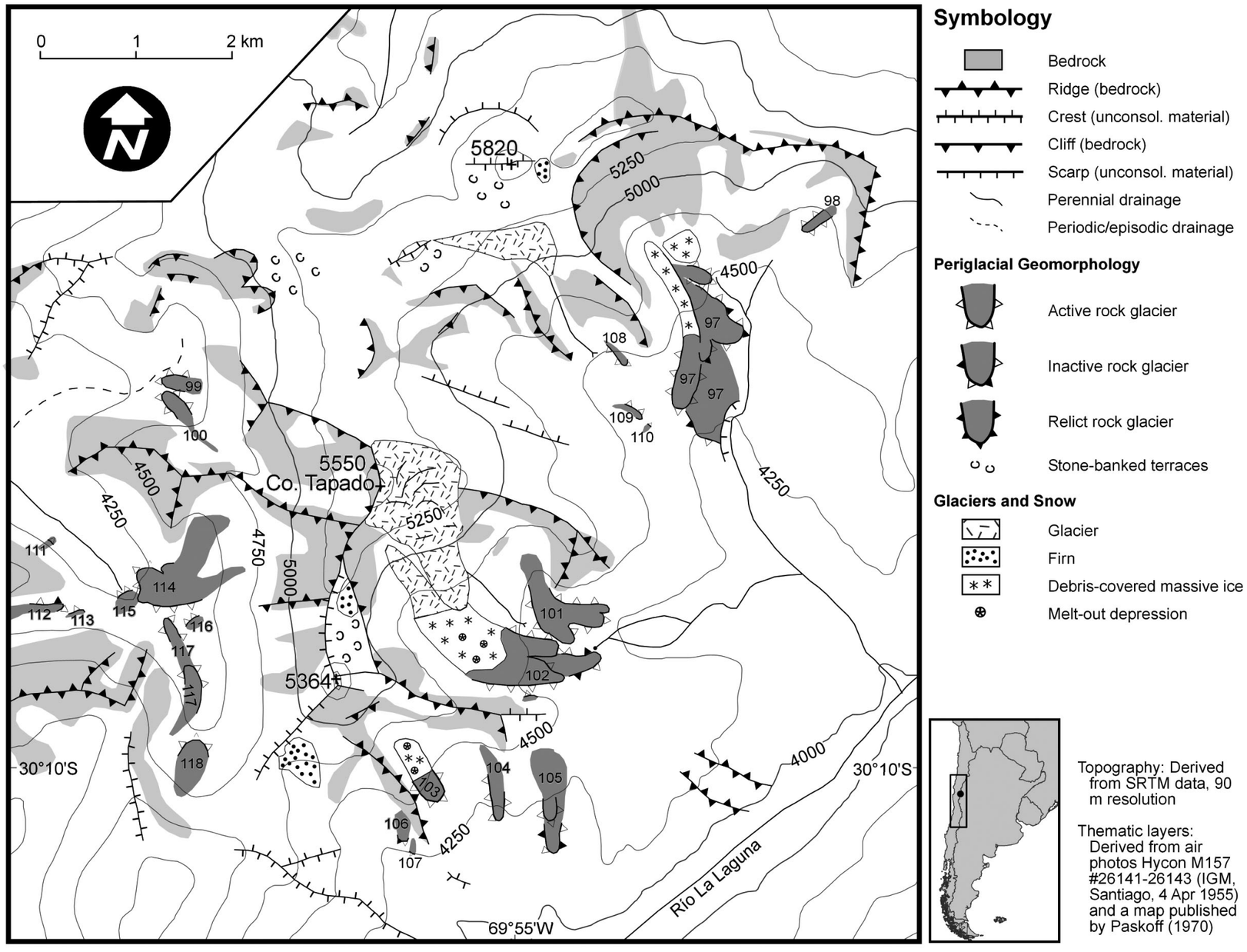

Figure C.3: Geomorphological map of Cerro Tapado (30° 08′ S).

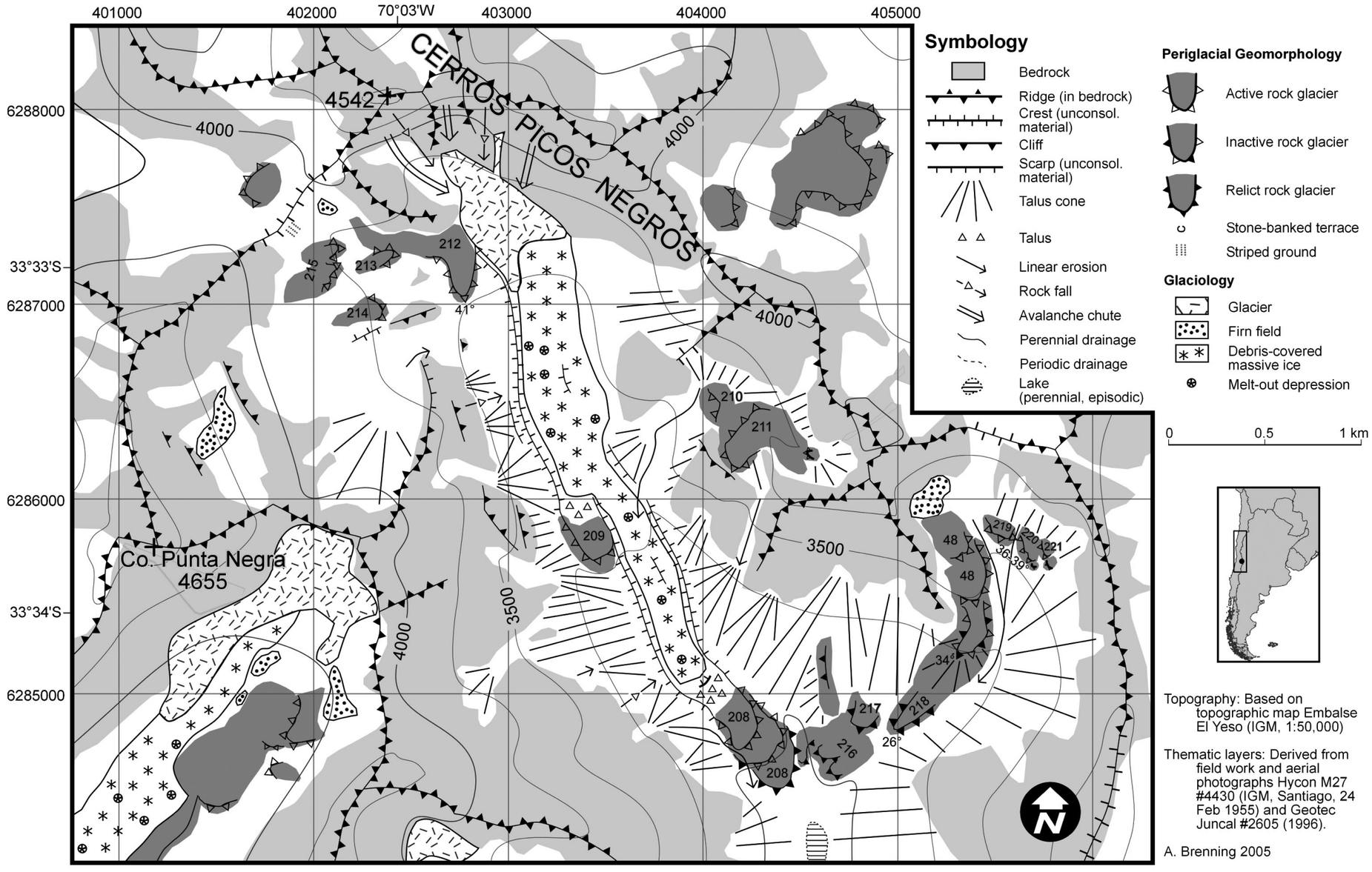

Figure C.4: Geomorphological map of the Cajón de la Casa de Piedra, Cerros Picos Negros area (33° 33′ S). After Brenning (2003), modified.

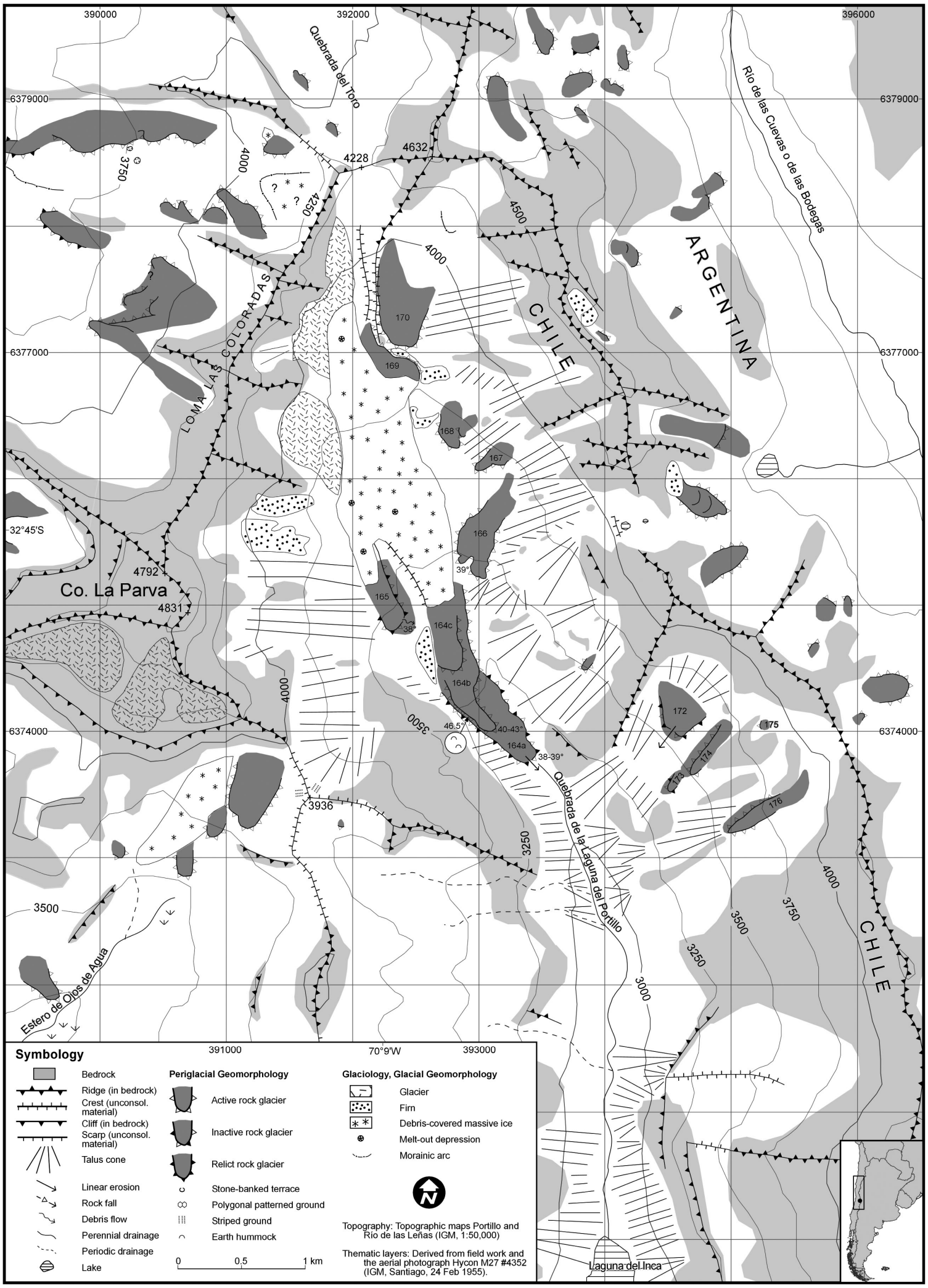

Figure C.5: Geomorphological map of the Laguna del Inca catchment, Cerro La Parva area (32° 45′ S).

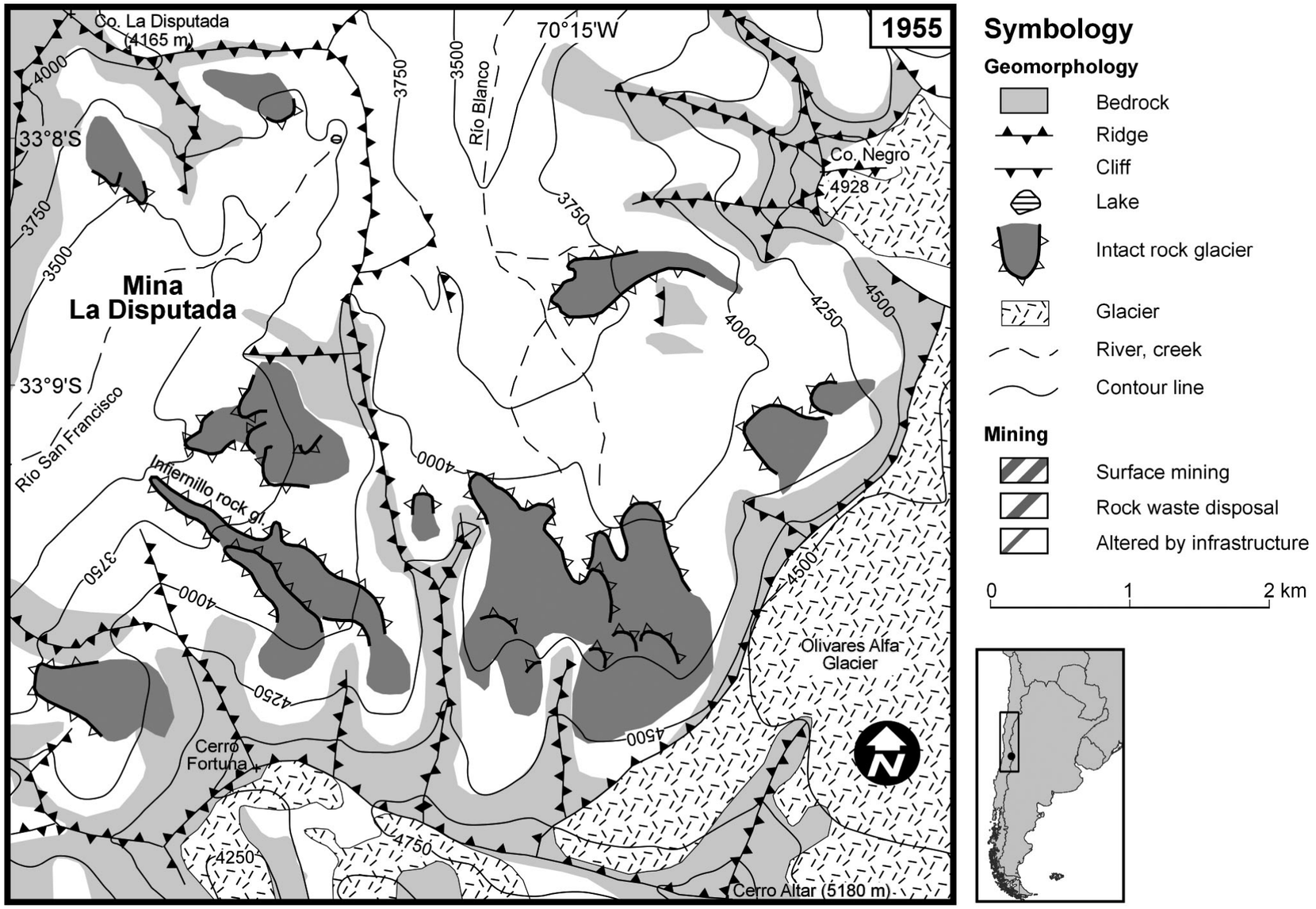

Figure C.6: Geomorphological impact of open-pit mining on rock glaciers at Codelco División Andina and Disputada de Las Condes Los Bronces mine (continued on the next page; 33° 09′ S). Cartography is based on Lliboutry (1961), Arcadis Geotécnica (2001) and aerial photographs Hycon (no. 4300; year 1955) and Geotec (flight Juncal, no. 5585; 1997).

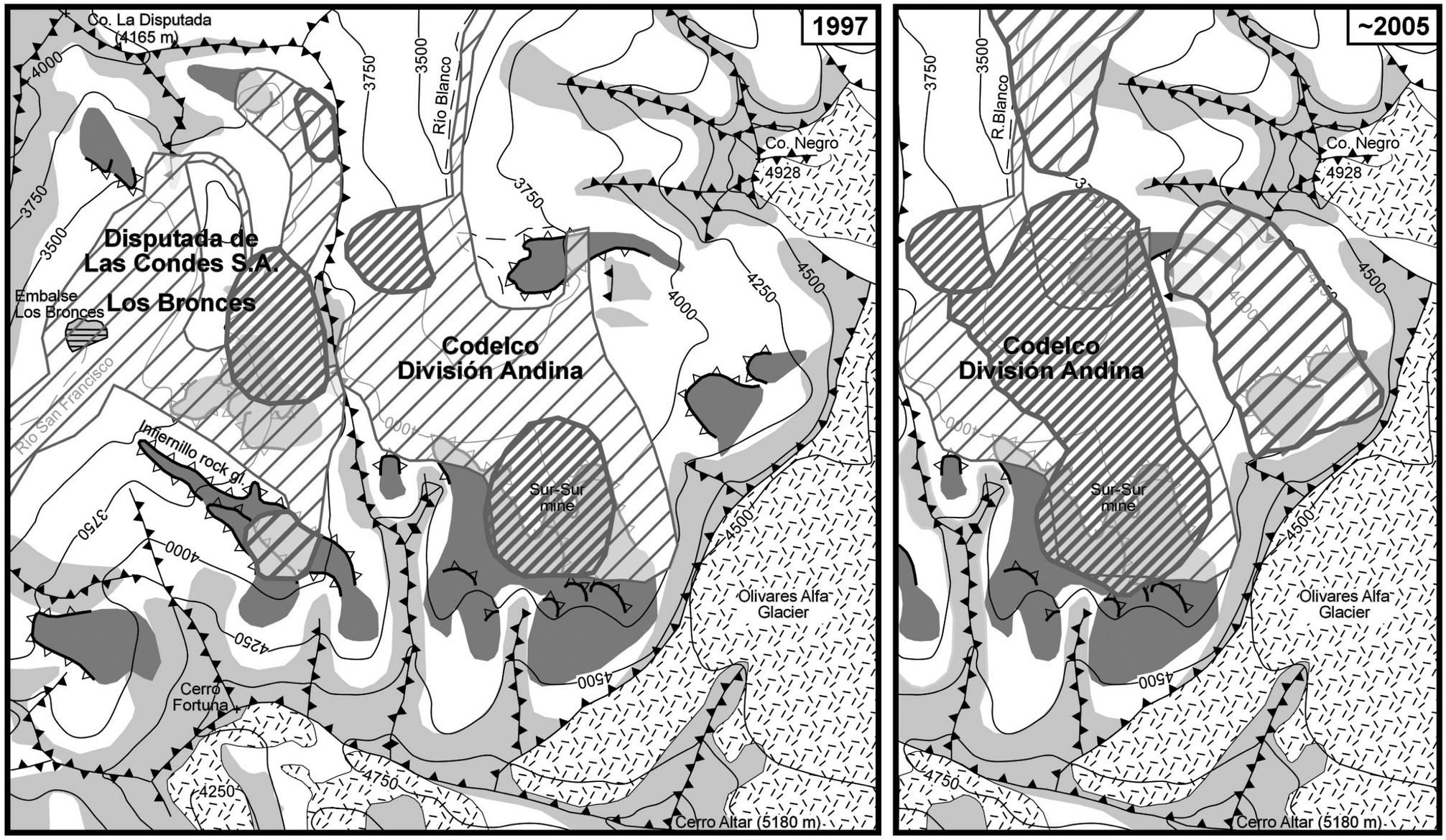
1997
Co. La Disputada
(4165 m)
Río Blanco
Co. Negro
4928
Disputada de
Las Condes S.A.
Los Bronces
Embalse
Los Bronces
Río San Francisco
Codelco
División Andina
Sur-Sur
mine
Olivares Alfa
Glacier
Cerro
Fortuna
Cerro Altar (5180 m)
~2005
R.Blanco
Co. Negro
4928
Codelco
División Andina
Sur-Sur
mine
Olivares Alfa
Glacier
Cerro Altar (5180 m)

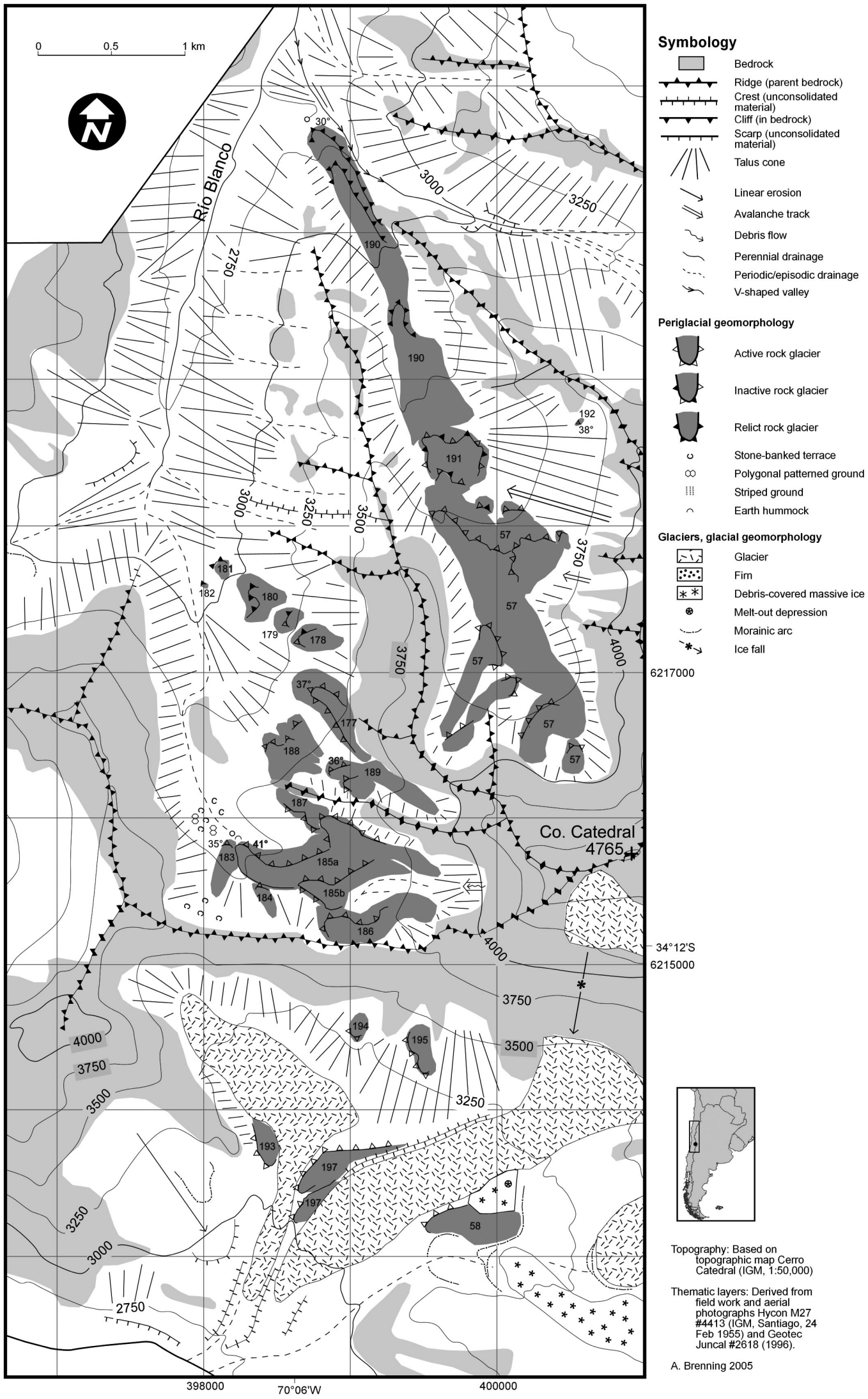

Figure C.7: Geomorphological map of the upper Río Blanco catchment, Cerro Catedral area (34° 12′ S).

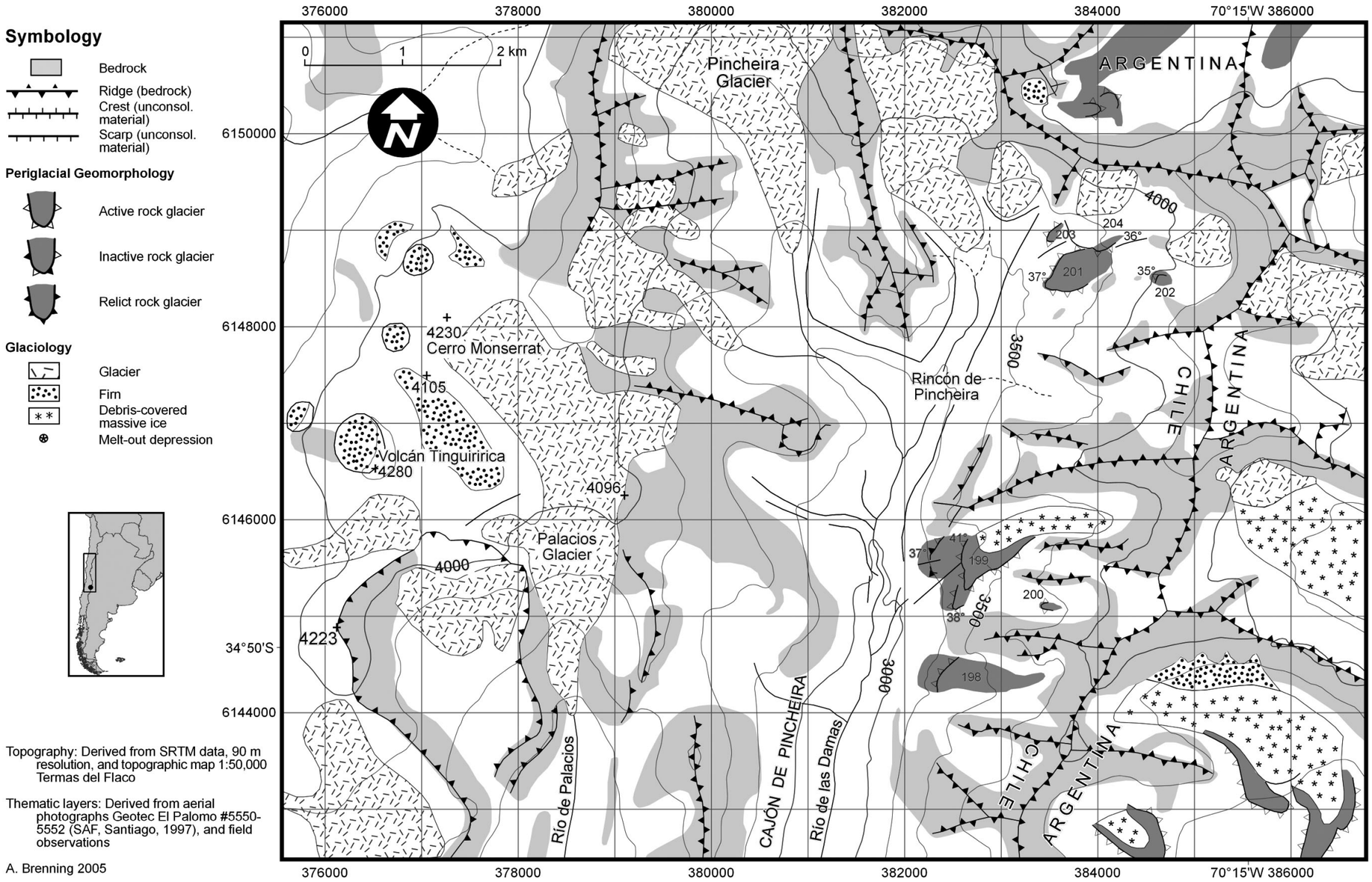

Figure C.8: Geomorphological map of the upper Río de las Damas catchment, Cerro El Moño area (34° 45′ S).

Lebenslauf

Name:	Alexander Brenning
Geburtsdatum, -ort:	15.09.1975, Bamberg
09/1985 – 06/1994	Clavius-Gymnasium Bamberg; Abitur
10/1994 – 09/1995	Wehrdienst in Donauwörth
11/1995 – 06/2001	Studium der Mathematik mit dem Nebenfach Geographie: Friedrich-Alexander-Universität Erlangen–Nürnberg, Pontificia Universidad Católica de Chile (DAAD-Stipendium), Technische Universität Bergakademie Freiberg
06/2001	Abschluss als Diplom-Mathematiker, TU Freiberg Diplomarbeit: „Geostatistics without Stationarity Assumptions within Geographical Information Systems“
08/2001 – 08/2002	Wissenschaftlicher Mitarbeiter Institut für Geographie, Universität Erlangen–Nürnberg
09/2002 – 02/2005	Wissenschaftlicher Mitarbeiter Geographisches Institut, Humboldt-Universität zu Berlin
02 – 04/2002, 03 – 04/2004	DAAD-Stipendiat, Pontificia Universidad Católica de Chile, und Instituto Argentino de Nivología y Glaciología (Mendoza)
Seit 03/2005	Wissenschaftlicher Mitarbeiter Institut für Medizininformatik, Biometrie und Epidemiologie, Universität Erlangen–Nürnberg

Alexander Brenning
19. April 2005

Selbständigkeitserklärung

Hiermit erkläre ich, die vorliegende Arbeit selbständig ohne fremde Hilfe verfasst und nur die angegebene Literatur und Hilfsmittel verwendet zu haben.

Alexander Brenning
19. April 2005